DOCOSAHEXAENOIC ACID (DHA) EXERTS ITS ANTI-ATHEROGENIC EFFECTS IN ENDOTHELIAL CELLS VIA EPIGENETIC AND TRANSCRIPTIONAL MECHANISMS

By

Shiqi Huang

A thesis

Submitted to the Faculty of Graduate Studies of

The University of Manitoba

In Partial Fulfillment of the Requirements for the Degree of

MASTER OF SCIENCE

Department of Food and Human Nutritional Sciences

University of Manitoba

Winnipeg, Manitoba, Canada

ABSTRACT

Atherosclerosis, the main contributor to a range of cardiovascular diseases, can be regulated by various epigenetic and transcriptional mechanisms, including p38 mitogen-activated protein kinase (MAPK) and nuclear factor κB (NF-κB) signaling. Docosahexaenoic acid (DHA) is widely assumed to have atheroprotective effects but the underlying mechanisms remain largely unknown. Our laboratory previously reported that DHA activates p38 MAPK differently in growing and quiescent human endothelial cells, which represent the atherogenic and healthy states *in vivo*, respectively. Also, DHA can inhibit NF-κB in endothelial cells. Thus, we hypothesized that DHA may exert its atheroprotective effects in endothelial cells via epigenetic and transcriptional mechanisms involving p38 MAPK/NF-κB signaling. EA.hy926 cells were cultured on Matrigel-coated plates for growing and quiescent states and were treated with DHA and inhibitors for p38 MAPK or other enzymes downstream of p38 MAPK. The activation and/or protein levels of various cell signaling and epigenetic players were detected by Western blotting. In general, DHA was found to activate eNOS, mediate eNOS expression, regulate the transactivation of NF-κB and CREB, influence histone H3 phosphorylation, affect cell cycling, and alter cyclin D1 protein levels. Most of these effects of DHA showed concentration-, time-, and endothelial cell growth state-dependency. While 125 μM DHA may be deleterious for endothelial cells, 20 μM DHA showed potential atheroprotective effects that were superior in quiescent cells compared to growing cells. The effects of DHA likely result from the modulation of certain transcription factors such as NF-κB and histone marks, with some involvement of p38 MAPK signaling. Overall, DHA was able to exert its atheroprotective effect via epigenetic and transcriptional mechanisms. These findings may lead to further research to help refine the recommendations for DHA intake under different health conditions and identify potential therapeutic targets and/or diagnostic markers for endothelial functions and atherosclerosis.

ACKNOWLEDGEMENTS

First and foremost, I would like to express my deepest gratitude towards my two advisors Dr. Carla Taylor and Dr. Peter Zahradka, who are not only experienced researchers but also nurturing educators. They have given me enormous support, guidance, encouragement, and patience throughout my Master's study, especially during the hardship of the pandemic. Also, thanks to my committee members Dr. James Davie and Dr. Peter Eck; your inputs inspired me a lot, and your help along the way really means a lot to me.

I would like to thank my wonderful lab members, our Canadian Centre for Agri-Food Research in Health and Medicine as well as St. Boniface Research Centre staff, and our department graduate program assistant Emily Gregorchuk, for creating such a cheerful and professional workplace and study environment for me. I also want to expression my appreciation to Dr. Peter Pelka who generously shared the protocol for analysing the cell cycle by flow cytometry, and Dr. Christine Zhang who helped and guided me through the flow cytometry process. In addition, I would like to extend my gratitude to my funding sources: Research Manitoba Master's Studentship Award, Mark G. & Patricia N. Smerchanski Endowed Studentship from the St. Boniface Hospital Foundation, and the Graduate Enhancement of Tri-Council Stipends, the International Graduate Student Scholarship and the International Graduate Student Entrance Scholarship from the University of Manitoba.

Finally, I want to thank all my family and friends for their support and encouragement throughout my whole journey of study and pursuing research, especially my husband who has always been there for me and took care of me during the whole course of my Master's.

Table of Contents

List of Figures

List of Tables

List of abbreviations

ABCA1	ATP-binding cassette A1
ACE	angiotensin converting enzyme
ACh	acetylcholine
acLDL	acetylated low-density lipoprotein
ADP	adenosine diphosphate
ALA	α-linolenic acid
AngII	angiotensin II
AP-1	activator protein 1
APOA1	apolipoprotein A1
ApoB100	apolipoprotein B100
APOE	apolipoprotein E
APS	ammonium persulfate
ASCEND	A Study of Cardiovascular Events in Diabetes
ATP	adenosine triphosphate
BCA	bicinchoninic acid
BP	blood pressure
BRD4	bromodomain-containing protein 4
BSA	bovine serum albumin
CaM	calmodulin
CaMKII	Ca^{2+}/calmodulin-dependent protein kinase II
CBP	CREB-binding protein
CCII	CREB-CBP interaction inhibitor
CDK	cyclin-dependent kinase
COX-2	cyclooxygenase-2
CREB	cAMP-response-element binding protein
CRP	C-reactive protein
CTK	C-terminal kinase
CVD	cardiovascular disease
CXCL16	C-X-C motif ligand 16
DAG	diacylglyceride
DHA	docosahexaenoic acid
DMEM	Dulbecco's modified Eagles' medium

DMSO	dimethyl sulfoxide
DNA	deoxyribonucleic acid
ECL	enhance chemiluminescence
ECM	extracellular matrix
ED	endothelial dysfunction
EGR-1	early growth response factor-1
eNOS	endothelial nitric oxide synthase
EPA	eicosapentaenoic acid
ERK1/2	extracellular-signal regulated kinase 1/2
ET-1	endothelin 1
FBF	forearm blood flow
FBS	fetal bovine serum
FFA	free fatty acid
FFAR	FFA receptor
FMD	flow-mediated dilation
FOXO1	foxhead box O1
FOXO3α	foxhead box O3α
GGPP	geranylgeranyl pyrophosphate
HAEC	human aortic endothelial cell
HCAEC	human coronary artery endothelial cell
HDAC	histone deacetylase
HDL	high-density lipoprotein
HEPES	4-(2-hydroxyethyl)-1-piperazineethanesulfonic acid
HLB	hypotonic lysis buffer
HMG-CoA	3-hydroxy-3-methyl-glutaryl-coenzyme A
HO-1	heme oxygenase-1
HR	heart rate
HRP	horseradish peroxidase
HUVEC	human umbilical vein endothelial cell
ICAM1	intercellular adhesion molecule 1
IDL	intermediate density lipoprotein
IEG	immediate-early gene
IHR	intermittent hypoxia/reoxygenation
IKK	IκB kinase

IL	interleukin
INFγ	interferon γ
Inh	inhibitor
iNOS	inducible nitric oxide synthase
LDL	low-density lipoprotein
LDL-C	low-density lipoprotein-cholesterol
LDLR	low-density lipoprotein receptor
lncRNA	long-non-coding RNA
LOX-1	lectin-like oxLDL receptor-1
LPL	lipoprotein lipase
LPS	lipopolysaccharide
LSS	laminar shear stress
MAG	monoacylglyceride
MAPK	mitogen-activated protein kinase
MAPKAPK	mitogen-activated protein kinase activated protein kinase
MCP-1	monocyte chemoattractant protein-1
MG	Matrigel®
MI	myocardial infarction
miRNA	microRNA
MMP	matrix metalloproteinase
mRNA	messenger ribonucleic acid
MSK	mitogen- and stress-activated protein kinase
n3 PUFA	omega-3 polyunsaturated fatty acids
NADPH	nicotinamide adenine dinucleotide phosphate
NCEP-II	National Cholesterol Education Program II
ncRNA	non-coding RNA
NEFA	non-esterified fatty acid
NF-κB	nuclear factor-κB
NO	nitric oxide
NRF2	nuclear factor erythroid 2 related factor 2
NTK	N-terminal kinase
OSA	obstructive sleep apnea
oxLDL	oxidized low-density lipoprotein
PAF	platelet-activating factor

PAGE	polyacrylamide gel electrophoresis
PBS	phosphate-buffered saline
PGC1α	peroxisome proliferator-activated receptor γ coactivator 1α
PGI_2	prostaglandin I2
PI	propidium iodide
PI3K	phosphoinositide-3-kinase
PKA	protein kinase A
PKAc	catalytic subunit of PKA
PKC	protein kinase C
PLC	phospholipase C
Pol II	RNA polymerase II
PPAR	peroxisome proliferator-activated receptor
P-TEFb	positive transcription elongation factor b
PTM	post-transcriptional modification
PVDF	polyvinylidene difluoride
RAAS	renin-angiotensin-aldosterone system
RBC	red blood cell
REDUCE-IT	Reduction of Cardiovascular Events with Icosapent Ethyl–Intervention Trial
RHD	Rel homology domain
RLP	remnant-like particle
ROS	reactive oxygen species
RSK	p90 ribosomal S6 kinase
SAP	shrimp alkaline phosphatase
2×SB	2 times sample buffer
SDS	sodium dodecyl sulphate
SEM	standard error of the mean
siRNA	small interfering RNA
SIRT1	sirtuin 1
SPM	specialized pro-resolving mediator
STAT1	signal transducer and activator of transcription 1
STRENGTH	Statin Residual Risk Reduction with Epanova in High CV Risk Patients with Hypertriglyceridemia
TAD	transcriptional activation domain
TBST	tris-buffered saline with Tween-20

TC	total cholesterol
TEMED	N,N,N',N'-tetramethylethylenediamine
TF	transcription factor
TG	triglyceride
TGFβ	transforming growth factor β
TNFα	tumor necrosis factor α
t-PA	tissue-type plasminogen activator
VC	vehicle control
VCAM1	vascular cell-adhesion molecule 1
VEGF	vascular endothelial growth factor
VITAL	Vitamin D and Omega-3 Trial
VLDL	very low-density lipoprotein
VSMC	vascular smooth muscle cell
vWF	von Willebrand factor

LITERATURE REVIEW

Introduction

Cardiovascular disease (CVD), especially ischemic heart disease and stroke, the primary causes of death worldwide for nearly 2 decades [1], results in tremendous economic and social burden. The main contributor to ischemic heart disease, stroke, and other related CVD is atherosclerosis, the narrowing of blood vessels due to plaque formation as a result of endothelial dysfunction (ED) [2]. Endothelial cells line the vessel walls, and are typically quiescent in the healthy state. Damage to the vessels will activate endothelial cells. These cells should return to their quiescent state after the vessel wall has been repaired. However, endothelial cells can remain activated even when there is no physical damage to the vessel, and this is termed ED. These active cells make the vessel permissive to plaque formation as a consequence of decreased nitric oxide (NO) production. Additionally, the reduction in endothelial nitric oxide synthase (eNOS) activity enables arterial remodeling, which ultimately leads to arterial stiffness [3]. All of these processes occur due to changes in endothelial cell state, eventually progressing to atherosclerosis and a high risk of death.

Omega-3 polyunsaturated fatty acids (n3 PUFA), especially eicosapentaenoic acid (EPA) and docosahexaenoic acid (DHA), which have longer chain lengths, are well-known for their cardioprotective effects. Although controversies remain, it is generally agreed that n3 PUFA, particularly those from marine sources like EPA and DHA, can reduce both plaque formation and ischemic events [4], but the underlying mechanisms by which they function still largely remain unknown. Being bioactive molecules with many bioactive metabolites, understanding how n3 PUFA signal in the cell may help to resolve those controversies and may even help in discovering new therapies and/or targets for CVD. Previous work [5] and some other preliminary data obtained in the Taylor and Zahradka labs (University of Manitoba) have demonstrated that DHA, but not EPA or α-linolenic acid (ALA), can reduce the proliferation, DNA synthesis and migration of cultured endothelial cells, by inducing a quiescent state. Further experiments done by the lab showed that DHA was able to induce p38 mitogen-activated protein kinase (MAPK) activity and p38-activation showed different response patterns to DHA in growing and quiescent endothelial cells [6]. These results suggest that DHA may exert its beneficial effects via p38 MAPK, an important player in oxidative stress and the inflammatory response. Thus, this project will focus on the potential atheroprotective mechanisms by which DHA affects endothelial cell function via p38 MAPK-related pathways.

Endothelial cells and atherosclerosis

Endothelial cells

Endothelial cells form a single layered sheet (endothelium) lining the luminal side of all blood-containing chambers, from heart to blood vessels [7]. The endothelial cells discussed in this thesis refer to vascular endothelial cells, the ones in blood vessels. They are the very first cells that all nutrients and other constituents in the blood will encounter when going into tissues and organs. Besides controlling the passage of all substances, including white blood cells, between the bloodstream and underlying tissues, endothelial cells also serve a critical role in maintaining the homeostasis of the cardiovascular system and regulate many physiological processes in our body [8,9]. They control blood fluidity, modulate vascular tone, and participate in the inflammatory response.

In healthy, normal conditions, endothelial cells maintain blood fluidity by preventing platelet aggregation via membrane-bound ectonucleotidases that hydrolyze ATP and ADP [10] and secretion of anti-thrombotic agents like prostaglandin I2 (PGI_2) [11] as well as NO [12,13]; by supporting fibrinolysis via tissue-type plasminogen activator (t-PA) and urokinase [8,14]; and by promoting the anti-coagulant protein C/protein S pathway [15,16]. Upon injury, however, endothelial cells are activated and shift to favor platelet aggregation and coagulation. They release platelet-activating factor (PAF), von Willebrand factor (vWF) and other factors to activate circulating platelets and promote blood clotting [17,18]. This helps to repair damaged vessels and regain hemostasis.

Endothelial cells are also key in regulating vasomotor tone. PGI_2 and NO, important vasodilators released from endothelial cells, act on vascular smooth muscle cells (VSMC) beneath the endothelium during resting conditions [8,19]. In response to certain stimuli, such as hypoxia and adrenaline, endothelial cells will instead produce vasoconstrictors, such as endothelin 1-3 (ET-1 to ET-3) [20]. Besides expressing vasodilators and vasoconstrictors, endothelial cells regulate blood flow by taking part in the renin-angiotensin-aldosterone system (RAAS). Two of the most important enzymes in the RAAS, angiotensin converting enzyme (ACE) and ACE2, are predominantly expressed in endothelial cells [21,22]. ACE and ACE2 are responsible for the production and hydrolysis of angiotensin II (AngII), a potent vasoconstrictor, respectively.

When exposed to pro-inflammatory stimuli, like cytokines and lipopolysaccharides (LPS), endothelial cells are activated to synthesize and secrete more cytokines, chemokines and even growth factors to aid the communication and recruitment of leukocytes [8].

Endothelial cells also produce otherwise transcriptionally-suppressed adhesion molecules, such as vascular cell-adhesion molecule-1 (VCAM-1), intercellular adhesion molecule-1 (ICAM-1), and E-selectin, to mediate the attachment and migration of leukocytes on and across the endothelium [23,24]. All these actions support leukocyte function in fighting infection and repairing tissue damage. In healthy conditions, endothelial cells should return to the resting, quiescent state after inflammation resolves.

Endothelial cells also play a critical role in angiogenesis. Once physical damage occurs in the vessels and/or is stimulated by chemicals, endothelial cells will be activated from the usual quiescent state and be able to migrate and proliferate for vessel repair or grow new vessels. Endothelial cells are also responsible for producing growth factors, such as vascular endothelial growth factor (VEGF), angiopoietins, and ephrins, that are involved in the initiation, remodeling and maturation of the new vasculature [8]. Normally, the activated endothelial cells should return to the quiescent state once damage has been repaired and/or the stimuli eliminated, a process called resolution [24]. In the diseased state, however, endothelial cells usually remain in the activated state and fail to resolve back to the quiescent state, resulting in ED. This is especially indispensable during oncogenesis where new blood vessels are in high demand [25], and during atherosclerosis [26] which will be discussed later.

Endothelial dysfunction

Ludmer and his colleagues [27] found that acetylcholine (ACh), a widespread neurotransmitter, induced vasoconstriction in patients with atherosclerosis. This opened up the research field for studying ED. Since then, ED has been described in many disease conditions, including diabetes, chronic renal failure, metabolic syndrome, and especially atherosclerosis-related CVD [28]. ED usually develops as impaired endothelium-dependent vasodilation, which occurs due to switching of endothelial cells to the more proinflammatory, prothrombotic, and proliferative active state [28]. As mentioned above, inflammation-related stimuli can activate endothelial cells to such a state. If the stimuli do not cease and chronic inflammation sets in, endothelial cells will be kept activated and enter this vicious cycle of producing more chemokines (e.g. monocyte chemoattractant protein-1 (MCP-1)), adhesion molecules (e.g. VCAM-1 and ICAM-1), and pro-coagulants (e.g. vWF) [24]. More importantly, chronic inflammation is usually accompanied by oxidative stress that will result in eNOS uncoupling—the switch from NO production to O_2^- generation by eNOS [3]. Initially regarded as a calcium-dependent and calmodulin (CaM)-modulated enzyme, eNOS functions as a homodimer and its activity is tightly regulated at multiple tiers (as reviewed in [3,29]). eNOS contains 3 major

domains: an N-terminal oxygenase domain that binds heme, L-arginine (the substrate), and other co-factors, the CaM binding domain, and a C-terminal reductase domain that interacts with reduced nicotinamide adenine dinucleotide phosphate (NADPH). Under normal conditions for NO synthesis, electrons derived from NADPH are transferred to the heme with the assistance of CaM, so that O_2 can be recruited by the heme iron at which point oxidation of L-arginine to NO and citrulline is then catalyzed. The activity of eNOS is heavily regulated by phosphorylation, especially at the Ser-1177 site, which is located within the reductase domain of eNOS [29]. Phosphorylation at this site is believed to enhance electron transfer to the oxygenase domain that catalyzes the production of NO from L-arginine and prevents CaM dissociation when the calcium concentration is low [30]. Under certain conditions, such as an oxidative environment [3], the electron flux is uncoupled from L-arginine oxidation and is instead transferred to O_2 to generate superoxide. The consequent reduction in NO bioavailability is the key in ED. This gaseous intercellular signaling molecule has pleiotropic functions. Apart from its well-known role as a vasodilator and anti-platelet aggregation agent [8], NO also modulates the release and/or action of other endothelium-derived mediators like ET-1, scavenges superoxide, prevents leukocyte adhesion, and inhibits VSMC proliferation [31]. Thus, as NO production and bioavailability are reduced in the ED state, the protective effects associated with this molecule are curtailed. The resulting responses will eventually enable plaque formation and atherosclerosis. Therefore, NO can be regarded as the gate-keeper for endothelial function [32] and the release of NO may be used to determine the "healthiness" of endothelial cells. To measure NO in real life, however, is challenging due to its gaseous nature and very short half-life of 1-2 sec. Thus, other methods have been developed to assess endothelial function.

One of the earliest methods for assessing endothelial function uses ACh. The infusion of ACh and subsequent comparison of artery diameter *ex vivo* can determine the endothelium's responsiveness. ACh induces vasodilation via NO with normal endothelium but vasoconstriction if the endothelium is dysfunctional, as first described by Ludmer et al [27]. However, this is an invasive method, and non-invasive methods have become more popular now with the aid of high-resolution ultrasound. Among those, flow-mediated dilation (FMD) is one of the most common clinical research methods, measuring changes in branchial artery diameter in response to resumption of blood flow following its restriction via cuff inflation [33,34]. The restored flow creates reactive hyperemia. The resulting elevated shear stress can immediately act on endothelial cells to stimulate NO release and vasodilation [28,32,34]. The basis of most clinical methods for endothelial function assessment is endothelial-dependent

vasomotion which relies on the release of NO and/or other endothelial-released vasoactive compounds [34].

Endothelial cell lines

Both primary endothelial cells and endothelial cell lines are employed for research purposes. First isolated in the 1970s, human umbilical vein endothelial cells (HUVEC) have become the major *in vitro* model to expand our knowledge about endothelial cell function [35]. However, HUVEC may not be representative for all *in vivo* conditions due to the great heterogeneity seen in the gene expression profiles of endothelial cells originating from different tissues [36]. Therefore, other primary endothelial cells are often isolated, such as aortic endothelial cells (HAEC) and human coronary artery endothelial cells (HCAEC), and used to study ED and inflammation. Although primary cells have the advantage of more closely resembling the vascular endothelium *in vivo*, their short life span (less than 10 passages) and diverse donor origins indicate primary endothelial cell lines are not ideal for long-term experiments and comparable results from cells of different sites and donors. Thus, the demand for permanent endothelial cell lines arises.

EA.hy926 is the best characterized permanent macrovascular endothelial cell line used in research. It was generated in the early 1980s via hybridization of HUVEC and A549 cells derived from human lung carcinoma [37]. A comparative study using a range of primary endothelial cells and permanent cell lines revealed that EA.hy926 was the only macrovascular endothelial cell line among some other cell lines to retain most of its endothelial properties [38]. Typical characteristics of endothelial cells that EA.hy926 cells have preserved include the presence of Weibel-Palade-bodies (endothelial-specific rod-shaped organelles), constitutive expression of endothelial markers like vWF, inducible expression of adhesion molecules and cytokines such as ICAM-1 and MCP-1, uptake of acetylated low-density lipoprotein (acLDL), and possession of ACE activity [35,37–39]. Its plasma membrane also has endothelin converting enzyme [40]. Although morphologically similar to primary cells, this cell line does not show contact inhibition when cultured to high density [38]. Indeed, recent data from our lab suggest that when grown on naked plastic, the proliferation and DNA synthesis rates remain high even when the cells are confluent [5]. It is only when they are grown on Matrigel® (MG), a commercialized gelatinous mixture rich in extracellular matrix (ECM) proteins, that cell proliferation and DNA synthesis rates decline significantly and continuously after the cells reach confluency. This may imply that the cells switch back to a quiescent state similar to that of an intact vessel. The differential responses of EA.hy926 cells

to the same set of PUFA treatments when cultured with and without MG [6] further corroborates the effects MG may have on EA.hy926 cell growth and culture. Only when grown on MG do the cells show signs of quiescence and exhibit differential p38 MAPK activation upon DHA stimulation. Therefore, MG will be used to culture the EA.hy926 cell line throughout this project.

Atherosclerosis

ED is recognized to have great prognostic value for many diseases as mentioned above, and especially as an important early marker and proposed predictor for atherosclerosis [26,32,41]. Partially due to limitations in assessment techniques [34], however, the prognostic value of ED has not been applied clinically. Currently, widely-used clinical biomarkers for atherosclerosis are circulating levels of lipoproteins and lipids [42] that are going to be discussed later. Atherosclerosis is a progressive chronic inflammatory disease condition characterized by the narrowing of the arterial lumen due to subendothelial accumulation of fatty substances, matrix proteins and inflammatory cells, i.e. plaque, at specific sites. Although the exact cause remains elusive, it is generally agreed that a series of complex interacting processes, "involving lipoprotein retention, inflammatory cell recruitment, foam cell formation, apoptosis and necrosis, VSMC proliferation and extracellular matrix synthesis, calcification, angiogenesis, arterial remodeling, fibrous cap rupture, thrombosis, and more" [43] finally lead to full atherosclerosis. Common risk factors for atherosclerosis include elevated serum lipids, hypertension, obesity, diabetes, smoking, and family genetics [44], most of which are linked to ED. As discussed above, dysfunctional endothelial cells secrete pro-inflammatory cytokines and adhesion molecules, produce reactive oxygen species (ROS), and release growth factors. These promote inflammatory cell recruitment and attachment, create a local oxidative environment favoring the formation of oxidized LDL (oxLDL), and stimulate the underlying VSMC. Dysfunctional endothelial cells also promote recruitment of monocytes which enter the subendothelial space and are activated into macrophages that can engulf oxLDL and lead to formation of foam cells. With stimulated VSMC switching their phenotype, all of these dysfunctional cells and accumulated lipids will manifest into the initial atherosclerosis lesion or the "fatty streak" [45].

Atherosclerosis can happen in many arteries and cause severe outcomes, such as atherosclerosis in coronary arteries leading to heart attack, in carotid arteries resulting in stroke, and in renal arteries contributing to chronic kidney disease [44]. The symptoms of atherosclerosis, however, can hardly be observed until the lesions grow to a size that can

severely interfere with artery functions leading to onset of medical emergencies. Thus, predictive biomarkers, diagnostic markers and therapeutic targets are needed. Cholesterol level, or LDL-cholesterol (LDL-C) to be more specific, is a well-recognized risk factor for atherosclerosis and related CVD at a population level, and is employed as a surrogate endpoint for clinical trials [42]. However, several trials found that additional cholesterol lowering had no further clinical benefit on top of the effect of statins [46–48]. Statins, which function as 3-hydroxy-3-methyl-glutaryl (HMG)-CoA reductase inhibitors, are so far the only class of LDL-C-lowering drugs that can prevent the morbidity and mortality caused by atherosclerosis and related CVD [48,49]. HMG-CoA reductase is the rate-limiting enzyme in endogenous cholesterol biosynthesis. The same pathway also produces other isoprenoids like geranylgeranyl pyrophosphate (GGPP), which is essential in the translocation and subsequent activation of RhoA — a small GTPase protein that can inhibit eNOS activity [50,51]. Emerging evidence suggests that the beneficial effects of statins lie not only in the cholesterol-lowering effect, but also by inhibiting production of those isoprenoid intermediates [48]. Therefore, it is necessary to further understand the underlying pathways/mechanisms and discover better biomarkers and targets.

Cell signaling, epigenetics and transcriptional control of atherosclerosis

Although closely related to chronic inflammation and dyslipidemia, atherosclerosis can also be viewed as an epigenetic disease involving extensive alterations in cell signaling [52,53]. The modern definition of epigenetics encompasses all the factors acting on chromatin that govern gene expression beyond the actual DNA sequence [54]. It includes, but is not limited to: histone modifications or histone marks (methylation, acetylation, etc.) and DNA methylation; transcription factors (TFs) such as nuclear factor-κB (NF-κB), peroxisome proliferator-activated receptor gamma (PPARγ), and activator protein 1 (AP-1); chromatin remodeling factors like SWI/SNF (SWItch/Sucrose Non-Fermentable) that can be recruited by certain TFs to act on chromatin allowing it to switch between a condensed state and an open state. Histone and DNA modification as well as the activities of some TFs are modulated by specific enzymes whose activity can then be regulated by other kinases and phosphatases. All these signal transductions can be initiated from many physio-pathological stimuli, such as CVD risk factors (e.g. hypertension and dyslipidemia), smoking, and diet [52]. Cell signaling can cause changes in epigenetic status/marks and TF activities that eventually lead to gene expression alterations that then affect all the downstream cellular processes and pathways.

p38 MAPK

p38 MAPK is a member of the MAPK family that responds to extracellular stress signals including inflammation [55]. It has four main isoforms: α, β, γ, and δ, all encoded by different genes. p38 MAPK can be further divided into two subsets: α and β versus γ and δ, based on amino acid sequence similarity, susceptibility to the selective pyridinyl imidazole class inhibitors like SB202190, and substrate selectivity [56]. Activation of p38 MAPK is usually achieved by dual phosphorylation of their characteristic Thr-Gly-Tyr motif, while dephosphorylation downregulates activity [57]. So far, p38α MAPK is the best studied and the most important isoform, since p38α MAPK knockout mice cannot survive, but knockouts of the other 3 isoforms are viable and fertile [56]. Also, p38α is expressed ubiquitously while the other isoforms have their own expression patterns in different cells, although activation of p38α shows cell-type dependency even to the same stimulus [57].

In response to inflammatory stimuli, p38 MAPK, especially p38α, can mediate this process by affecting the activity of the pro-inflammatory TF, NF-κB, via its direct downstream kinase mitogen- and stress- activated protein kinase 1 and 2 (MSK1/2) [55]. p38 MAPK also plays a role in cell cycle regulation and cell survival through the modulation of different cyclins and cyclin-dependent kinases (CDKs) [56,58]. Furthermore, p38 MAPK may directly and/or indirectly interact with SWI/SNF to open up the chromatin of target genes, thus allowing the upregulation of the genes *in situ* [59,60]. SB203580, a p38α/β specific inhibitor, blocks the migration of endothelial cells [61] and VSMC [62]. This p38 MAPK-related migration may also involve MSK1/2 [63]. Trempolec and her colleagues [64] have categorized a list of p38α MAPK substrates and their effects upon phosphorylation.

MSK1/2

MSKs are among the 11 members of the MAPK activated protein kinase (MAPKAPK) family, and are largely activated by p38 MAPK and extracellular-signal regulated kinase 1/2 (ERK1/2), another member of the MAPK family [65]. Various *in vitro* and *in vivo* studies showed that p38α is the most crucial p38 MAPK for MSK activation, while p38γ/δ are dispensable [66]. While MSK1 and MSK2 share great similarities in their structure and functions, they also display distinct substrate specificity especially when responding to certain stimuli [66]. However, the amino acid sequences of MSK1 and MSK2 are highly conserved especially around the activation/phosphorylation sites. Therefore, there is considerable difficulty in using only antibodies to distinguish the contributions of MSK1 or MSK2 to certain functions, since the antibodies currently available lack specificity to identify these homologues

[66]. Approaches exhibiting greater specificity, possibly certain genetic tools (e.g. specific knock-out/-down animal models or cell cultures), are therefore needed for this purpose.

MSKs have two functional kinase domains (C-terminal kinase (CTK) domain and N-terminal kinase (NTK) domain) in the same polypeptide and their activation by ERK1/2 and p38 MAPK occurs via sequential phosphorylation of several key sites along the polypeptide: the MAPKs first phosphorylate Thr-581 and Thr-700 to activate its CTK-domain; then the activated CTK-domain auto-phosphorylates the Ser-212, Ser-376 and Ser-381 sites that activate the NTK-domain and stabilize the enzyme in a conformation optimal for its kinase activity [66]. There are many other phosphorylation sites involved but Ser-212, Ser-376 and Thr-581 are the essential ones for both MSK1 and MSK2, accounting for more than 95% of the kinase activity [67,68].

MSKs have versatile roles in transcriptional regulation and inflammatory responses. They directly phosphorylate certain TFs (e.g. cAMP-response-element binding protein (CREB) and NF-κB), histone H3, and some other chromosomal proteins. MSKs phosphorylate CREB at its critical Ser-133 activation site that is essential for recruiting the CREB-binding protein (CBP)/p300 coactivators [69]. CBP and p300 are acetyltransferases that act on both histone proteins and non-histone proteins like TFs. They share high homology in structure and certain functions but are unique in some other functions and substrate selection (reviewed in [70,71]). CBP/p300 induces gene transcription by increasing chromatin accessibility, interacting with TFs to recruit RNA polymerase II (Pol II) to the promoter, and enhancing the transcriptional activities of certain TFs such as NF-κB [71,72]. The NF-κB subunit RelA (p65) can be phosphorylated by MSKs at Ser-276, which promotes the recruitment of CBP/p300 to acetylate RelA [73–76]. MSKs also phosphorylate H3 at Ser-10 and Ser-28, which activates the associated genes, but the two marks are usually not on the same H3 tail [77]. All of these events contribute to the regulation of target gene expression, especially the inflammation related genes thanks to CREB and NF-κB [65,72,78].

NF-κB

The NF-κB superfamily comprises a group of proteins whose functions are conserved from fruit flies to humans [79]. In the human context, the superfamily has two subfamilies: the "Rel" proteins (RelA or p65, RelB, and c-Rel) that contain a C-terminal transcription activation domain (TAD), and the "NF-κB" proteins (p105/p50 or NF-κB1, and p100/p52 or NF-κB2) whose C-terminal domains are comprised of multiple ankyrin repeats. All five members share a highly conserved Rel homology domain (RHD) for DNA binding and dimerization. The

major NF-κB dimer is formed by RelA and p50, while p50 and p52 can also homodimerize to bind to κB sites. Lack of the TAD, however, may repress transcription instead of positively regulating the genes associated as when p50 or p52 are heterodimerized with a Rel protein [80,81]. In the following text, the term "NF-κB" refers to the dimer TF, especially RelA/p50 since it is the most studied and paradigmatic dimer of NF-κB.

Usually, NF-κB complexes require activation to translocate from the cytoplasm to the nucleus to perform their function. There are two major ways to activate NF-κB in the cytoplasm: the canonical pathway requiring the dissociation of NF-κB from its inhibitor IκB , and the non-canonical pathway involving proteolytic degradation of the C-terminal ankyrin repeats on RelB-associated p100 to yield a shorter, active RelB/p52 form [80–82]. Further activation of NF-κB relies heavily on post-transcriptional modifications (PTMs), including phosphorylation, acetylation, and more (reviewed in [83,84]). Then NF-κB can recruit more co-factors depending on the PTM patterns and mediate expression of the target genes, which are often involved in immune and inflammation responses, cell survival and proliferation [85,86]. Being such an important mediator in so many critical pathophysiological processes, the activation and activity of NF-κB are tightly regulated via its PTMs, inhibitor IκB, and IκB kinase (IKK) as reviewed in the literature mentioned above. Besides, NF-κB can also be inhibited by another TF, PPARγ, most likely via upregulating IκB expression and inducing p65 degradation [87–89]. PPARγ belongs to the PPAR (PPARα, PPARβ/δ, and PPARγ) nuclear receptor family, which is a subfamily of TFs that require ligand binding for activation. The ligands of PPARs are fatty acids, especially PUFAs [90].

Cell cycle and cyclins

As mentioned, proliferation is a key feature of active endothelial cells and is required for angiogenesis. Cell proliferation, or cell cycle progression — a series of highly regulated events leading to cell division — to be more accurate, is driven by a superfamily of proteins called cyclins. Together with their catalytic partners, CDKs, a few subfamilies with defined features of cyclins govern cell cycle entry and progression, although there are more than 30 genes encoding products matching the traditional definition of cyclins [91]. In brief, external mitogens trigger the formation of cyclin D-CDK4/6 complexes making the cell enter G1 (Gap 1) phase from the quiescent state and progress through it; E-type cyclins (cyclin E1 and E2) mark the entry into S (Synthesis) phase and control DNA replication, while cyclin A (A1 and A2) is induced during the S phase and contributes to DNA replication and also modulates cell cycle progression through the G2 phase; the subsequent activation of cyclin B-CDK1 regulates

entry into M (Mitosis) phase [92–94]. There are many other cyclins involved in cell cycle regulation but they are less well-defined [93]. Apart from controlling cell cycle progression, cyclins also function in transcription control independent of CDKs, repairing DNA damage, and regulating cell death, cell differentiation, cell migration, and metabolism [92]. Deregulation of the cell cycle, mostly due to mutations and/or deregulation in cyclins and CDKs, is a characteristic of oncogenesis [95] and many other diseases.

Among all these cyclins, cyclin D (D1, D2, and D3) is worth special attention: they are the G1 mitogen sensors that link the external signals to cell cycle initiation and progression; they promote the expression and activation of other cell cycle proteins including cyclin E and cyclin A; they also have the most identified non-canonical functions mentioned above, especially for cyclin D1 [92,93]. Cyclin D1 is often deregulated in tumor cells and ranks second from the top in a list of overexpressed genes in solid cancers [96]. Cyclin D1 can also bind and modulate the transcriptional activity of some TFs like PPARs [97]. Its level is tightly regulated during the cell cycle: expression is largely induced by a few signaling cascades including the Ras/ERK and phosphatidylinositide-3-kinase (PI3K)/AKT pathways upon receiving mitogenic signals; during S phase, its degradation requires phosphorylation at Thr-286 [93,97]. Although the most common kinase for this site is glycogen synthase-3β, Thr-286 phosphorylation of cyclin D1 can also be catalyzed by p38 MAPK and ERK1/2 [98].

Epigenetics and transcription

As defined earlier, epigenetics involves multiple components and eventually leads to regulation of transcription, thus affecting cellular processes and even phenotypes of cells and individuals. A typical example of the power of epigenetic regulation is the immense range of different cell phenotypes in one's body, even though they are all derived from a single zygote. In the nucleus, DNA does not exist naked nor is it freely accessible for transcription into RNA including messenger RNA (mRNA) at all times. Rather, DNA is usually wrapped around histone core proteins to form chromatin that can be then condensed into chromosomes and packed into a tiny nucleus [99]. A core histone octamer consists of four types of histone proteins, H2A, H2B, H3, and H4, and all of them can carry various PTMs [100]. Together with DNA methylation, histone modifications play an important role in regulating chromatin structure and consequently gene accessibility [101]. If chromatin is less compact and less wrapped then DNA can be easily accessed by TFs and other pieces of the transcriptional machinery, and thus expression of the gene can occur. In contrast, condensed chromatin interferes with DNA-protein interactions, therefore inhibiting gene transcription. Acetylation

and phosphorylation of histones are generally considered as active marks, modifications that generally loosen chromatin structure and promote transcription [100–102], whereas DNA methylation is a repressive mark [100,101]. Methylation of histones can be either active (e.g. on H3 Lys-4) or repressive (e.g. on H3 Lys-9 and Lys-27) depending on the specific site modified. In most cases, when the chromatin is at an "open" state or in euchromatin to be accurate, active genes that can be transcribed require binding of TFs to their distal regulatory regions [103]. Those TFs will then recruit other co-factors, chromatin remodeling complexes (e.g. SWI/SNF), and histone modifying enzymes (e.g. CBP/p300 and histone deacetylases (HDACs)), which can further alter the histone marks and/or chromatin structure near the promoters of the genes [104]. Collaboratively, those factors will finally lead to faster and/or more binding, or activation of Pol II at the gene promoters for transcription initiation as well as elongation (transcription activation) [103,105], or downregulate the recruitment of Pol II to the promoters (transcription repression) [106]. Besides, histone marks and chromatin condensation are also important to DNA replication during cell cycle [107].

Epigenetic and transcriptional control of atherosclerosis

Emerging evidence indicates that epigenetic and transcriptional mechanisms play an important role in the pathogenesis of atherosclerosis, shedding light on potential therapeutic applications for drugs which target these epigenetic mechanisms [52]. As discussed below, many risk factors of atherosclerosis are linked with epigenetic modulations around the promoters of some key proteins in endothelial cells, such as eNOS, thus affecting the transcription of those genes. These epigenetic mechanisms may involve p38 MAPK and NF-κB signalling as well.

Intermittent hypoxia/reoxygenation (IHR) is a key contributor to the pathogenesis of atherosclerosis in people with obstructive sleep apnea (OSA). In children with OSA, their *NOS3* (the gene encodes eNOS) promoter area is DNA hypermethylated [108]. Hypoxia can also reduce overall H3 acetylation around the *NOS3* promoter area in endothelial cells and the SWI/SNF complex is believed to play a part in the epigenetic changes in this region [109]. In adult OSA, IHR has been found to increase p38 MAPK activity, and subsequently activate NF-κB and induce the expression of many pro-inflammatory genes [110]. Increased activation of NF-κB in an endothelial-specific PPARγ mutant mouse model revealed another player in the pathway. In this model, the loss of PPARγ activity, caused by mutation, accelerated AngII-induced development of ED [111]. A separate study demonstrated that PPARγ's transcription factor activity relies substantially on the activation of p38 MAPK via the free fatty acid (FFA)

receptor 1 (FFAR1), which then activates PPARγ coactivator 1α (PGC1α) to regulate the activity of PPARγ [112]. Phosphorylation of p300 by p38 MAPK may also be involved in regulating PPARγ activity. Intriguingly, p300 activation via p38 MAPK phosphorylation was reported in a different setting linked to NF-κB signalling. Specifically, in human astrocytes, activated p300 acetylates RelA at Lys-310. It has been reported that RelAK310Ac enhances the transcriptional ability of NF-κB but not its DNA-binding ability, thus leading to increased expression of inducible nitric oxide synthase (*iNOS*) [113]. This p38 MAPK/NF-κB/iNOS pathway does not engage other common phosphorylation activation sites of NF-κB such as RelA Ser-276 and Ser-536, and this differs from activation of the NF-κB signalling pathway described earlier.

Circulating oxLDL, a prevalent risk factor for atherosclerosis, can increase the repressive mark H3K9me3 on the eNOS promoter, while decreasing active marks, such as the overall acetylation status of H3 and H4, as well as H3K4me2 [114]. In the same study, it was also found that oxLDL can increase the level of ICAM-1 mRNA by recruiting RelA to the *ICAM1* promoter. In addition, oxLDL was found to enrich the active H3K4me3 mark on the promoter of some pro-inflammatory genes, such as tumor necrosis factor α (TNFα), MCP-1, interleukin-6 (IL-6), and IL-18 [115]. And eNOS uncoupling can be induced by exposure to oxLDL in HAEC, and downregulation of HDAC2 was involved in this process [116].

Another mentioned risk factor for ED and atherosclerosis is diabetes. It was found that transient exposure to high glucose can cause persistent elevation of RelA mRNA by increasing H3K4me1 levels on the *RELA* promoter in primary HAEC [117]. This led to prolonged escalation of VCAM-1 and MCP-1 mRNA levels even after the cells had been returned back to low glucose media for days. High glucose was also found to induce *EDN1* (the gene encodes ET-1) expression via p300 activation in endothelial cells [118]. Activation of p300 can acetylate histones, which are active marks as mentioned above. Indeed, increased H4 acetylation was found around the *EDN1* promoter at a few conserved NF-κB recognition sites after stimulation by the pro-inflammatory cytokines TNFα and interferon γ (IFNγ) [119]. This can be linked to impaired vasodilation during atherogenesis.

Flow induced pressure on vessel walls has a profound impact on vasculature health and hypertension is an important risk factor for atherosclerosis and other CVD. Laminar shear stress (LSS) is atheroprotective, while disturbed flow, due to impaired vasomotor tone and/or plaque formation, is detrimental [120]. Illi et al. [121] found that LSS can induce phosphorylation of H3 at Ser-10 and global acetylation at H3 as well as H4. These actions likely functioned through the p38 MAPK/MSK signalling pathway and promoted formation of

CREB/CBP complexes. They also found that c-Fos and c-Jun mRNAs were elevated by LSS via this mechanism [121]. Heterodimerization of c-Fos and c-Jun forms AP-1, an essential TF for *NOS3* transcription activation. LSS-induced AP-1 availability may be one of the origins for flow-mediated changes in gene expression in the endothelium. *NOS3* transcription was also induced by the deacetylase sirtuin 1 (SIRT1) via the TF foxhead box O1 (FOXO1) in EA.hy926 cells [122], while SIRT1 mRNA levels and its activity are affected by blood flow: LSS induces SIRT1 and disturbed flow decreases SIRT1 expression [123]. SIRT1 can also inhibit NF-κB signaling, through which it exerts its anti-oxidative and anti-inflammatory properties [124]. Oxidative stress in turn can downregulate SIRT1 activity, causing an increase in H4K16ac and decrease in FOXO3α/PGC1α complex formation, diminishing the expression of anti-oxidative genes [125,126]. SIRT1 also participates in arterial remodeling partially via its crosstalk with eNOS (reviewed in [123]). As one of the most important genes in endothelial cells, transcription of the *NOS3* gene is tightly controlled. Cell-type-specific patterns of histone modification in the promoter of *NOS3* have been detected. Endothelial cells have denser active histone marks, like H3K4me2/3, H3K9ac and H4K12ac, than VSMCs [127,128]. In non-endothelial cells, the transcription of *NOS3* is prohibited by DNA methylation of its promoter [128] and *NOS3* is made temporarily quiescent in vasculogenic progenitor cells by the H3K27me3 mark [129].

Non-coding RNA (ncRNA) is an emerging hot topic in epigenetic and transcriptional control. Depending on the nucleotide length, it can be roughly categorized into two main groups: long-non-coding RNA (lncRNA) and small non-coding RNA that comprises microRNA (miRNA) and small interfering RNA (siRNA). The roles and mechanisms of miRNA and lncRNA in atherosclerosis have been reviewed in [130] and [131], respectively. Plausible treatments using ncRNA have been suggested as well [132]. Unlike other players discussed above, little involvement of dietary components in relation to ncRNA in atherosclerosis has been demonstrated.

Nutrition, epigenetics, and transcription regulation

Fig. 1 illustrates the discussed epigenetic mechanisms in atherosclerosis. It is not hard to spot the possible influence of diet on some pathways. For example, resveratrol from red grapes is a well-known SIRT1 activator arising from the famous “French paradox” [133]. Also, PUFAs are potent ligands for PPARs, while serum oxLDL levels are greatly affected by diet, especially PUFA, due to their susceptibility to peroxidation [134,135]. All of these nutrients have been found to directly or indirectly affect epigenetics as discussed above.

Indeed, the fact epigenetics is dynamic and reversible in nature allows it to be responsive to environmental factors, and nutrition plays a large part here [136]. One well-known example is the relationship between folate and DNA methylation [137]. Folate-deficiency resulting in DNA hypomethylation might be one of the causes of neural tube defects in newborns [138]. It has been recognized that maternal and early life nutrition can alter the epigenome which can lead to plausible phenotypic changes [136], profound impacts on health status later in life [136,139–141], and potential transgenerational inheritance [139–142]. There are a few ways nutrients can affect epigenetics:

- modulate TF activity directly (as ligands for nuclear factors such as PUFA and PPARs [90,143]) or indirectly via cell signaling as partially shown in Fig. 1;
- serve as sources for epigenetic modifiers, for example:
    - glucose for histone glycation [144];
    - folate, vitamin B12, choline, and methionine involved in one-carbon metabolism as methyl-donors for histone and DNA methylation [145];
    - acetyl-CoA from glycolysis or fatty acid β-oxidation as the main donor for histone acetylation [146];
- regulate the activity of chromatin modifying enzymes, for instance:
    - DHA [147] and sulforaphane from cruciferous vegetables [148] can function as HDAC inhibitors;
    - resveratrol can activate SIRT1 [133] as mentioned above.

The importance of epigenetics in the pathophysiology of many diseases, including atherosclerosis, and the interaction with nutrition has been well acknowledged [149–152]. Nutrients and bioactive compounds in the diet can regulate expression of key genes via epigenetic modifications. These changes in gene expression can then alter key metabolic pathways that eventually result in disease phenotypes and/or traits [149–152]. For example, overfeeding human subjects with PUFA or saturated fatty acids was found to differentially affect the degree of DNA methylation on different gene promoters as well as different transcript levels in adipose tissue, and these differences might be related to the differential lipid profile responses in the two diet groups [153]. Also, circulating n3 PUFAs were found to alter DNA methylation status on the promoters of *APOE* (encoding apolipoprotein E), *ABCA1* (encoding ATP-binding cassette A1), and *IL6*, genes important in lipid metabolism or inflammation and strongly correlated to CVD [154]. In addition, certain bioactive compounds in the diet may have therapeutic potential for certain diseases via epigenetic mechanisms, such as those

functioning as HDAC inhibitors may prevent atherosclerosis progression [155,156]. Epigenetics can act as a bridge between external signals, especially nutritional ones, and intracellular transcriptional regulation. These differences in gene expression can then program our body differently in response to different diets.

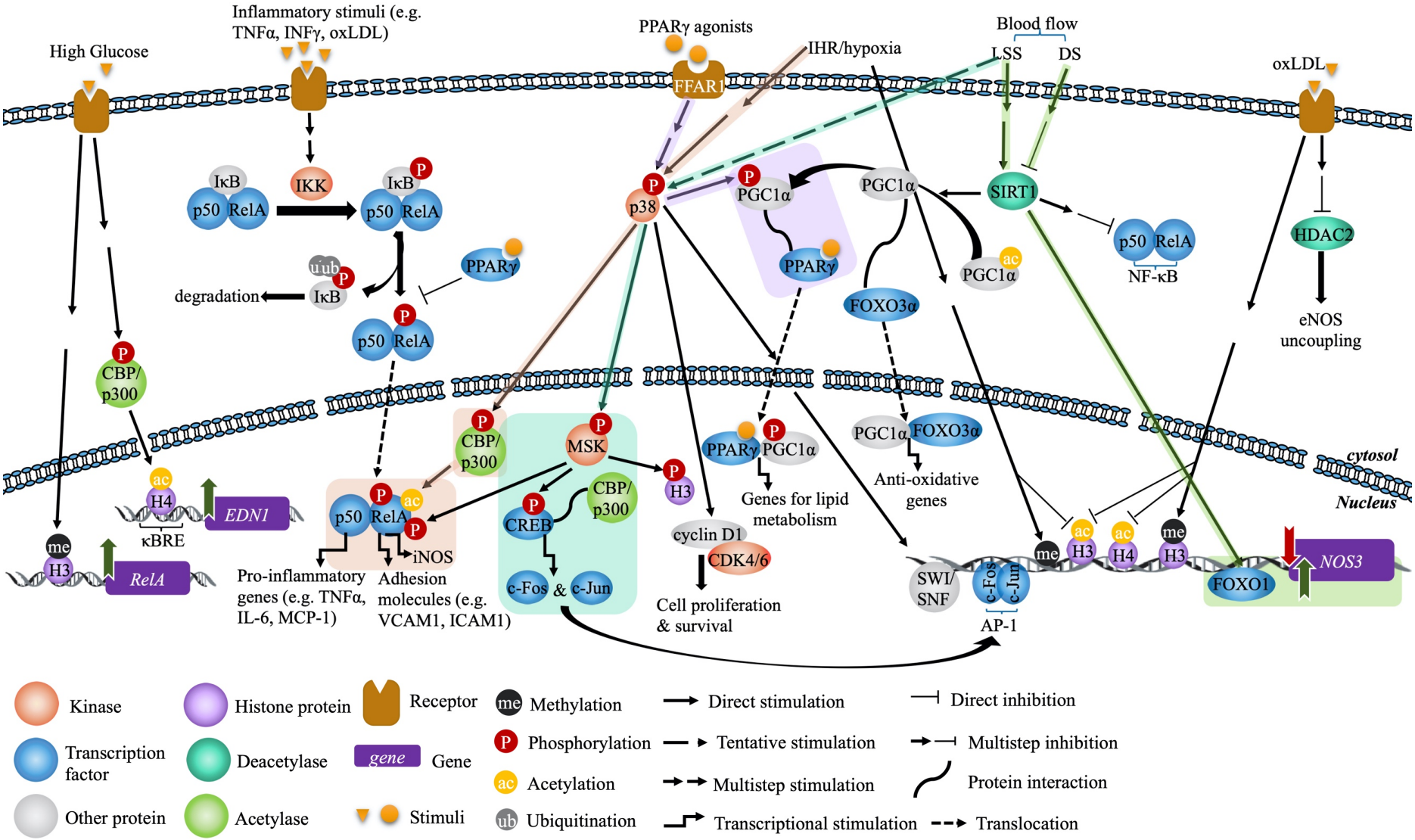
High Glucose
Inflammatory stimuli (e.g. TNFα, INFγ, oxLDL)
PPARγ agonists
IHR/hypoxia
Blood flow
LSS
DS
oxLDL
FFAR1
IKK
IκB
p50 RelA
degradation
PPARγ
p38
PGC1α
SIRT1
HDAC2
NF-κB
eNOS uncoupling
FOXO3α
CBP/ p300
MSK
cytosol
Nucleus
κBRE
EDN1
RelA
iNOS
Pro-inflammatory genes (e.g. TNFα, IL-6, MCP-1)
Adhesion molecules (e.g. VCAM1, ICAM1)
CREB
c-Fos & c-Jun
cyclin D1
CDK4/6
Cell proliferation & survival
Genes for lipid metabolism
Anti-oxidative genes
SWI/ SNF
AP-1
NOS3
FOXO1
Kinase
Transcription factor
Other protein
Histone protein
Deactylase
Acetylase
Receptor
Gene
Stimuli
Methylation
Phosphorylation
Acetylation
Ubiquitination
Direct stimulation
Tentative stimulation
Multistep stimulation
Transcriptional stimulation
Translocation
Direct inhibition
Multistep inhibition
Protein interaction

Figure 1. Possible epigenetic and transcriptional mechanisms active in endothelial cells and associated with atherogenic processes.

This schematic was customized to show the various inter-relationships described in the Literature Review that are relevant to the topic of the thesis. Different colored shading distinguishes specific signaling pathways. Green upwards arrows on genes indicate higher expression, while the red arrows indicate lower expression. H3 methylation on the *NOS3* promoter region is at Lys-9 position, a repressive marker, while methylation of *RELA* is at Lys-4 is an activation marker. This custom-designed figure was prepared by S. Huang using Microsoft PowerPoint software.

Omega-3 fatty acids

N3 PUFAs are characterized by the presence of the first double bond from the methyl end at the third carbon atom. There are 3 main n3 PUFAs in our diet: ALA (C18:3n3), EPA (C20:5n3) and DHA (C22:6n3). ALA is an essential fatty acid because the human body cannot synthesize it and we must acquire it from food to maintain normal functioning and health [157], while EPA and DHA can be synthesized in our body via elongation and desaturation from the precursor ALA. Due to the relatively low conversion rates [158,159], however, dietary intake of EPA and DHA is still recommended in most cases [160]. This is especially true for DHA, since its conversion rate from dietary ALA can be lower than 0.1% [161]. Canola and flaxseed oils as well as chia seeds are rich in ALA, while EPA and DHA are typically found in marine sources, such as deep-ocean fish.

In foods and supplements, there are 4 main structures into which n3 PUFA are incorporated: triglycerides (TGs), phospholipids, FFAs, and ethyl esters. The bioavailability data found in the literature for each n3 PUFA have been summarized [162], with FFAs and TGs appearing to be more bioavailable than ethyl esters. To make n3 PUFA bioavailable from diet, digestion of those esterified lipids begins in mouth with lingual lipase and phospholipase. Then fat droplets enter stomach and some TGs inside are partially broken down by gastric lipase into diacylglycerides (DAGs) and FFAs. The mechanical movement of stomach helps to disperse fats and form emulsions of TGs + DAGs + FFAs + other lipids. Even though some lipid digestion occurs in the mouth and stomach, the majority of fat digestion happens in the intestinal tract through the combined action of bile salts and pancreatic lipase. The resulting FFAs and monoacylglycerides (MAGs) can then be absorbed into enterocytes. The esterification position of n3 PUFAs in TGs also affects their absorption: FFAs cleaved from sn-1 and sn-3 positions of a TG can only be absorbed via a specific transporter, while the resulting 2-MAGs, together with the FA attached to it, can go into enterocytes via simple passive diffusion. Inside the intestinal cells, 2-MAGs will be re-esterified with FFAs to TGs that are packaged with cholesterol, phospholipids, and other lipids into chylomicrons before being extruded into the lymph and subsequently entering the bloodstream at the thoracic duct. In the bloodstream, TGs in chylomicrons will be hydrolyzed by lipoprotein lipases (LPL) attached to the surface of the endothelium, resulting in chylomicron remnants containing less TG. The FAs released by LPL enter tissues (especially muscle and adipose).

Similar to other lipids, n3 PUFAs circulate in blood postprandially in chylomicrons, and in the post-absorptive and fasting states, either as FFAs (released from stored TGs via

hormone-sensitive lipase) and bound to plasma albumin or in other lipoproteins. While chylomicron remnants deliver dietary lipids to the liver, very low density lipoproteins (VLDLs) transport the lipids from the liver to bloodstream for uptake of fatty acids into tissues and cells for storage and/or metabolism. LDLs are formed from VLDLs during this process with the aid of LPL as well, and LDL can be taken up by many tissues, including the liver, via the LDL receptor (LDLR). High density lipoproteins (HDLs), on the other hand, transport lipids (especially cholesterol) from cells to the liver for disposal.

The endothelium has a critical function in the lipid exchange process between lipoproteins in the blood and surrounding tissues and cells. Apart from containing different types of receptors (such as LDLR, scavenger receptors, and ATP-binding cassette transporter G1) to aid the transportation of various lipoproteins across endothelial cells, LPL and endothelial lipases on the plasma membrane of endothelial cells hydrolyze lipids from TG in lipoproteins and release FFAs for uptake by endothelial cells [163,164]. Compared to n3 PUFAs inside lipoproteins, those in the form of FFAs or non-esterified FAs (NEFA) make up a relatively small portion of total plasma n3 PUFA (~ 1.6% to 13.8% depending on age cohorts) in fasting samples [165]. Also, plasma FFA levels are believed to be positively associated with ED and CVD risk [166–168].

Health benefits of n3 PUFAs have been reported for many diseases especially CVD [162], partially attributed to their anti-oxidant and anti-inflammatory properties as reviewed in [169–171]. The first report associating n3 PUFA from fish consumption with beneficial effects against CVD was made in the 1970s in a Greenland Inuit population [172]. Since then, several observational and epidemiological studies have drawn the same conclusion [173–177], supporting the cardioprotective effects of n3 PUFA. More evidence from human trials and animal models has strengthened the link [176,178–184]. Therapeutic use of EPA and DHA (2-4 g/day) has been recommended by the American Heart Association since 2002 for lowering triglycerides in hypertriglyceridemia patients; subsequently the US Food and Drug Administration has approved prescriptions of EPA and DHA for the same purpose [185]. Yet, 2 recent clinical trials using high purity therapeutic doses of n3 PUFA in statin-treated patients obtained different results. These two trials are also so far the only 2 large-scale (large study population size and long follow-up period) randomized clinical trials using such a high dose of highly purified n3 PUFAs. The Reduction of Cardiovascular Events with Icosapent Ethyl–Intervention Trial (REDUCE-IT) gave 4 g/day icosapent ethyl (pure EPA ethyl ester) to dyslipidemia patients already on statin with a median follow-up period of 4.9 years, and showed a significant reduction in both primary (a combination of death from CVD, nonfatal

myocardial infarction (MI), nonfatal stroke, coronary revascularization, or hospitalization for unstable angina) and secondary (a composite of CVD death, nonfatal stroke, or nonfatal MI) endpoints for the EPA group compared to the placebo group [186], consistent with other EPA-only trials [187]. The Statin Residual Risk Reduction With Epanova in High CV Risk Patients With Hypertriglyceridemia (STRENGTH) trial, however, was terminated prematurely (maximum follow-up of 5 years) due to low prospect of any beneficial effect in the treatment group [188]. The 4 g/day omega-3 carboxylic acids (EPA+DHA FFA, Epanova) did not exhibit superior performance compared to the corn oil control in terms of reducing either primary or secondary endpoint events (the same as in REDUCE-IT) or additional secondary endpoint events (CVD death with or without other events such as nonfatal MI or stroke) [189]. Actually in 2015, the National Lipid Association in the US already warned against the use of DHA-containing long-chain n3 PUFA for TG lowering, since it may elevate LDL-C in patients with extremely high TG [190]. Those contradictory recommendations and divergent outcomes in clinical trials with EPA only or EPA+DHA make us wonder why the inclusion of DHA may possibly interfere with the beneficial effects observed for EPA on statin-treated patients while other evidence, especially those from observational and epidemiologic studies, supports the beneficial role of DHA on CVD. However, it may be noteworthy that no trial to date has examined the effect of a high DHA/low EPA formulation.

DHA

DHA is mainly found in marine fish, particularly deep-water ones like sardines, salmon, tuna, mackerel, and herring, which consume certain DHA-synthesizing marine microalgae [162]. In all these sources, DHA almost always exists with EPA. According to the Food Surveys Research Group in the US, the average dietary intake of DHA in Americans is 0.05 g/day, and is slightly higher in adults than in minors [191]. This intake amount has not changed for nearly 2 decades and is well below the recommendation of 250 mg/day EPA plus DHA by the 2015-2020 Dietary Guidelines for Americans [192] and many other authoritative bodies and scientific organizations in different regions and countries [160] such as the European Food Safety Authority [193]. Another study estimated DHA intake in 175 countries based on the food balance sheets from the Food and Agriculture Organization of the United Nations, and found that the estimated median intake may range from 47 mg/day to 192 mg/day, and these intakes are directly related to the income levels of the countries [194]. For pregnant and lactating women as well as young children, there are additional recommendations for just DHA intake [160,194]. Although recommendations for the long chain n3 PUFAs vary among

different organizations and different subpopulations, they usually do not fall below 250 mg /day for the general adult population [160,195]. To meet the dietary recommendations, omega-3 supplements can be taken. Supplements usually contain around 1000 mg n3 PUFA of fish oil per capsule with about 300 mg DHA, while high DHA (more than 500 mg) low EPA supplements are also available commercially. Contaminants like mercury that usually bio-magnify in seafoods have not been found in supplements yet thanks to current processing and purification methods [157] as well as regulations regarding monitoring for heavy metal contaminants. Interestingly, different types of n3 PUFA supplements can differentially affect the plasma n3 PUFA levels: DHA-only supplements were found to increase both plasma EPA and DHA levels [196–200], while EPA-only supplements elevated plasma EPA levels but not DHA levels [196,197,200]. Neither plasma EPA nor DHA levels showed an obvious rise with ALA-only supplementation [198,199], consistent with the low conversion rate. In generally healthy adults, plasma DHA content can vary from 7.2 μM to 237.5 μM [165,201], while after supplementation, plasma DHA levels can surge up to 588 μM (in obese females) [199].

The dietary intake recommendations for DHA in certain subpopulations should be accredited to its important role for functioning of the brain and retina. In our body, DHA is mainly found in the phospholipids of cell membranes, particularly in the brain and retina, and contributes greatly to membrane fluidity and certain cell signaling process. The accumulation of DHA in the brain starts during mid-to-late pregnancy until age 2 [202]. As a major structural constituent of the plasma membranes in the human central nervous system, DHA also participates in neural cell survival, functioning, and signal transmission [203]. Therefore, DHA offers protection against cognitive decline [204] and may improve cognitive function under certain circumstances [205,206]. In addition, DHA levels in the brain were found to be lower in patients with depression [207,208]. Together with EPA, DHA is essential for retinal health, especially in the prevention of age-related macular degeneration [209,210]. Also, DHA may play a role in skeletal muscle synthesis, metabolic syndrome, and cystic fibrosis [211–215]. Apart from the possible benefits in CVD as discussed and going to be discussed in more detail, DHA, as well as EPA, may act as a blood thinner and cautions should be taken when administrating it together with other anti-coagulants [169,216].

DHA and atherosclerosis

To date, most of clinical trials have focused on the effects of overall n3 PUFA or EPA+DHA as mentioned above (summarized in [185]). Despite the discouraging results from the STRENGTH trial, several recent meta-analyses [217–219], including a Cochrane review

[220], still demonstrated strong evidence of EPA+DHA's protective effects against adverse CVD outcomes, even when taking the STRENGTH trial into consideration [218,219]. Again, the idea that EPA-only is more effective in this context is supported by some [218,221], most likely due to the great success of the REDUCE-IT trial, while others think more evidence is needed to draw a conclusion since the range and absolute amount of DHA doses used across the EPA+DHA studies are relatively small [217]. Clinical trials with more concentrated or even purified DHA at larger dosages may be needed to further address the debate.

When searching for clinical trials focusing on DHA, only a handful are available as listed in Table 1, let alone those with purified DHA. Most of these trials are double-blind, randomized, and placebo-controlled with some using a crossover design, and can be considered as relatively high-quality evidence. However, they are not as large-scale as REDUCE-IT or STRENGTH, and only followed the participants for less than half a year. The effects of DHA on endothelial function were inconclusive due to the contradictory FMD results obtained in different studies [222–224]. In some other aspects of vascular health, DHA performed, if not better than, at least equally to EPA for decreasing blood pressure [225], being anti-thrombotic [222], and reducing inflammation [226,227]. In terms of effects on lipid and lipoprotein profiles, DHA consistently lowered TGs [197,224,228,229], even more than EPA in some cases [196,227]. The only study showing no change in TGs after intervention already had high n3 PUFA content in the background diet [223]. Compared to EPA, DHA also consistently raised the levels of HDL-cholesterol (HDL-C), the "good cholesterol" [196,223,224,227], and HDL_2-C, a sub-class of HDL also inversely associated with CVD risk [197,228]. These results agree with another clinical study using different mixture of oils to create varying compositions of n3, n6, and n9 PUFA: only the DHA-rich canola oil group increased HDL-C after the intervention and had greatest decline in TGs among all other 4 groups [230]. Although DHA also increased the "bad cholesterol", LDL-C [196,197,223,224,227–229], as mentioned earlier, it did not significantly change apoprotein B (ApoB, the main protein found on LDL) levels compared to EPA [196,227]. The ApoB level can be regarded as a superior indicator for CVD risk compared to LDL-C [231], and no difference was observed in this parameter between DHA and EPA interventions in other studies as well [185,217]. This may indicate that instead of an increase in number, the LDL particles may be shifted to a larger size in the DHA group, and larger LDL is believed to be less atherogenic [217,232]. Indeed, the increase in LDL particle size was reported in those trials as well [197,229,233,234]. Therefore, the controversies around DHA's beneficial effects on CVD still skew strongly toward the positive side.

Some discrepancies in the results can be explained by other confounding factors and differences in study designs. While most recent meta-analyses and systemic reviews support the positive association between n3 PUFA (including DHA) and cardiovascular protection as mentioned above, some early meta-analyses concluded there was no significant association [235,236]. All studies included in these 2 meta-analyses used EPA and/or DHA up to 1.8 g/day, considerably lower than the 3 to 4 g/day dosage used in the studies shown in Table 1. Indeed, dosage is one important factor affecting the final outcome of a clinical trial, as pointed out by Casula et al. [221]. The effective dose of DHA for various conditions, however, remains largely debatable. And unlike EPA, currently there is no prescription formulation that is DHA-only. Thus, understanding the mechanisms of action of DHA's cardioprotective effects becomes important and fundamental for resolving these controversies.

Table 1. **List of randomized clinical trials investigating the effects of DHA, instead of combinations of n3 PUFA, on CVD (in chronological order).**[1]

Treatment	Dosage	Duration	Outcomes	Subjects	Ref
DHA or EPA or Placebo (corn oil)	~4 g/day each, highly purified[2]	7 wks	Only DHA increased HDL-C and the DHA group had a greater reduction in TG. Only EPA decreased TC.	224 healthy nonsmoking men	[196]
DHA or EPA or Placebo (olive oil)	~4 g/day each, highly purified[2]	6 wks	Only DHA decreased ambulatory BP and HR; increased LDL-C & LDL particle size, HDL_2-C, FBF, and dilator responses; & attenuated constrictor responses. Both EPA and DHA decreased TG but had no effect on TC.	56 overweight & mildly hyperlipidemic men	[197,225, 237]
DHA or EPA or Placebo (olive oil)	~4 g/day each, highly purified[2]	6 wks	No change in glycemic parameters (fasting insulin, glycated hemoglobin etc.) or FMD. DHA group had a greater increase in HDL_2-C. Only DHA increased LDL particle size, decreased collagen aggregation and collagen-stimulated thromboxane release.	Hypertensive and type 2 diabetes: 39 men & 12 postmenopausal women	[222,228, 233]
NCEP-II diet with DHA or Placebo (corn oil)	6 g/day n3 PUFA in the diet + 1.2 g/day DHA or corn oil	6 wks each, crossover	DHA supplementation increased FMD and TG was unchanged; DHA supplementation increased LDL-C & HDL-C. No change in biomarkers for oxidative stress & inflammation.	20 hyperlipidemic & hypercholesterolemic children	[223]

DHA oil from microalgae or Placebo (olive oil)	7.5 g/day (contains 3 g/day DHA)	90 days	DHA decreased TG, large VLDL, IDL and VLDL size. DHA increased concentrations of LDL-C, small VLDL, large LDL and LDL particle size. DHA decreased RLP-C and inflammatory markers (IL-6 & CRP), and increased the RBC n-3 index and anti-inflammatory MMP2.	34 hypertriglyceridemic men	[226,229, 238]
DHA in carrier oil or Placebo (olive oil)	4 g/day (contains 1.6 g/day DHA)	16 wks	DHA group had lower FMD, TG, VLDL, and a trend for higher LDL-C ($p = 0.06$) and HDL-C ($p = 0.08$).	328 healthy younger adults (<40 years old)	[224]
EPA or DHA or Placebo (corn oil)	~3 g/day each, highly purified[2]	10 wks each, crossover	DHA had greater effects than EPA on: decreased IL-18, TG, & TC:HDL-C ratio; and increased adiponectin, HDL-C, LDL-C, LDL particle size, & both the catabolic rate and production rate of the LDL ApoB100 fraction. Both DHA & EPA decreased CRP, IL-6, and TNFα.	Otherwise healthy men (48) and women (106) with abdominal obesity & mild inflammation	[227,234]

[1]Abbreviations: BP: blood pressure, HR: heart rate, FBF: forearm blood flow, TG: triglyceride, TC: total cholesterol, FMD: flow-mediated dilation, LDL: low density lipoprotein, HDL: high density lipoprotein, NCEP-II: National cholesterol education program II, VLDL: very low-density lipoprotein, IDL: intermediate density lipoprotein, RLP: remnant-like particle, IL: interleukin, CRP: C-reactive protein, RBC: red blood cell, MMP: matrix metalloproteinase, ApoB100: apolipoprotein B100, TNFα: tumor necrosis factor-α.

[2] Capsules used in those trials contained highly purified (>90%) preparations of EPA or DHA.

Mechanisms for the anti-atherogenic effects of DHA

As an important bioactive molecule, DHA is able to bind various cell surface receptors and trigger signaling cascades, or bind intracellular nuclear receptors like PPARs, to regulate gene expression [165]. This DHA-modulated signaling may eventually lead to alterations in key metabolic pathways in our body. Fig. 2 summarizes the possible atheroprotective pathways through which DHA may operate in the three main cell types that are central to atherogenesis.

In endothelial cells, as illustrated in Fig. 1, pro-inflammatory stimuli such TNFα are able to induce NF-κB signaling which leads to increased expression of its target genes, such as *VCAM1* and *ICAM1*. Wang et al. [239] demonstrated in HAEC that DHA was able to attenuate those TNFα-induced adverse effects. To be specific, DHA inhibited TNFα-stimulated NF-κB signaling by downregulating the subsequent nuclear translocation of NF-κB via suppression of IKK and IκB phosphorylation. Translocation of TNFα-activated AP-1 was blocked by DHA as well. Moreover, DHA also decreased the protein levels of both NF-κB and AP-1 in response to TNFα treatment. All these changes led to less VCAM-1 and ICAM-1 expressed in DHA-treated HAEC and reduced monocyte adhesion to the endothelial cells. In another human endothelial cell line, DHA was found to reverse the TNFα-dependent downregulation of *NOS3* expression [240]. This may be related to the TNFα-induced expression of *MAPK14* (the gene encoding p38α MAPK) [240], since p38α MAPK can inhibit *NOS3* promoter activity [241]. In addition, DHA was able to attenuate oxLDL-enhanced monocyte adhesion to endothelial cells, which can be largely attributed to NF-κB signaling as well [242]. As a ligand for PPAR activation, DHA can inhibit NF-κB activation via PPARs [243,244]. Also, DHA was found to inhibit ERK1/2 activation via FFA receptor 4 (FFAR4) [245], while ERK1/2 is upstream of NF-κB. The relation of endothelial NF-κB signaling and atherosclerosis is deliberate as demonstrated *in vivo* by Gareus et al [246] who showed that mice with endothelial-specific abolition of NF-κB signaling developed fewer atherosclerotic lesions. Since the NF-κB pathway is positively linked to atherosclerosis and can be inhibited by DHA, p38 MAPK, an upstream activator of NF-κB, should be inhibited by DHA as well. Intriguingly, however, early activation of p38 and ERK1/2 by DHA has been observed from 5 to 30 min after DHA treatment [6,247]. In addition, a second peak of p38 activation occurred 4 to 8 hours after DHA treatment in growing endothelial cells, but not in confluent quiescent cells [6]. As stimulation of FFAR1 can activate p38 MAPK [112], the activation of p38 MAPK by DHA may be partially mediated through FFAR1.

Macrophages are a key cell type contributing to the inflammatory response and atherosclerosis progression. There are two main phenotypes of macrophages: the M1 macrophages that are classically activated and are pro-inflammatory and atherogenic, and the M2 macrophages that are alternatively activated and are anti-inflammatory and atheroprotective [248]. DHA exerted its anti-inflammatory effects in macrophages by inhibiting LPS-activated MAPK/NF-κB signaling and the expression of several pro-inflammatory proteins, such as TNFα, IL-6, IL-1β, and iNOS [249,250]. Besides suppressing those M1 markers, DHA also upregulated the expression of IL-10 and transforming growth factor β (TGFβ) which favor M2 polarization, and as a result, potentiated macrophage efferocytosis—the removal of apoptotic cells by macrophages [250]. Enhanced efferocytosis by increased M2 polarization is critical in plaque regression [248]. PPARγ is required in the DHA-induced M2 polarization process but not in DHA's suppression of M1 polarization and/or the expression of those pro-inflammatory proteins [250]. DHA was also found to inhibit TNFα-induced expression of the Lectin-like oxLDL receptor-1 (LOX-1) and NADPH oxidase 2 (NOX2) via PI3K in a human macrophage cell line, leading to reduced uptake of acLDL and less production of ROS [251]. LOX-1 is a critical transmembrane receptor for modified LDL. OxLDL is the most potent ligand for LOX-1 and it triggers a vicious cycle among oxLDL, LOX-1 and NF-κB, which can finally result in foam cell formation through NF-κB-induced inflammation and increased oxLDL update by macrophages [252]. LOX-1 is also expressed in endothelial cells and VSMC, contributing to ED and formation of foam cells, respectively. In endothelial cells, LOX-1 was found to activate RhoA thus inhibiting eNOS, promoting monocyte attachment via adhesive molecule production, and inducing apoptosis via ERK1/2 and p38 MAPK signaling [252].

Apart from its anti-inflammatory effects, DHA can inhibit VEGF-induced activation of ERK1/2/eNOS signaling in HUVEC and prevent subsequent cell migration, probably via FFAR4 [253]. NO production by eNOS was found to be elevated by DHA in another study, concentration-dependently via induction of SIRT1 expression [254]. DHA-induced SIRT1 expression was found to affect both the mRNA and protein levels in a concentration- and time-dependent manner. And DHA may act through SIRT1 to deacetylate eNOS at its CaM-binding domain, hence increasing eNOS activity [254]. DHA was also able to attenuate palmitic-acid-induced apoptosis and intracellular lipid droplet accumulation in endothelial cells [255]. These ameliorative effects of DHA are likely due to its transcriptional modulation of different genes. For example, pro-inflammatory and pro-apoptotic genes were inhibited by DHA treatment,

while anti-apoptotic genes were activated, together with genes in lipid metabolism like *APOA1* (encoding apolipoprotein A1) and *LPL* [255].

Heme oxygenase-1 (HO-1, gene name: *HMOX1*) is another key player in DHA's atheroprotective actions. HO-1 is an inducible isoform of HO, controlling the rate-limiting step of heme degradation, and is only expressed in high amounts as a cyto-protection mechanism when stimulated by pathological stress [256]. HO-1 plays an important role in preventing atherosclerosis and related CVD via its anti-inflammatory and anti-oxidative properties [257]. *HMOX1* transcription requires binding of AP-1, NF-κB, and most importantly nuclear factor erythroid 2-related factor 2 (NRF2, a TF regulating the expression of anti-oxidative genes) to its proximal promoter region [256]. DHA was found to induce *HMOX1* expression in a ROS-dependent manner via NRF2 in both EC [258] and VSMC [259]. In EA.hy926 cells, DHA-stimulated phosphorylation of PI3K/AKT, p38 MAPK, and ERK1/2 may induce NRF2 translocation for *HMOX1* transcription activation [258]. The upregulation of HO-1 inhibited the TNFα-stimulated NF-κB activity leading to less *ICAM1* transcription and subsequent reduced immune cell adhesion to EC [258], and attenuated oxidative stress and apoptosis in VSMC [259].

Moreover, in human aortic SMC, DHA can decrease INFγ-induced oxLDL uptake by downregulating the expression of a specific chemokine, C-X-C motif ligand 16 (CXCL16) [260]. TF signal transducer and activator of transcription 1 (STAT1) may be involved in this downregulation of INFγ-induced CXCL16 expression: INFγ usually activates STAT1 by phosphorylation and DHA was able to decrease STAT1 phosphorylation in the experiment [260]. Also, DHA can prevent the stimulation of rat SMC proliferation by reducing cyclin D1 expression via inhibition of ERK1/2-dependent expression of early growth response factor-1 (EGR-1, a TF involved in mitogenesis and cell differentiation) [261].

While DHA was found to regulate the transcriptional activities of many TFs in relation to its athero-protective effect as discussed above, the effect of DHA on other epigenetic components, such as histone and chromatin modulation, has not been studied extensively in the context of atherosclerosis yet.

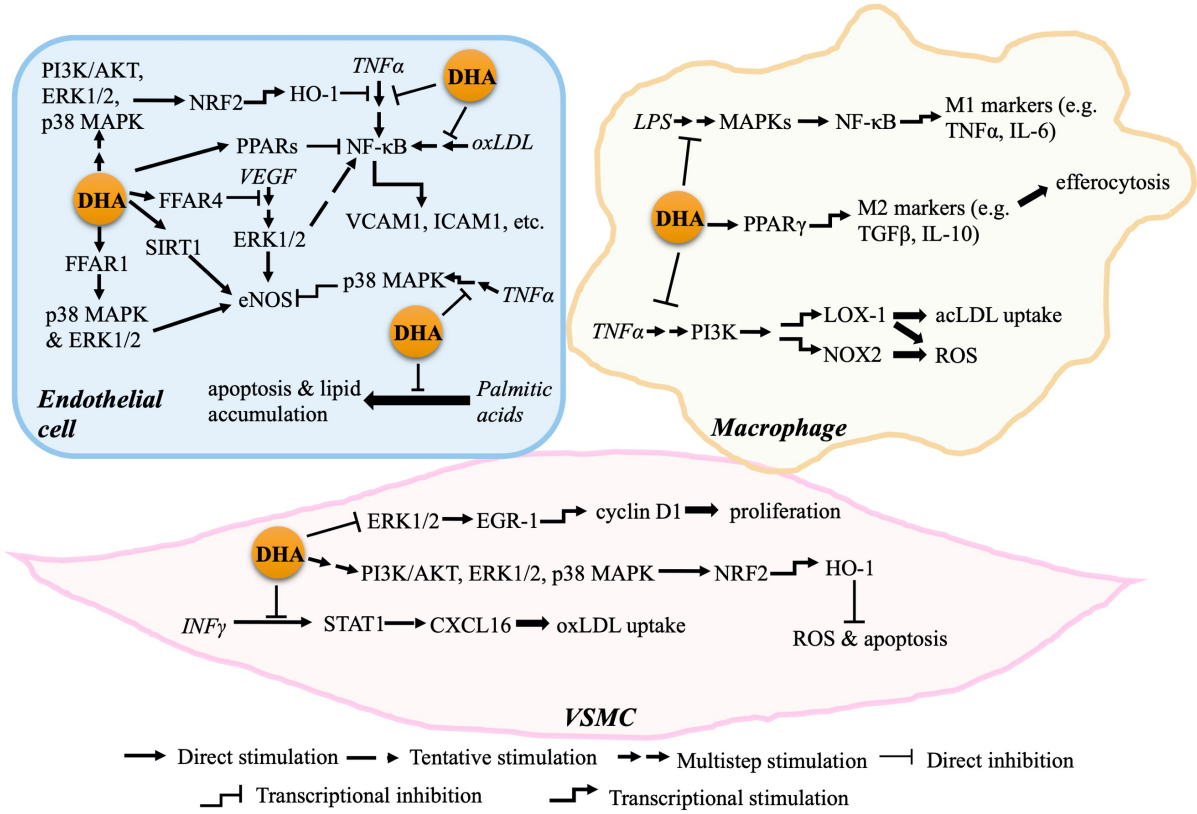

Figure 2. Possible pathways in the 3 major cell types through which DHA may exert its atheroprotective effects.

This schematic was customized to show the various potential anti-atherogenic mechanisms that DHA can mediate as described in this section of the Literature Review. This custom-designed figure was prepared by S. Huang using Microsoft PowerPoint software.

STUDY RATIONALE

Endothelial cells are crucial for vasculature health, and dysfunction of endothelial cells predestines the onset of atherosclerosis [26]. Atherosclerosis can be viewed as an epigenetic disease with multi-tier epigenetic and transcriptional regulatory mechanisms influencing its progression [52,53]. And these systems can be heavily modulated by dietary factors including DHA. Although generally recognized as anti-atherogenic, DHA supplementation together with EPA showed limited health benefits in CVD management in some randomized clinical trials compared to pure EPA therapy [186,187,189]. The solution to these controversies around DHA as an aid for prevention and management of atherosclerosis may lie in better understanding its mechanisms of action. Previous investigations of the epigenetic and transcriptional controls of atherosclerosis revealed several important players including MAPKs and NF-κB [61,110,246]. Furthermore, NF-κB can be activated by the MAPK/MSK pathway [262]. DHA is known to repress stimulus-induced NF-κB activity [239,242]. For the activation of MAPKs, however, DHA has contradictory effects [245,247], especially for p38 MAPK where DHA's effects are growth-state-, concentration-, and time-dependent in EA.hy926 cells [6]. The differential activation pattern of p38 MAPK by DHA may be the clue to DHA's anti-atherogenic effects in endothelial cells along with the NF-κB signaling axis. The link between p38 MAPK and NF-κB signalling pathways upon DHA stimulation, however, has not been validated or studied in detail. In addition, few studies have investigated the epigenetic effects of DHA in endothelial cells to determine how they might contribute to the atheroprotective effects of DHA.

HYPOTHESIS

The overarching hypothesis, as the title suggests, is that DHA exerts its anti-atherogenic effects via epigenetic and transcriptional mechanisms. Specifically, it is hypothesized that DHA acts through p38 MAPK/NF-κB signalling to promote an atheroprotective state in endothelial cells. Additionally, it is hypothesized that the beneficial effects of DHA involve modification of RelA and modulation of other TF and/or histone marks along the p38 MAPK/MSK/NF-κB signalling axis, such as CREB and histone H3.

OBJECTIVES

1. To validate the link between p38 MAPK/NF-κB signalling in response to DHA *in vitro* in different endothelial cell growth states using EA.hy926 cells as the model;
2. To assess the effects of DHA on eNOS and cell cycling under different endothelial growth states, and determine whether p38 MAPK/NF-κB signaling is involved in the responses;
3. To determine whether DHA can modulate CREB activity and histone H3 modification via p38 MAPK/MSK signalling.

MATERIAL AND METHODS

Cell culture

EA.hy926 endothelial cells (ATCC, CRL 2922) were cultured in Dulbecco's modified Eagles' medium (DMEM, Gibco, #12100046) supplemented with 20 mM 4-(2-hydroxyethyl)-1-piperazineethanesulfonic acid (HEPES, Millipore, #391340), 100 units/mL penicillin/streptomycin (Gibco, #15140163), and 10% fetal bovine serum (FBS, Hyclone, #SH30071). The cells were incubated at 37 ºC in a humidified 5% CO_2 atmosphere, and were sub-cultured once ~80% confluency was reached. Only cells within passage 20 were used for subsequent treatments.

To obtain quiescent cells, EA.hy926 endothelial cells must be cultured on MG-coated dishes and plates [5]. Growth factor reduced MG (Corning®, #356231) was diluted in cold serum-free DMEM before adding onto pre-chilled well-plates at a concentration of ~99.3 μg/cm^2. A total of 2 mL DMEM+MG mixture for 12-well plates or 3 mL for 6-well plates was added into each well gently and then allowed to set at room temperature for at least 1 h. Then, the media was removed and the wells were washed twice with serum-free DMEM before cell seeding at 9000 cells/cm^2. Taking the seeding day as day 0, the cells would reach confluency at day 8 and become quiescent at day 10 according to previous findings in our lab [5].

Cell treatment

For DHA and inhibitor treatment, sub-confluent cells at day 4 were used as growing cells, while cells at day 10 were quiescent cells as mentioned. DHA (Cayman, #90310) was first diluted 10-fold with ethanol, then bound to 5% fatty-acid-free bovine serum albumin (BSA, Roche, #10775835001) dissolved in phosphate-buffered saline (PBS) with another 10-fold dilution. Then this BSA-bound DHA was added directly into each well at the indicated concentrations. Ten-fold diluted 5% BSA-PBS in ethanol was used as a vehicle control (VC) and the volume added to the cells matched to the highest concentration of DHA of that particular set. p38α/β MAPK-specific inhibitor SB202190 (Tocris, #1264), MSK inhibitor SB747651A (Tocris, #4630), and CREB-CBP interaction inhibitor (CCII, Calbiochem. #217505), if used, were dissolved in dimethyl sulfoxide (DMSO) as a 1000× concentrated stock solution and added 30 min prior to DHA treatment at final concentrations of 1 μM [263], 5 μM [264], and 20 μM [265], respectively. An appropriate volume of DMSO was added to the VC well as well. Cells were harvested after the indicated treatment time was reached. At least 3 independent experiments were performed for each condition.

Western blotting

The activation and total levels of the proteins of interest were quantified by the classic method, Western blotting. The activation state of a protein was expressed as the band intensities of its key PTM normalized to those of its total protein, while the total levels of a protein were expressed as its total protein normalized to the total protein load measured by Ponceau S staining [266,267].

Protein extraction and quantification

Cells grown on MG-coated 12-well plates were lysed directly on the plate by addition of 100 µL of 2× sample buffer (2×SB: 125 mM Tris-HCl pH 6.8, 2% sodium dodecyl sulphate (SDS), and 20% glycerol) to extract protein. The cell lysates were collected in 0.6 mL microfuge tubes and then sonicated (Sonic dismembrator Model 100, Thermo Fisher) for about 3 seconds with the intensity node turned to 1, cooled on ice, and stored at -20 ºC until used.

Protein was quantified using the bicinchoninic acid (BCA) assay kit (Pierce, 23225) according to the manufacturer's protocol. Briefly, 10 µL of standards (diluted from stock 2.0 mg/mL BSA in the kit with 2×SB to 0.2, 0.4, 0.6, 0.8, and 1.0 mg/mL), samples (undiluted for Day 4; 2× diluted for Day 10), and blank (2×SB) were added in duplicate into a 96-well plate (NUNC™, #167008), followed by 200 µL of reaction mixture (mixing Reagent A and B at 50:1 ratio). The reaction plate was covered with a lid and sealed with parafilm and then incubated at 37 ºC for 30 min before reading with a FLUOstar Omega plate reader (BMG LABTECH) at 550 nm. The total protein amount in each cell lysate was calculated with reference to the BSA standard curve.

SDS-polyacrylamide gel electrophoresis (SDS-PAGE) and transfer

Protein samples for loading were prepared as follows: aliquoting out 15 µg of protein from respective cell lysates, topping up to a total volume of 20 µL with 2×SB, adding 1 µL of sample loading dye (1:1 mixture of 10% bromophenol blue (w/v) and 2-mercaptoethanol), and boiling for 5 min. Then, 7%, 10% or 14% separating gels and 5% stacking gels were prepared according to Table 2 in a triple-wide glass cassette with a 63-well comb. Once the gels were set, the glass cassette was assembled onto the electrophoresis system (CBS Scientific, #MGV-202-33), and the prepared protein samples from 3 independent experiments of that set were loaded into the wells together with a protein ladder (Froggabio, #PM007). Only one gel was run at one time in 1× running buffer (25 mM Tris, 192 mM glycine, and 0.1% SDS) at 75 mA for approximately 90 to 100 min until the dye front reached the bottom of the gel.

When the run was completed, the glass cassette was carefully separated to expose the gel inside. Then only the separating gel was gently transferred onto a pre-wetted sponge pad/filter paper half sandwich. A proper-sized polyvinylidene difluoride (PVDF) membrane (Roche, #03010040001) was pre-treated with 100% methanol for at least 1 min before placing it onto the gel. Then the transfer sandwich was finished with another layer of filter paper and sponge pad. This sandwich was locked inside the gel transfer cassette after bubbles were carefully removed with a roller layer by layer. The cassette was placed into a transfer tank filled with 1× transfer buffer (25 mM Tris, 192 mM glycine, and 20% methanol) and ice pads. The whole blotting system (CBS Scientific, #EBU-302) was then placed onto a magnetic stirrer at 4 ºC for constant stirring while transferring at 100 V for 75 min.

Table 2. Recipe for triple-wide separating and stacking gels.

Separating	**20% Acrylamide* (mL)**	**H_2O (mL)**	**1.5 M Tris-HCl, pH 8.8 (mL)**	**10% SDS (µL)**	**10% APS* (µL)**	**TEMED* (µL)**
7%	7	8.3	4.5	200	200	16
10%	10	5.3	4.5	200	200	16
14%	14	1.3	4.5	200	200	16
Stacking	**20% Acrylamide (mL)**	**H_2O (mL)**	**0.5 M Tris-HCl, pH 6.8 (mL)**	**10% SDS (µL)**	**10% APS (µL)**	**TEMED (µL)**
5%	2	3.75	2	80	80	20

*: 2× diluted from 40% Acrylamide: Bis-Acrylamide 29:1 (Fisher, #BP1408); APS = ammonium persulfate (Bio-Rad, #1610700), TEMED = N,N,N',N'-tetramethylethylenediamine (MP Biomedicals # 805615)

Immunoblotting

The PVDF membrane (referred to as the blot hereby) was removed from the transfer sandwich immediately after completion, and was washed once with 1× Tris-buffered saline with Tween-20 (TBST, 20 mM Tris-HCl, pH 7.4, 150 mM NaCl, 0.05% Tween-20) before staining with Ponceau S (VWR, 82009-945) for at least 2 min. The stained blot was rinsed gently with 1×TBST twice and then imaged on a ChemiDoc imaging system (Bio-Rad). After the Ponceau S stain was washed away from the blot with 1×TBST (3 × 5 min), the blot was blocked with 3% BSA-TBST for at least 1 h on a shaker at room temperature. All primary

antibodies were diluted in 3% BSA-TBST as shown in Table 3, and applied to the blot, allowing for probing overnight at 4 ºC on a rocker. The following day, the blot was washed 5 times for 5 min each time with 1×TBST. Then, the blot was probed with a corresponding secondary antibody (diluted in 1% BSA-TBST as indicated in Table 3) for 1 h at room temperature with shaking. The blot was washed with 1xTBST (5 × 5 min). An appropriate amount of Western blotting chemiluminescent substrate (Immobilon Crescendo Western HRP (horseradish peroxidase) substrate, Millipore, # WBLUR0500; or SignalFire™ Plus ECL (enhanced chemiluminescence) Reagent, Cell Signaling, #12630) was applied to the blot. The blot was incubated in the substrate for 1 min in the dark, and then immediately imaged on the ChemiDoc. Then, all acquired images were analyzed with Image Lab software (Bio-Rad) for band intensity quantification according to the manufacturer's instruction. For normalization,

Table 3. List of antibodies used.

Primary antibody	Supplier	Catalog #	Dilution	Secondary antibody
p-p38 MAPK (Thr-180/Tyr-182)	Cell Signaling	9211	1:1000	Rabbit, 1:10,000
p38 MAPK	Cell Signaling	9212	1:1000	Rabbit, 1:10,000
p-eNOS (Ser-1177)	Cell Signaling	9571	1:1000	Rabbit, 1:10,000
eNOS	Cell Signaling	9572	1:1000	Rabbit, 1:10,000
p-MSK1 (Ser-376)	Cell Signaling	9591	1:1000	Rabbit, 1:10,000
p-MSK1 (Thr-581)	Cell Signaling	9595	1:1000	Rabbit, 1:10,000
MSK1	Cell Signaling	3489	1:1000	Rabbit, 1:10,000
p-RelA (Ser-536)	Cell Signaling	3036	1:1000	Mouse, 1:10,000
p-RelA (Ser-276)	Cell Signaling	3037	1:1000	Rabbit, 1:10,000
RelA (acetyl Lys-310)	Abcam	ab19870	1:750	Rabbit, 1:10,000
RelA	Cell Signaling	8242	1:1000	Rabbit, 1:10,000
p-CREB (Ser-133)	Cell Signaling	9198	1:1000	Rabbit, 1:10,000
CREB	Cell Signaling	9197	1:1000	Rabbit, 1:10,000
p-Histone H3 (Ser-10)	Epigenetek	C10014-1	1:1000	Rabbit, 1:10,000
p-Histone H3 (Ser-28)	Epigenetek	C10014-1	1:1000	Rabbit, 1:10,000
Histone H3	Cell Signaling	9717	1:1000	Rabbit, 1:10,000
p-Cyclin D1 (Thr-286)	Cell Signaling	3300	1:1000	Rabbit, 1:10,000
Cyclin D1	Cell Signaling	2926	1:1000	Mouse, 1:10,000

the “total lane protein” mode was selected if analyzing a blot probed for a total protein and normalized to the Ponceau S blot, while the “housekeeping protein bands” mode was selected if analyzing a blot probed for a specific PTM of that protein and normalized to that total protein blot. Outputs from the software were exported into a Microsoft Excel file for documentation and further statistical analysis.

Membrane stripping

If the blot was to be probed for another antibody (usually the total protein antibody of the PTM previously probed), after imaging, the blot would be washed once with 1×TBST and stripped with 50 mL stripping buffer (0.2 M glycine-HCl, pH 2.0, 1% SDS, supplemented with 400 µL 2-mercaptoethanol before use) for 15 min at room temperature on a shaker. Then, the blot was washed immediately with 1×TBST for at least 5 × 5 min, until the odour disappeared. The blot was then be blocked and probed again or stored in 1×TBST at 4 ºC until needed. Each blot was only stripped 2 times at most.

Cell cycle analysis by flow cytometry

Measuring the DNA content in a cell is the most common approach to determining the stage of the cell cycle: DNA starts to replicate during S phase until it finishes doubling and reaches the G2 phase; the DNA content is held at double the amount throughout G2 and M phase; once mitosis finishes, DNA content returns to the usual amount with the daughter cells starting in G0/G1 phase again [268]. DNA can be stained with fluorescent dyes, and since fluorescence intensity corresponds well with DNA content, the fluorescent signal can thereby be used to determine the cell cycle stage. One of the most commonly used DNA dyes for flow cytometry is propidium iodide (PI), and the method developed by Tate et al. [269] was adopted.

Ethanol fixation

Cells grown on MG-coated 6-well plates were treated as indicated and harvested with trypsinization. The resulting cell suspensions were centrifuged at 760 ×g for 5 min, the supernatant was removed, and the cell pellets were re-suspended with 75% ethanol-PBS (5 mL per well per treatment per tube) and allowed to fix for at least 2 h. Pipetting was carefully done while suspending cells to achieve a single cell suspension. The cells in ethanol were stored at 4 ºC for at most 1 week until the next stage of DNA staining and flow cytometry analysis.

DNA staining

On the day of analysis, the cells were centrifuged at 300 ×g for 5 min at room temperature to remove the ethanol. Then, the cell pellets were washed once with cold 1×PBS before being resuspended in 0.5 mL PI solution (50 µg/mL PI (Sigma, #P4864), 4 mM Na citrate, 0.1% Triton X-100 (Sigma, T8787), 50 µg/ml RNase A (NEB, T3018L), pH adjusted with NaOH to 7.8). The cells were incubated in the dark for 10 min at 37 ºC, and 50 µL of 1.38 M NaCl was added to the 0.5 mL solution in each tube immediately after incubation. A single cell suspension was prepared by careful pipetting, and the cells were ready for flow cytometry.

Flow cytometry

Flow cytometry was done at the University of Manitoba Flow Cytometry Core Facility on a CytoFlex LX Digital Flow Cytometry Analyzer 4 Laser System (Beckman Coulter). A 488 nm laser and fluorescent channel 610/20 BP (mirror/filter) were selected to excite the DNA-PI dye complex and to detect the fluorescent signal in the 600 to 620 nm range, respectively. Data acquisition and cell cycle distributions were done inside the CytExpert software (Beckman Coulter) by the built-in algorithm. Histograms with population hierarchy data were displayed and exported for further statistical analysis.

Statistical analysis

The data for each experiment were collected from 3 independent biological replicates (i.e. 3 different passages of cell culture), with no technical replicates within each passage. All data were analyzed using IBM SPSS statistics version 27 (IBM Corp.) and plotted as means ± standard error of the mean (SEM) using GraphPad Prism version 9.0 (GraphPad software). Outliers were identified as those outside the range of mean ± 2.5 standard deviation of that data set and were removed prior to analysis. If the data were not normally distributed, log transformation was performed on those data sets before subjecting them to ANOVA. One-way ANOVA followed by post-hoc testing with Duncan's multiple range test (for homogenous data sets) or Dunnett's test (for non-homogenous data sets) was used for DHA concentration curve data and for time course data. For data studying the combined effects (interactions) of DHA × inhibitor, DHA × growth state, or DHA × time, two-way ANOVA followed by pair-wise mean comparison with Bonferroni correction was employed. Statistical significance was set at $p < 0.05$, except that an interaction in a two-way ANOVA was considered significant at $p < 0.1$. If there was a trend, it is indicated in the Results text, and defined as a p value is between 0.05 and 0.1 for post-hoc testing or pair-wise mean comparisons.

RESULTS

DHA regulated eNOS activation and total levels

It was previously reported by our the lab that DHA, but not other fatty acids, activated p38 MAPK differently in growing and quiescent EA.hy926 endothelial cells [6]. Since there is evidence that p38 MAPK can regulate eNOS activity in endothelial cells [270], it is plausible that DHA via p38 MAPK may be able to modulate the activity of eNOS. If this is the case, then DHA may have an atheroprotective effect. To evaluate this possibility, it was first necessary to establish the concentration and time course of eNOS activation in response to DHA treatment for both cell growth states. This information was required to provide the best combination of concentration and treatment time needed for the subsequent assessments.

Both growing and quiescent EA.hy926 cells were treated with varying concentrations of DHA for time periods extending to 24 h. Western blotting was subsequently used to examine the relative levels of total eNOS and p38 MAPK as well as their activated (phosphorylated) forms, and the blots are shown in Fig. 3, panels A-F. Visual inspection of these data indicates that there are transient increases in both p-eNOS and p-p38 MAPK in response to DHA, however, these responses are different when growing (Fig. 3A-C) and quiescent (Fig. 3D-F) cells are compared. Quantification of the band intensities and subsequent normalization versus the controls (total eNOS and p38 MAPK) enabled the data to be examined graphically (Fig. 3G-R). Time course treatment with 125 μM DHA revealed that eNOS was maximally activated at 2 h but suppressed at 16 and 24 h relative to the untreated control in growing cells (Fig. 3G), while p38 MAPK was transiently activated at the early (30 min) time point and was activated at a second, later (more than 8 h) treatment time (Fig. 3H). In contrast, neither eNOS nor p38 MAPK was significantly activated in quiescent cells under the same conditions (Fig. 3I & J). Interestingly, in growing cells, DHA did not have a demonstrable impact on eNOS activation (Fig. 3K), while DHA concentration-dependently activated p38 MAPK (Fig. 3L). In quiescent cells, however, eNOS was activated only with 20 μM DHA (Fig. 3M), while p38 MAPK activation was only at higher DHA concentrations (125 and 150 μM) (Fig. 3N). Further examination of the time course with 20 μM DHA revealed that, in growing cells, eNOS was activated after 2 h of treatment except at 8 h (Fig. 3O), while p38 MAPK remained activated to the 16 h time point (Fig. 3P). In quiescent cells, however, eNOS was activated at 8 h only (Fig. 3Q), and p-p38 MAPK was elevated only at 10 min compared to 2 – 24 h (Fig. 3R). Since 8 h is also the late activation timepoint for p38 MAPK in growing cells (Fig. 3H) but not in quiescent cells, this treatment time was selected for subsequent experiments for the 20 and 125

μM concentrations. In general, there is an inverse relationship between eNOS activation and p38 MAPK activation by DHA.

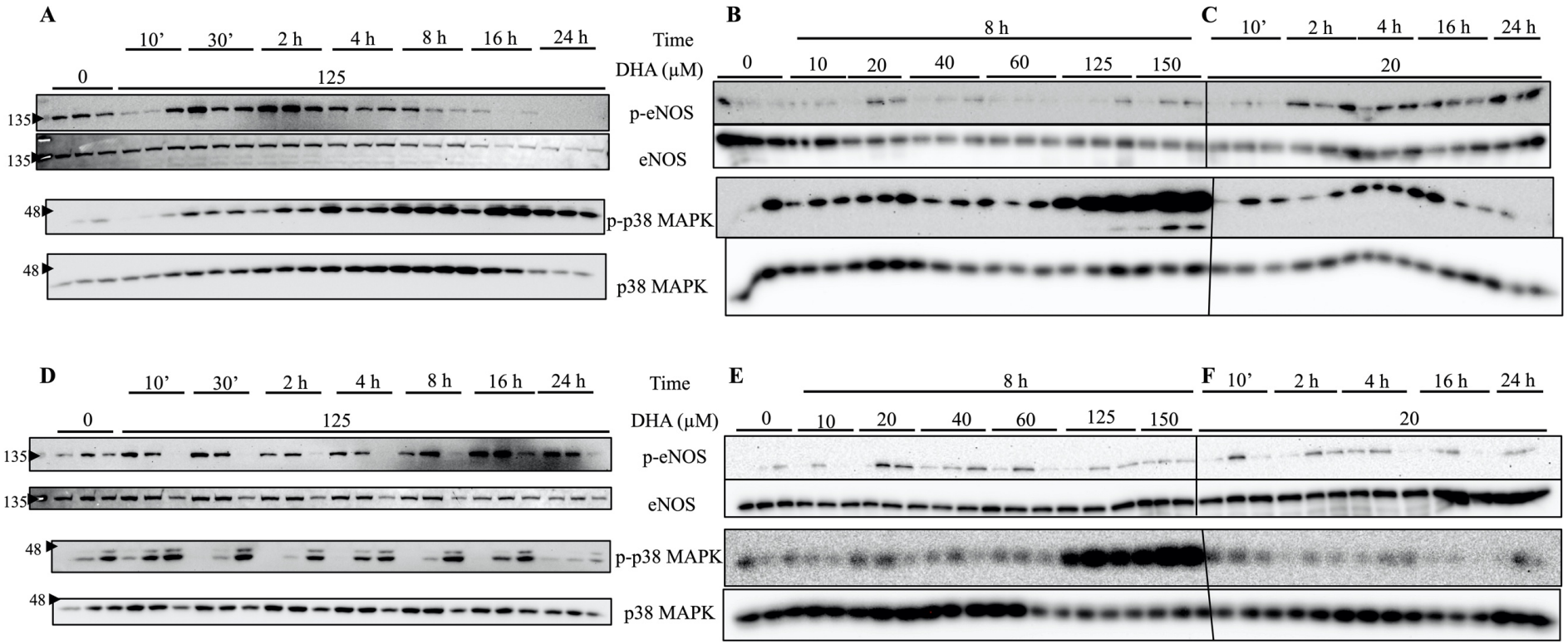
A
10’
30’
2 h
4 h
8 h
16 h
24 h
Time
0
125
DHA (μM)
135
p-eNOS
135
eNOS
48
p-p38 MAPK
48
p38 MAPK
B
8 h
0
10
20
40
60
125
150
C
10’
2 h
4 h
16 h
24 h
20
D
10’
30’
2 h
4 h
8 h
16 h
24 h
Time
0
125
DHA (μM)
135
p-eNOS
135
eNOS
48
p-p38 MAPK
48
p38 MAPK
E
8 h
0
10
20
40
60
125
150
F
10’
2 h
4 h
16 h
24 h
20

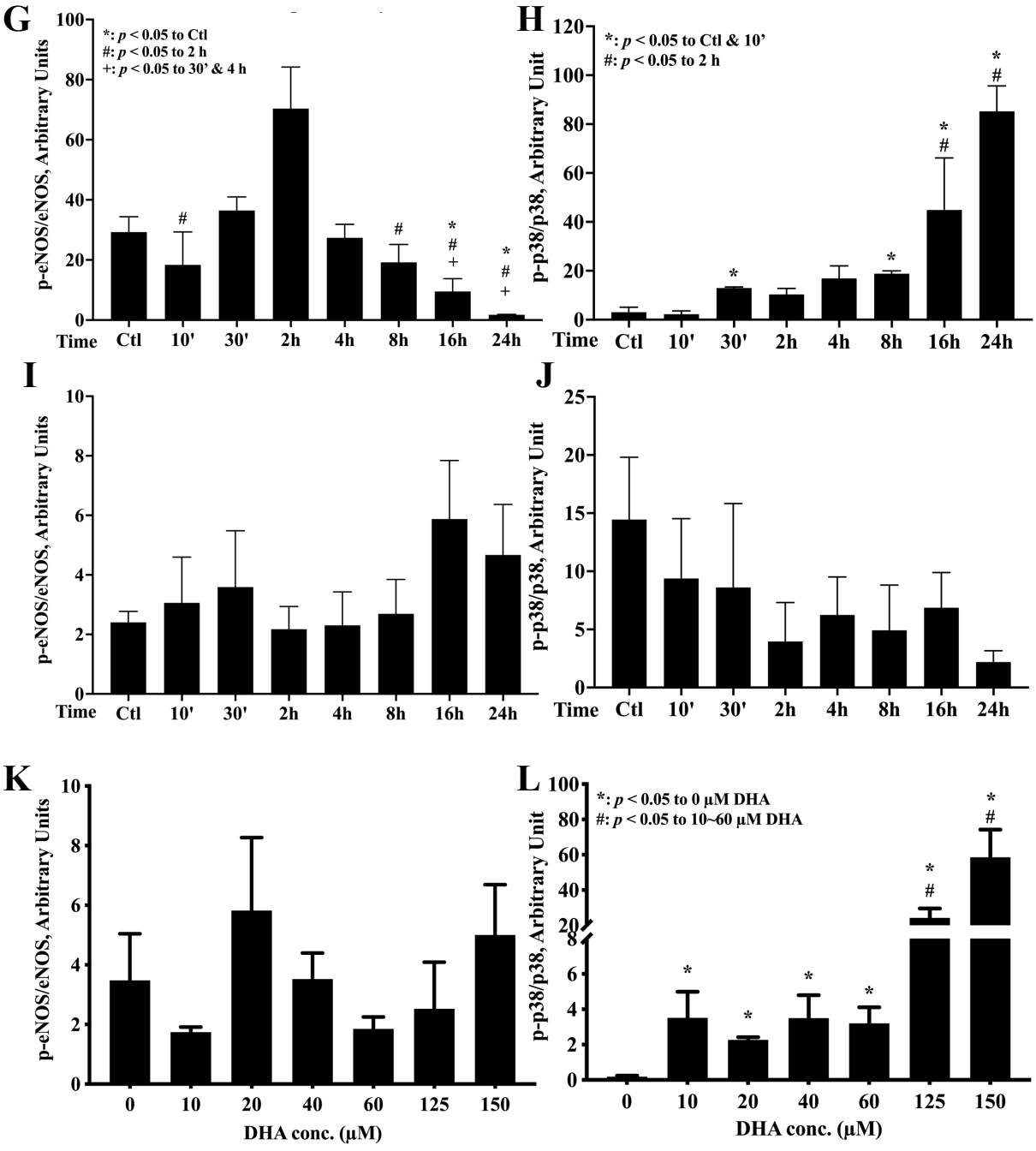
G
*: p < 0.05 to Ctl
#: p < 0.05 to 2 h
+: p < 0.05 to 30' & 4 h
p-eNOS/eNOS, Arbitrary Units
Time Ctl 10' 30' 2h 4h 8h 16h 24h
H
*: p < 0.05 to Ctl & 10'
#: p < 0.05 to 2 h
p-p38/p38, Arbitrary Unit
Time Ctl 10' 30' 2h 4h 8h 16h 24h
I
p-eNOS/eNOS, Arbitrary Units
Time Ctl 10' 30' 2h 4h 8h 16h 24h
J
p-p38/p38, Arbitrary Unit
Time Ctl 10' 30' 2h 4h 8h 16h 24h
K
p-eNOS/eNOS, Arbitrary Units
0 10 20 40 60 125 150
DHA conc. (μM)
L
*: p < 0.05 to 0 μM DHA
#: p < 0.05 to 10~60 μM DHA
p-p38/p38, Arbitrary Unit
0 10 20 40 60 125 150
DHA conc. (μM)

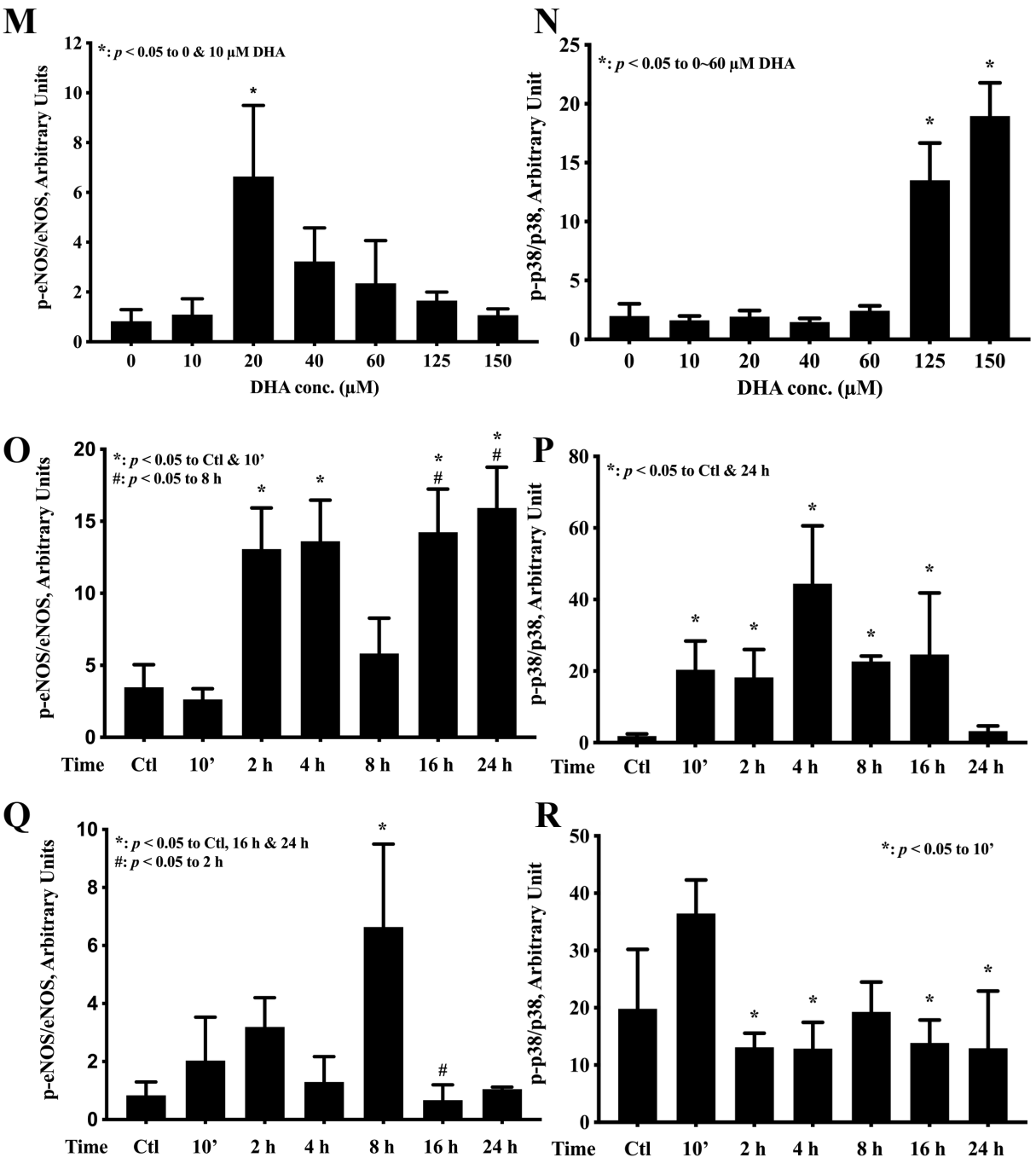
M
*: p < 0.05 to 0 & 10 μM DHA
p-eNOS/eNOS, Arbitrary Units
DHA conc. (μM)
0 10 20 40 60 125 150
N
*: p < 0.05 to 0~60 μM DHA
p-p38/p38, Arbitrary Unit
DHA conc. (μM)
0 10 20 40 60 125 150
O
*: p < 0.05 to Ctl & 10'
#: p < 0.05 to 8 h
p-eNOS/eNOS, Arbitrary Units
Time Ctl 10' 2 h 4 h 8 h 16 h 24 h
P
*: p < 0.05 to Ctl & 24 h
p-p38/p38, Arbitrary Unit
Time Ctl 10' 2 h 4 h 8 h 16 h 24 h
Q
*: p < 0.05 to Ctl, 16 h & 24 h
#: p < 0.05 to 2 h
p-eNOS/eNOS, Arbitrary Units
Time Ctl 10' 2 h 4 h 8 h 16 h 24 h
R
*: p < 0.05 to 10'
p-p38/p38, Arbitrary Unit
Time Ctl 10' 2 h 4 h 8 h 16 h 24 h

Figure 3. Effect of DHA and growth state on the activation of eNOS and p38 MAPK in EA.hy926 cells.

Growing and quiescent EA.hy926 cells were treated with various concentrations of DHA for different durations and Western blotting was used to measure p-eNOS (Ser-1177), total eNOS, p-p38MAPK (Thr-180/Tyr-182) and total p38MAPK. Panels A-C show Western blot data for 3 biological replicates per indicated treatment (A=time course with 125 μM DHA; B=DHA concentration titration for 8 h; C=time course with 20 μM DHA) for both eNOS (total and phosphorylated) and p38MAPK (total and phosphorylated) in growing cells, while panels D-F show the same in quiescent cells. The p-eNOS and p-p38MAPK band intensities (representative of eNOS and p38MAPK activation, respectively) were quantified and are graphically presented relative to the respective total eNOS and p38MAPK controls in panels G & H (time course with 125 μM DHA in growing cells), I & J (time course with 125 μM DHA in quiescent cells), K & L (DHA concentration titration for 8 h in growing cells), M & N (DHA concentration titration for 8 h in quiescent cells), O & P (time course with 20 μM DHA in growing cells), and Q & R (time course with 20 μM DHA in quiescent cells), respectively. In panels G-R, the data are presented as means ± SEM (n=3). Different symbols denote statistical significance ($p < 0.05$) between different treatment conditions as indicated inside the graph. Ctl: vehicle control with 0 μM DHA treatment. The band intensity data for Ctl and 8 h treatments were used for both DHA concentration titration for 8 h and 20 μM DHA time courses (B & C, and E & F), since the samples were identical for these conditions and included on the same blot.

It was also observed that total eNOS bands at 8 h to 24 h were fainter than the control bands (Fig. 3A and 3D), leading to speculation that DHA may affect total eNOS levels in endothelial cells as well. This was confirmed by comparing the total eNOS level against total protein load as defined by Ponceau S staining (Fig. 4). Visual inspection of the total eNOS blot showed that the 125 μM DHA bands were much fainter compared to 0 μM and 20 μM DHA, especially in quiescent cells (Fig. 4A), which was validified by quantification of the band intensities (Fig 4B). However, this concentration effect of DHA on eNOS expression was similar in both growth states. Nevertheless, cell growth state alone was found to affect total eNOS levels, which has not been reported by others yet. Quiescent cells had average eNOS levels that were about 1.5-fold higher relative to those of growing cells (Fig. 4B).

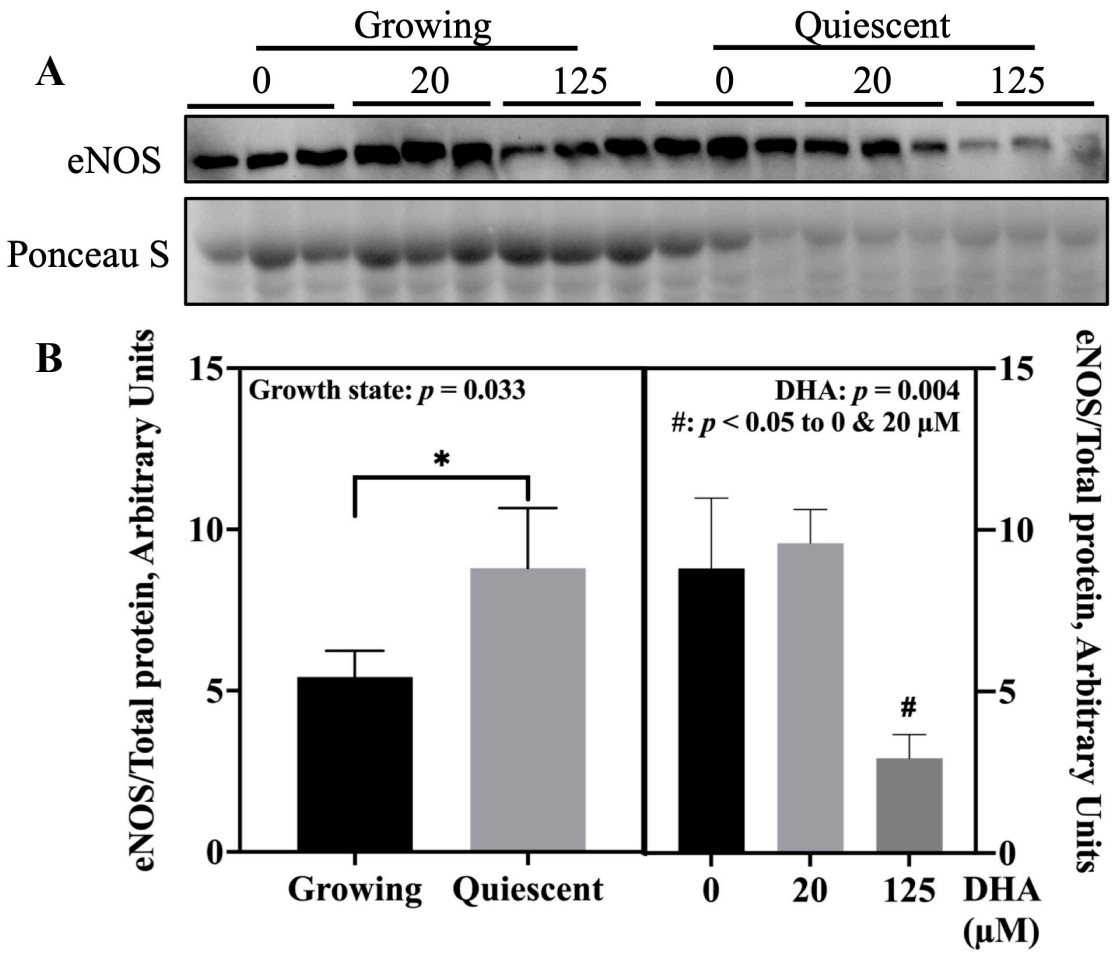

Figure 4. Effect of DHA and growth state of endothelial cells on total eNOS levels.

Growing and quiescent EA.hy926 cells were treated with 0, 20, and 125 µM DHA for 8 h and Western blotting was used to measure total eNOS relative to total protein load (Ponceau S staining). The blots (A) show 3 biological replicates per treatment. The total eNOS band intensities were quantified and are graphically presented in panel B relative to total protein load. Data are presented as means ± SEM for the main effects of growth state (n=9) and DHA concentration (n=6). Different symbols denote statistical significance ($p < 0.05$) between different treatment conditions as indicated in the graph.

After determining the concentrations of DHA and duration of treatment used in the subsequent experiments, SB202190, a p38α/β specific inhibitor [56], was employed to validate p38 MAPK's involvement in the modulation of eNOS by DHA. For this experiment, growing (Fig. 5) and quiescent (Fig. 6) cells were treated with DHA for 8 h in the presence and absence of the p38α/β inhibitor.

In growing cells, treatment with 20 and 125 μM DHA showed no sign of activating eNOS at 8 h compared to the 0 μM DHA treatment (Fig. 5B), consistent with the DHA concentration titration for 8 h as in Fig. 3K. When p38α/β was inhibited, however, a high concentration of DHA (125 μM) drastically augmented p-eNOS levels (Fig. 5A & B). The p38 MAPK inhibition seemed not to affect eNOS activation at other DHA concentrations (20 and 40 μM). For total eNOS levels, similar to what is visible in Fig. 4A, fainter total eNOS bands were observed in the 125 μM DHA treated samples compared to band intensities for other treatment (Fig. 5A), although this did not reach statistical significance (Fig. 5C). On the other hand, DHA at 20 μM significantly increased total eNOS levels in growing cells compared to 0 and 125 μM DHA (Fig. 5C).

In quiescent cells, DHA treatment without p38 MAPK inhibition at all 3 concentrations (20, 40, and 125 μM) did not activate eNOS compared to the vehicle control (0 μM DHA) (Fig. 6B), inconsistent with the DHA concentration titration results for 8 h as shown in Fig. 3M in which 20 μM DHA significantly activated eNOS compared to 0 μM DHA. The large variation in band intensities among the 3 independent experiments should have likely affected detection of statistical significance in this case, thus causing this inconsistency. Nevertheless, the average levels of p-eNOS with 20 μM DHA was still substantially higher (about 2.7-fold) than that of vehicle control (Fig. 6B). When p38α/β was inhibited, eNOS was activated tremendously in the absence of DHA, and this activation was largely prevented by DHA treatment at both 40 μM and 125 μM, with a trend ($p = 0.058$) for ~ 60% less activation in the presence of 20 μM DHA (Fig. 6A & B). Although visual examination of the blots of total eNOS did not show obvious patterns (Fig. 6A), quantification of the bands did reveal similar results to those in growing cells (Fig. 6C vs Fig. 5C): the increase in total eNOS levels by 20 μM DHA treatment were attenuated by p38α/β inhibition. Furthermore, in the absence of the inhibitor, 125 μM DHA significantly lowered total eNOS levels compared to 20 μM DHA (Fig. 6C).

In case the huge differences in band intensities overshadowed some details, the effect of p38α/β inhibition on eNOS only was examined separately (Fig. 7). Using this approach, it was obvious, both by visual examination of the blots (Fig. 7A) and after quantification (Fig. 7B), that while p38 inhibition activated eNOS in quiescent cells as shown in Fig. 6A & B, p38

inhibition suppressed eNOS activation in growing cells. The main effect for growth state was significant for total eNOS levels (Fig. 7C), with quiescent cells having more ~ 1.7-fold higher levels of total eNOS compared to growing cells, matching the observations in Figs. 4 to 6.

Taken together, the effect of DHA on eNOS activation is p38 MAPK-dependent, both in terms of concentration and growth-state. While decreasing total eNOS levels at high concentration (125 μM), DHA at 20 μM elevated total eNOS levels instead. This concentration-dependent effect of DHA on eNOS protein levels was not dependent on p38 MAPK, except for the 20 μM DHA treatment in quiescent cells.

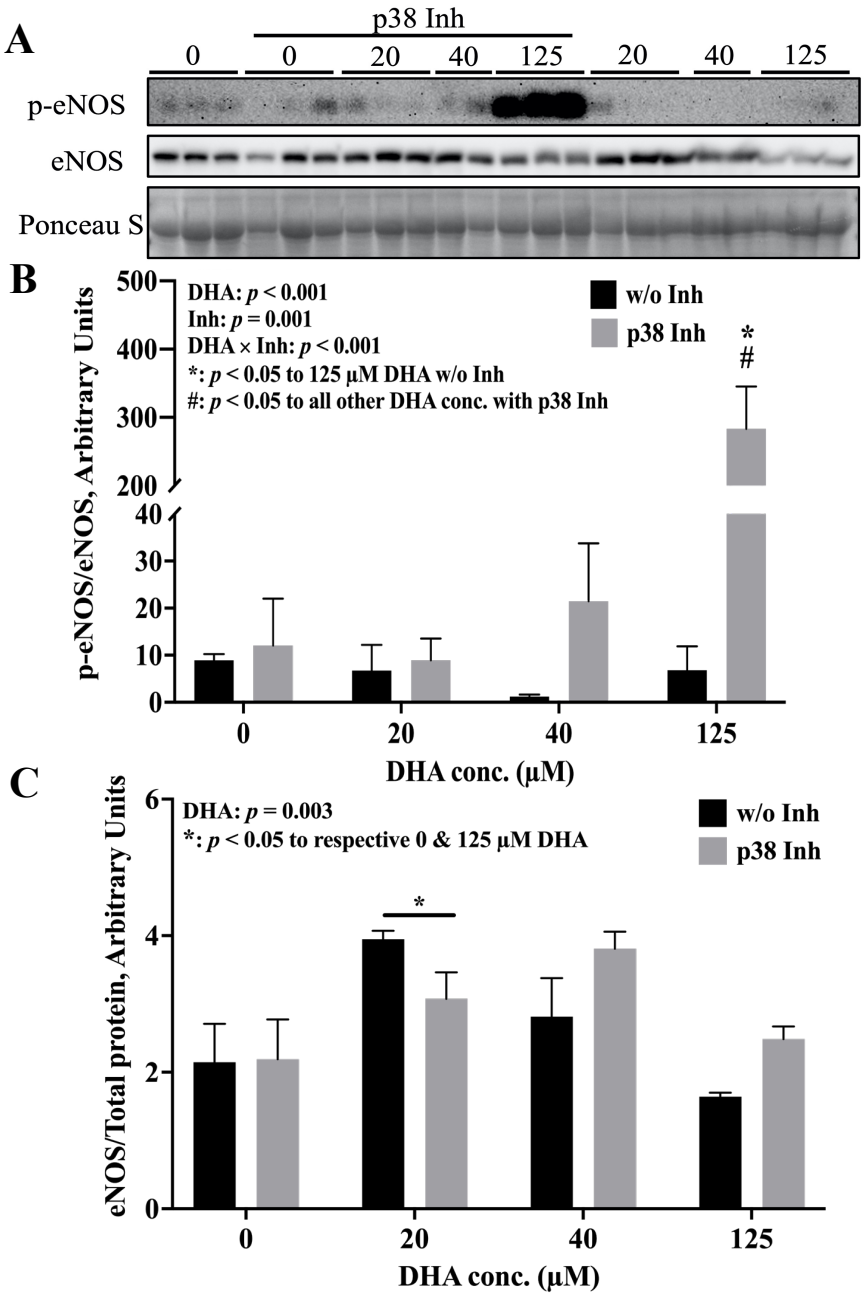

Figure 5. Effect of DHA and p38 MAPK inhibition on eNOS activation in growing cells.

Growing EA.hy926 cells were exposed to 0, 20, 40, and 125 µM DHA for 8 h with or without the p38 MAPK inhibitor, SB202190 (1 µM). Western blotting was used to measure p-eNOS (Ser-1177) and total eNOS, while Ponceau S staining provided total protein load. The blots (A) show 3 biological replicates per treatment. The p-eNOS band intensities (representative of eNOS activation) were quantified and are graphically presented in panel B relative to total eNOS band intensity. Likewise, the total eNOS band intensities were quantified and are graphically presented in panel C relative to total protein load. Data are presented as means ± SEM (n=3). Different symbols denote statistical significance ($p < 0.05$) between different treatment conditions as indicated in the graph. Inh: inhibitor.

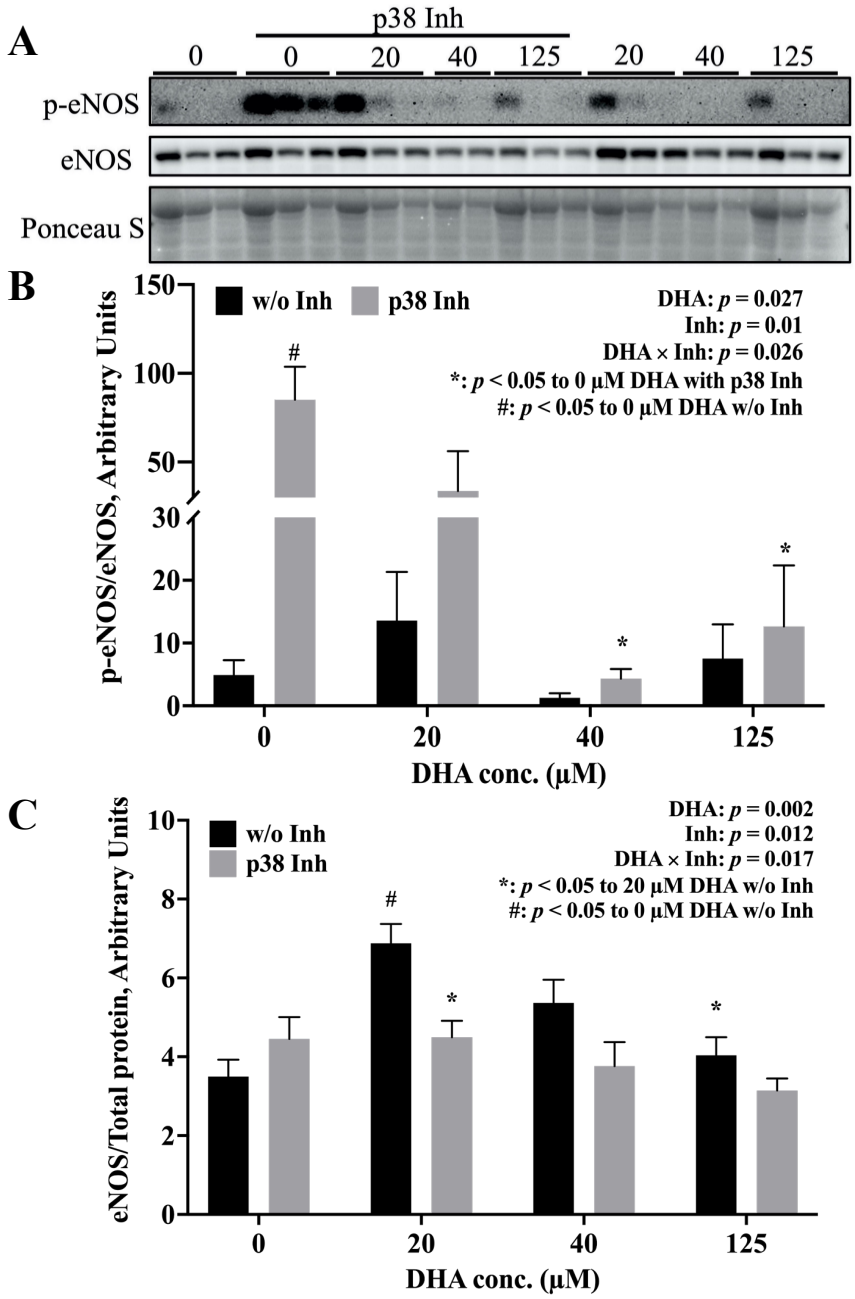

Figure 6. Effect of DHA and p38 MAPK inhibition on eNOS activation in quiescent cells.

Quiescent EA.hy926 cells were exposed to 0, 20, 40, and 125 µM DHA for 8 h with or without the p38 MAPK inhibitor, SB202190 (1 µM). Western blotting was used to measure p-eNOS (Ser-1177) and total eNOS, while Ponceau S staining provided total protein load. The blots (A) show 3 biological replicates per treatment. The p-eNOS band intensities (representative of eNOS activation) were quantified and are graphically presented in panel B relative to total eNOS band intensity. Likewise, the total eNOS band intensities were quantified and are graphically presented in panel C relative to total protein load. Data are presented as means ± SEM (n=3). Different symbols denote statistical significance ($p < 0.05$) between different treatment conditions as indicated in the graph. Inh: inhibitor.

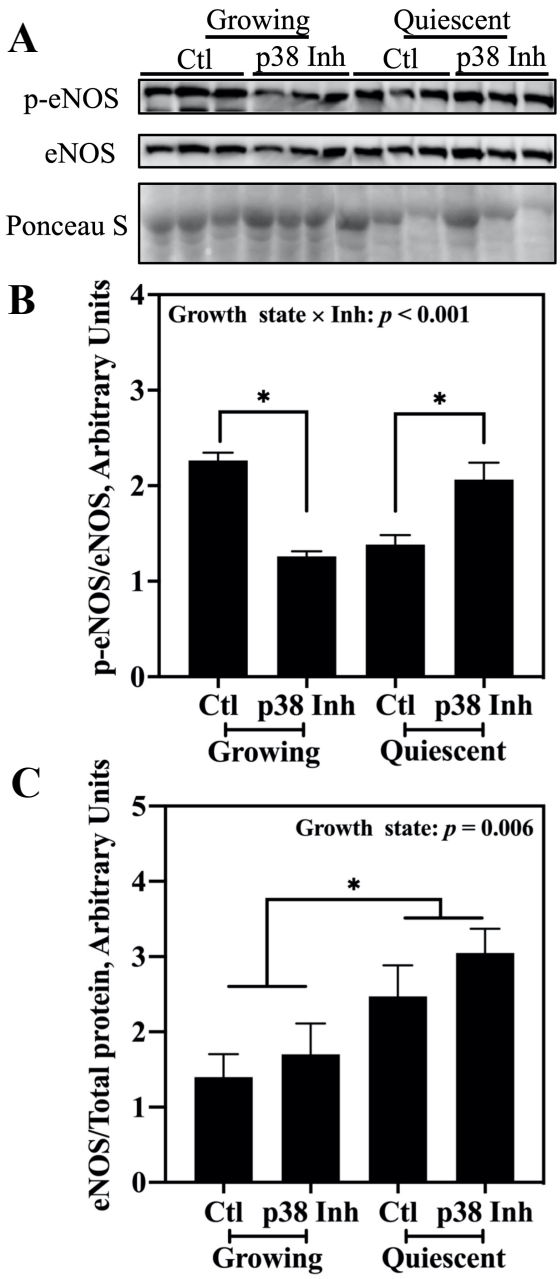

Figure 7. Effect of growth state of endothelial cells and p38 MAPK inhibition on eNOS activation and total protein levels.

Growing and quiescent EA.hy926 cells were treated with or without the p38 MAPK inhibitor, SB202190 (1 μM). Western blotting was used to measure p-eNOS (Ser-1177) and total eNOS, while Ponceau S staining provided total protein load. The blots (A) show 3 biological replicates per treatment. The p-eNOS band intensities (representative of eNOS activation) were quantified and are graphically presented in panel B relative to total eNOS band intensities. The total eNOS band intensities were quantified and are graphically presented in panel C relative to total protein load. Data are presented as means ± SEM (n=3). The asterisk denotes statistical significance ($p < 0.05$) between different treatment conditions as indicated in the graph. Ctl: vehicle control without inhibitor treatment; Inh: inhibitor.

To explore other possible mediators along the p38 MAPK/NF-κB axis for DHA's atheroprotective effects, MSK was considered a good candidate since it can be directly activated by p38 MAPK, which gives it the capacity to phosphorylate NF-κB. SB747651A is a potent inhibitor for MSK [264]. If the eNOS response to DHA after MSK inhibition is similar to that after p38 MAPK inhibition as shown above, it is highly likely that DHA's effect on eNOS is transduced via p38 MAPK/MSK to NF-κB.

To examine the involvement of MSK, EA.hy926 cells were treated with or without SB747651A prior to DHA treatment, the same as was done with p38 MAPK inhibition. In growing cells (Fig. 8), it is obvious from the blots that MSK inhibition reduced p-eNOS levels and there were fainter total eNOS bands in response to 125 μM DHA compared to other conditions (Fig. 8A). As determined by densitometry analysis, no effect was observed due to DHA, while MSK inhibition suppressed eNOS activation (Fig. 8B). However, neither DHA treatment nor MSK inhibition was found to affect total eNOS levels as in Fig. 8C.

In quiescent cells (Fig. 9), similar to what was observed in growing cells (Fig. 8A), visual examination of the blots showed that MSK inhibition downregulated p-eNOS levels, and fainter total eNOS bands at 125 μM DHA were seen compared to other conditions (Fig. 9A). Densitometric analysis revealed that DHA significantly activated eNOS at all 3 concentrations compared to the vehicle control, while MSK inhibition suppressed this DHA-induced eNOS activation at 20 and 40 μM DHA only (Fig. 9B). At 125 μM DHA, however, MSK inhibition did not downregulate p-eNOS levels, and eNOS remained activated compared to 0 and 20 μM DHA with MSK inhibitor treatment (Fig. 9B). For total eNOS levels in the absence of inhibitor (Fig. 9C), again, 125 μM DHA decreased eNOS protein levels, compared to both the control and 20 μM DHA treatment. Moreover, DHA at 40 μM also downregulated total eNOS levels when there was no inhibition. Surprisingly, the MSK inhibitor also reduced eNOS protein levels, slightly but significantly, in the absence of DHA treatment (0 μM) in quiescent cells. This reduction of total eNOS levels by MSK inhibition when compared to respective DHA-alone treatment, however, was not observed in the presence of DHA. On the other hand, the MSK inhibitor in combination with 125 μM DHA reduced total eNOS protein levels compared to MSK inhibition alone.

Overall, MSK was required for eNOS activation by DHA in both growth states but in different manners. And MSK was needed for basal eNOS expression in quiescent cells. However, the eNOS response patterns to p38 MAPK inhibition (Fig. 5 & 6) and MSK inhibition (Fig. 8 & 9) in conjunction with DHA treatment were not the same, and in some instances the responses were directly opposite (e.g. Fig. 6B vs Fig. 9B for quiescent cells).

Thus, although DHA can also mediate eNOS activation and expression via MSK as well as p38 MAPK, these two kinases operated separately when signaling to eNOS in response to DHA.

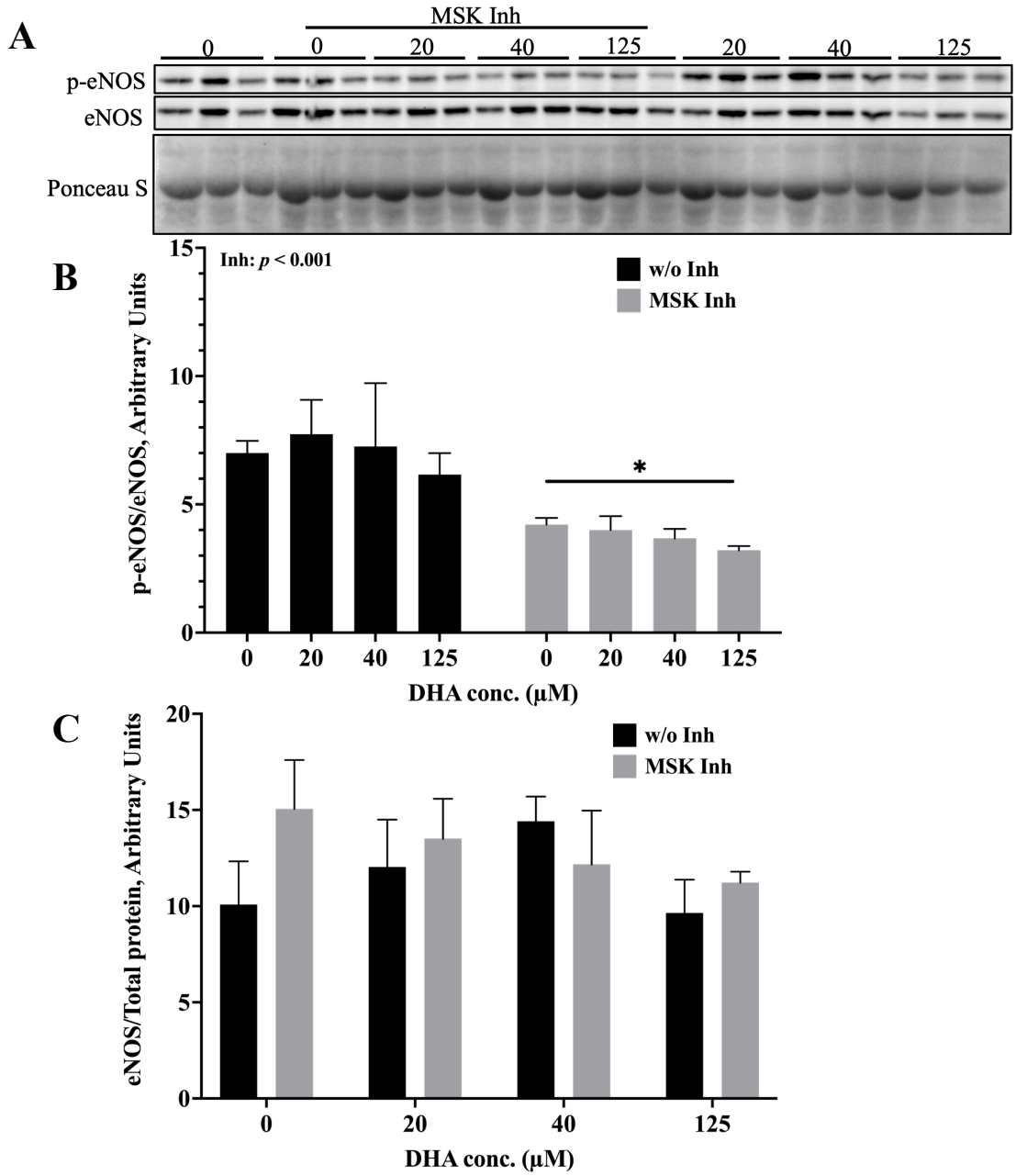

Figure 8. Effect of DHA and MSK inhibition on eNOS activation and total protein levels in growing cells.

Growing EA.hy926 cells were treated with 0, 20, 40, and 125 µM DHA for 8 h with or without the MSK inhibitor, SB747651A (5 µM). Western blotting was used to measure p-eNOS (Ser-1177) and total eNOS, while Ponceau S staining provided total protein. The blots (A) show 3 biological replicates per treatment. The p-eNOS band intensities (representative of eNOS activation) were quantified and are graphically presented in panel B relative to total eNOS band intensity. Likewise, the total eNOS band intensities were quantified and are graphically presented in panel C relative to total protein load. Data are presented as means ± SEM (n=3). The asterisk denotes the statistically significant ($p < 0.05$) main effect of MSK inhibition. Inh: inhibitor.

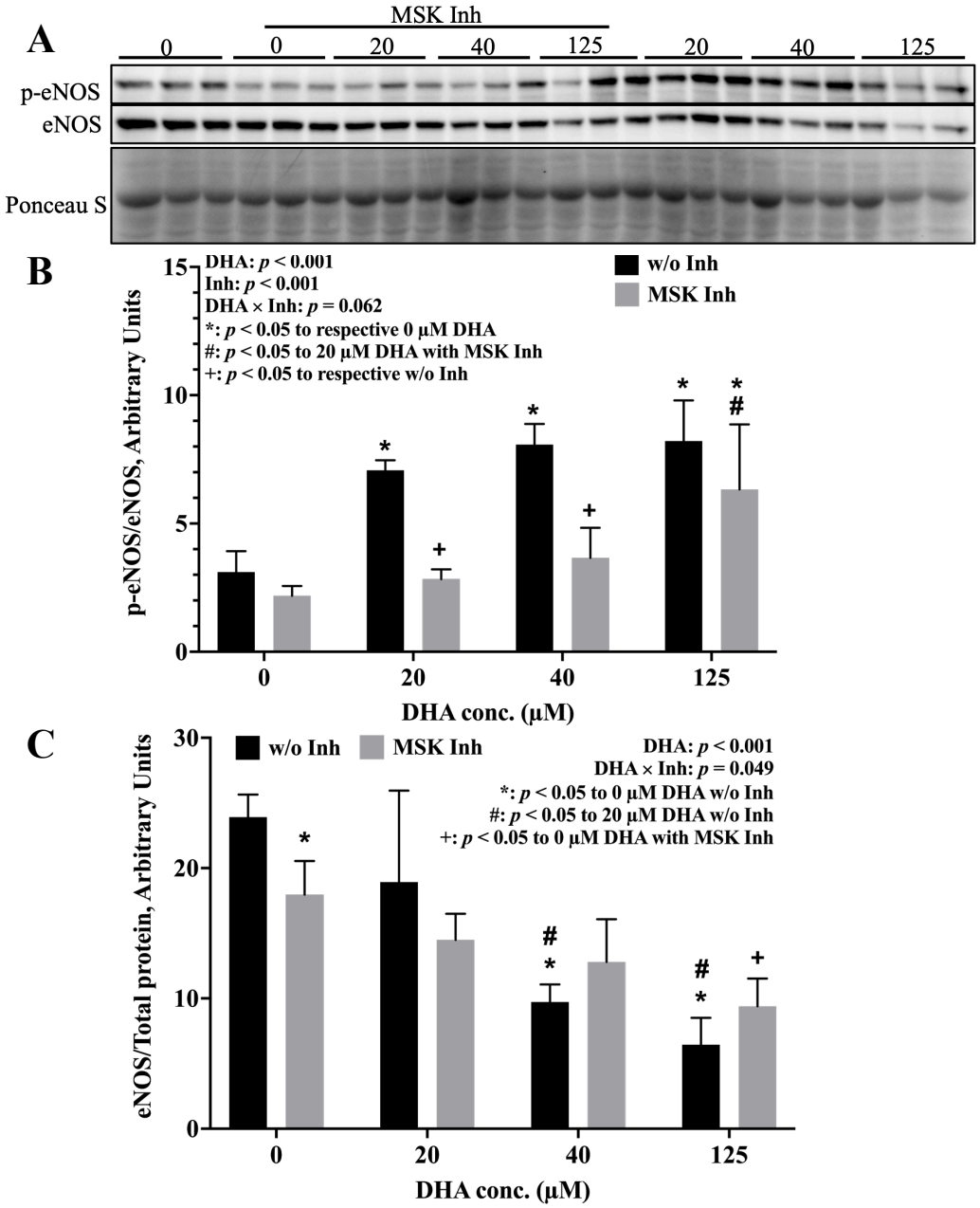

Figure 9. Effect of DHA and MSK inhibition on eNOS activation and total protein levels in quiescent cells.

Quiescent EA.hy926 cells were exposed to 0, 20, 40, and 125 µM DHA treatment for 8 h with or without MSK inhibitor, SB747651A (5 µM). Western blotting was used to measure p-eNOS (Ser-1177) and total eNOS, while Ponceau S staining provided total protein. The blots (A) show 3 biological replicates per treatment. The p-eNOS band intensities (representative of eNOS activation) were quantified and are graphically presented in panel B relative to total eNOS band intensity. Likewise, the total eNOS band intensities were quantified and are graphically presented in panel C relative to total protein load. Data are presented as means ± SEM (n=3). Different symbols denote statistical significance ($p < 0.05$) between different treatment conditions as indicated inside the graph. Inh: inhibitor.

To ensure that those inhibitors performed as expected, EA.hy926 cells grown on plastic without MG were stimulated with TNFα and kinase involvement was assessed by comparing the response with and without the specified inhibitors. Thr-581 is the site on MSK phosphorylated by p38α/β, while MSK can directly phosphorylate CREB at Ser-133. Upon stimulation, p-MSK and p-CREB levels were increased as shown in Fig. 10A and B, respectively. This stimulation of phosphorylation was clearly reduced when the inhibitors were present, thus proving that the inhibitors were working as expected. Even the non-stimulated p-MSK and p-CREB levels were visibly decreased by the inhibitors.

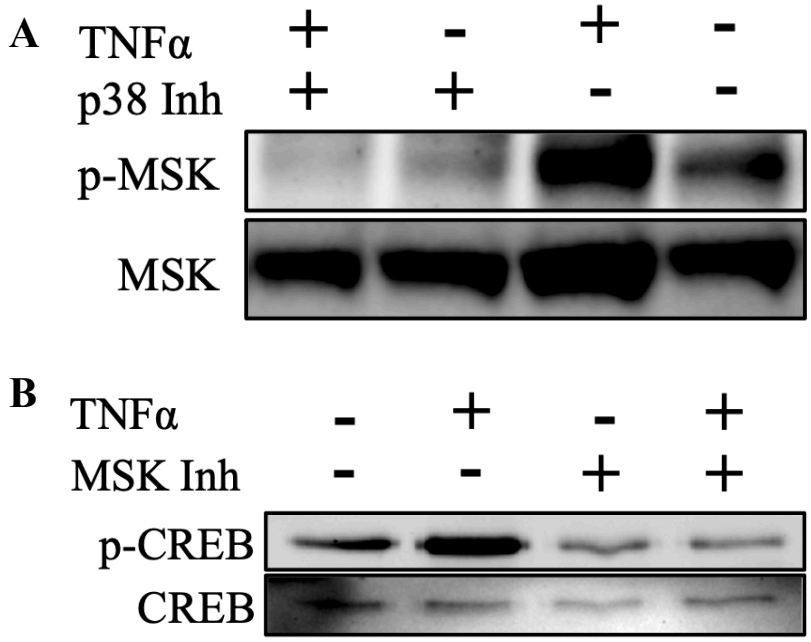

Figure 10. Quality check for the inhibitors used in the assays.

EA.hy926 cells (grown on bare plastic) were stimulated with 10 μM TNFα for 2 h or treated with an equal amount of DMSO (vehicle). Inhibitors (or vehicle) were added 30 min prior to the stimulation. Western blotting was used to examine the effectiveness of p38α/β MAPK inhibitor, SB202190 (1 μM), in panel A by measuring p-MSK (Thr-581) relative to total MSK; and to examine the effectiveness of MSK inhibitor, SB747651A (5 μM), in panel B by measuring p-CREB (Ser-133) relative to total CREB.

DHA modulated the status of transcription factors and histone marks

MSK is an important kinase directly downstream of p38 MAPK and can modulate many other TF and histone marks [72]. Phosphorylation of MSK at Thr-581 indicates its induction by upstream kinases (p38α/β MAPK and ERK1/2), while phosphorylation at Ser-376 indicates MSK is catalytically active and capable of phosphorylating its downstream substrates [66]. The effect of DHA on these 2 MSK PTMs via p38 MAPK were investigated by treating EA.hy926 cells with DHA under p38 MAPK inhibition as illustrated in Fig. 11 and 12.

In growing cells (Fig. 11), the blots showed that only a high concentration of DHA (125 μM) can activate MSK, while p38 MAPK inhibition reduced the intensity of the total MSK band (Fig. 11A). Indeed, 125 μM DHA induced MSK activation regardless of p38 MAPK (Fig. 11B), and there was a trend (p = 0.07) for upregulation of MSK catalytic activity by 125 μM DHA compared to the control of 0 μM DHA (Fig. 11C). Unexpectedly, p38 MAPK inhibition elevated p-MSK levels at both Thr-581 and Ser-376 (Fig. 11B and C). This further activation may be due to additional compensatory induction from another MSK activating kinase, such as ERK1/2. On the other hand, p38 MAPK inhibition significantly decreased MSK expression with no effect of DHA observed (Fig. 11D).

In quiescent cells (Fig. 12), similar patterns of MSK phosphorylation were observed to those of growing cells, while the total MSK levels differed (Fig. 12A). This affected the values of normalized p-MSK levels and the outcome thus appeared to be much different from that in growing cells. Although 125 μM DHA again induced MSK activation (Fig. 12B) and catalytic activity (Fig. 12C), p38 MAPK inhibition attenuated this induction of p-MSK levels at both Thr-581 and Ser-376 by DHA (Fig. 12B & C), instead of activating p-MSK as in growing cells (Fig. 11B & C). Apart from 125 μM DHA, the catalytic activity of MSK was also elevated by 20 μM DHA, again being dependent on p38 MAPK (Fig. 12C). p38 MAPK inhibition had no effect on total MSK levels but a high DHA concentration (125 μM) downregulated total MSK levels (Fig. 12D).

Taken together, DHA can induce MSK activity via two different routes in endothelial cells depending on growth state: MSK activation by DHA was independent of p38 MAPK in growing cells, but requires p38 MAPK in quiescent cells. Also, p38 MAPK inhibition decreased MSK expression in growing cells but not in quiescent cells. MSK, both its activity and expression, was more responsive to DHA in quiescent cells.

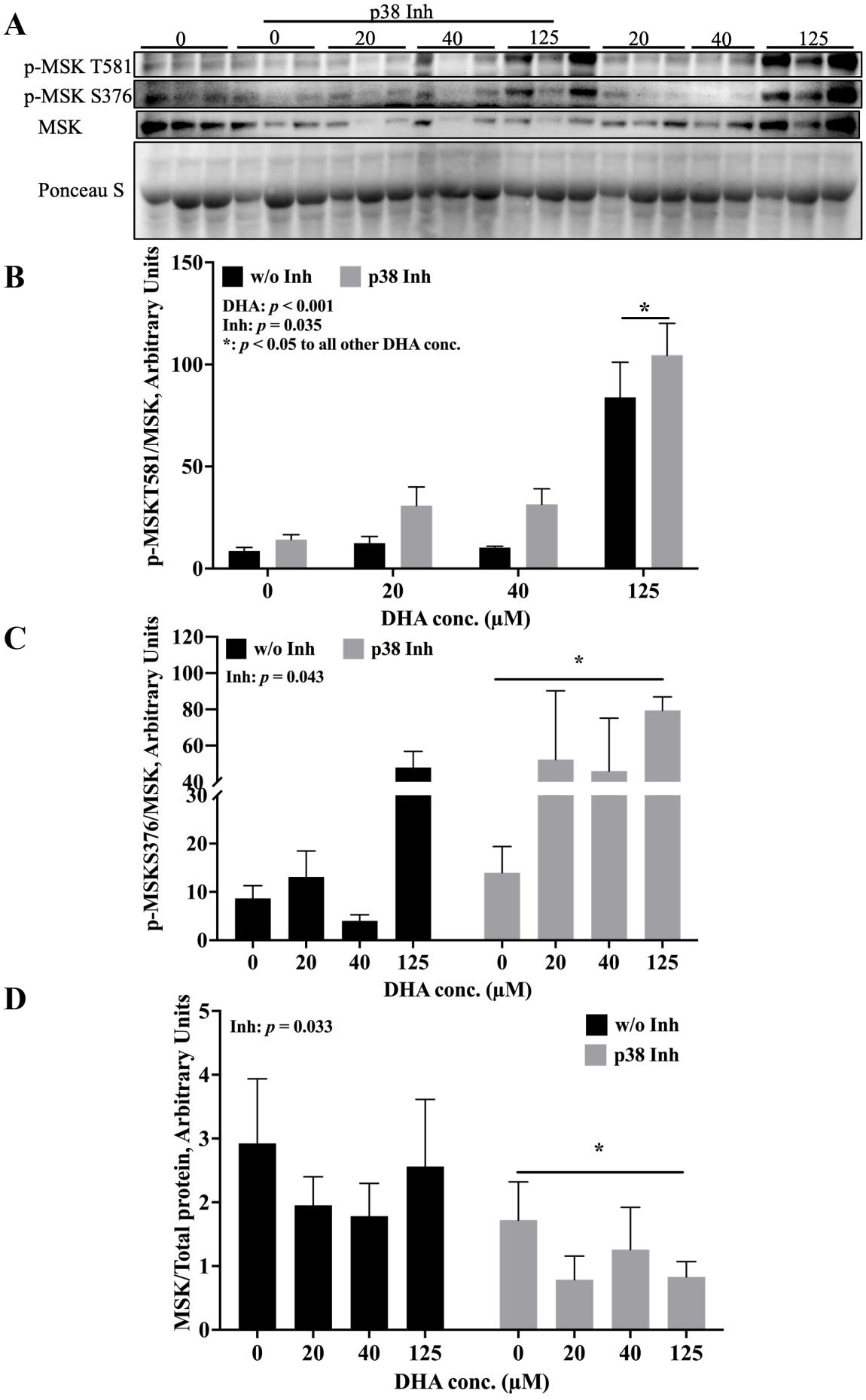
A
p38 Inh
0
0
20
40
125
20
40
125
p-MSK T581
p-MSK S376
MSK
Ponceau S
B
p-MSKT581/MSK, Arbitrary Units
w/o Inh
p38 Inh
DHA: p < 0.001
Inh: p = 0.035
*: p < 0.05 to all other DHA conc.
*
DHA conc. (μM)
C
p-MSKS376/MSK, Arbitrary Units
w/o Inh
p38 Inh
Inh: p = 0.043
*
DHA conc. (μM)
D
MSK/Total protein, Arbitrary Units
Inh: p = 0.033
w/o Inh
p38 Inh
*
DHA conc. (μM)

Figure 11. Effect of DHA and p38 MAPK inhibition on MSK activation in growing cells. Growing EA.hy926 cells were treated with 0, 20, and 125 μM DHA for 8 h with or without the p38 MAPK inhibitor, SB202190 (1 μM). Western blotting was used to measure p-MSK (Thr-581), p-MSK (Ser-376), and total MSK, while Ponceau S staining provided total protein load. The blots (A) show 3 biological replicates per treatment. The band intensities of p-MSK at Thr-581 (B) and Ser-376 (C) were quantified and are graphically presented relative to total MSK band intensity. The total MSK band intensities were quantified and are graphically presented in panel D relative to total protein load. Data are presented as means ± SEM (n=3). The asterisk denotes statistical significance ($p < 0.05$) between different treatment conditions as indicated in the graph. Inh: inhibitor.

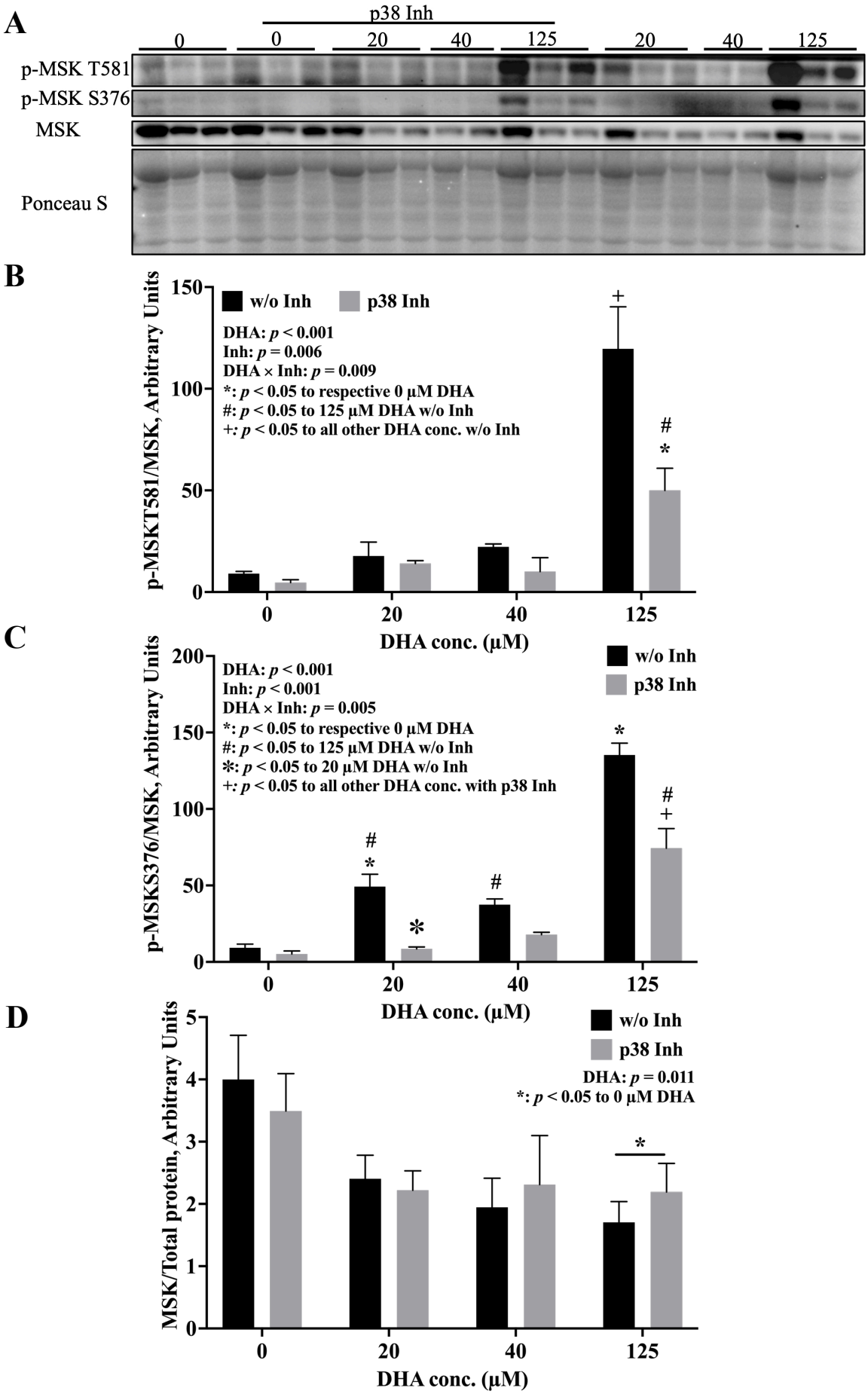
A
p38 Inh
0
0
20
40
125
20
40
125
p-MSK T581
p-MSK S376
MSK
Ponceau S
B
w/o Inh
p38 Inh
DHA: p < 0.001
Inh: p = 0.006
DHA × Inh: p = 0.009
*: p < 0.05 to respective 0 µM DHA
#: p < 0.05 to 125 µM DHA w/o Inh
+: p < 0.05 to all other DHA conc. w/o Inh
p-MSKT581/MSK, Arbitrary Units
DHA conc. (µM)
C
w/o Inh
p38 Inh
DHA: p < 0.001
Inh: p < 0.001
DHA × Inh: p = 0.005
*: p < 0.05 to respective 0 µM DHA
#: p < 0.05 to 125 µM DHA w/o Inh
*: p < 0.05 to 20 µM DHA w/o Inh
+: p < 0.05 to all other DHA conc. with p38 Inh
p-MSKS376/MSK, Arbitrary Units
DHA conc. (µM)
D
w/o Inh
p38 Inh
DHA: p = 0.011
*: p < 0.05 to 0 µM DHA
MSK/Total protein, Arbitrary Units
DHA conc. (µM)

Figure 12. Effect of DHA and p38 MAPK inhibition on MSK activation in quiescent cells.

Quiescent EA.hy926 cells were treated with 0, 20, and 125 μM DHA for 8 h with or without the p38 MAPK inhibitor, SB202190 (1 μM). Western blotting was used to measure p-MSK (Thr-581), p-MSK (Ser-376), and total MSK, while Ponceau S staining provided total protein load. The blots (A) show 3 biological replicates per treatment. The band intensities of p-MSK at Thr-581 (B) and Ser-376 (C) were quantified and are graphically presented relative to total MSK band intensity. The total MSK band intensities were quantified and are graphically presented in panel D relative to total protein load. Data are presented as means ± SEM (n=3). Different symbols denote statistical significance ($p < 0.05$) between different treatment conditions as indicated in the graph. Inh: inhibitor

To examine the link between p38 MAPK and NF-κB in response to DHA, the activation and activity of RelA, a critical NF-κB subunit, was investigated. This was achieved by examining phosphorylation of RelA at Ser-536, the modification that governs NF-κB activation and translocation into nucleus, in response to DHA treatment with or without p38 MAPK inhibition [83]. The results seen in Fig. 13 show slightly fainter bands with DHA-only treatment for both growing (Fig. 13A) and quiescent cells (Fig. 13B), but the quantification and analysis revealed no statistically significant differences for p-RelA levels at the Ser-536 site after normalization (Fig. 13C and D). No differences were observed in total RelA levels in response to DHA or p38 MAPK inhibition (results not shown). This can be interpreted to mean that RelA phosphorylation at Ser-536 is not modulated by p38 MAPK. Also, DHA seemed to have limited effects on the phosphorylation of RelA at Ser-536 in current context.

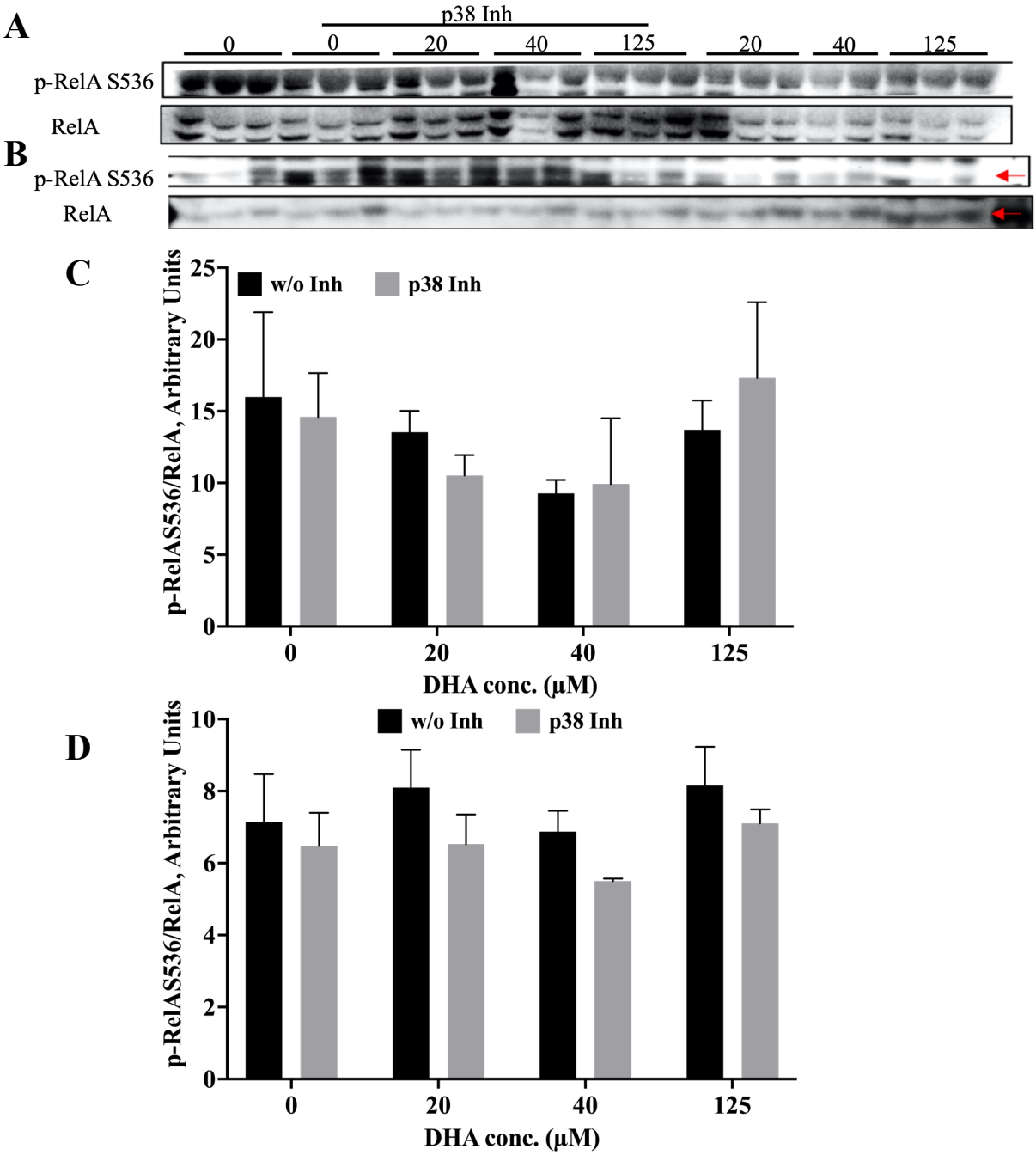

Figure 13. Effect of DHA and p38 MAPK inhibition on RelA phosphorylation at Ser-536 in endothelial cells.

Growing and quiescent EA.hy926 cells were treated with 0, 20, 40, and 125 µM DHA for 8 h with or without the p38 MAPK inhibitor, SB202190 (1 µM). Western blotting was used to measure p-RelA (Ser-536) and total RelA. The blots show 3 biological replicates per treatment in growing cells (A) and quiescent cells (B). The band intensities of p-RelA were quantified and are graphically presented relative to total RelA band intensity in growing cells (C) and quiescent cells (D). Data are presented as means ± SEM (n=3). No statistical significance was detected. Inh: inhibitor.

DHA may affect RelA acetylation via p38 MAPK and MSK

Another important RelA modification that can dictate the transcriptional activity of NF-κB is acetylation at Lys-310 (RelAK310ac). The involvement of p38 MAPK in the acetylation of RelA in response to DHA was examined similar to that of p-RelA Ser-536 with a combined treatment of p38 MAPK inhibitor and DHA on endothelial cells as shown in Fig. 14. From the Western blots, it was apparent that the bands for RelAK310ac were not as intense in the presence of the p38 MAPK inhibitor as the DHA-only treatment counterparts in both growing (Fig. 14A) and quiescent cells (Fig. 14B). For the growing cell condition, although the quantification results agree with what is seen visually, no statistically significant differences were detected for either the effect of DHA nor p38 MAPK inhibition (Fig. 14C). In quiescent cells, however, DHA significantly increased RelAK310ac levels at all 3 concentrations compared to vehicle control, while p38 MAPK inhibition significantly attenuated this induction by DHA at 20 and 40 μM but not 125 μM DHA treatment (Fig. 14D). This showed that in quiescent cells, DHA can induce RelAK310ac via p38 MAPK at lower concentrations (20 and 40 μM) but not at a high concentration of 125 μM, while this modification responded to neither DHA treatment nor p38 MAPK inhibition in growing cells. Therefore, the link between p38 MAPK and NF-κB signaling in response to DHA may partially lie with RelAK310ac but not with p-RelA Ser-536.

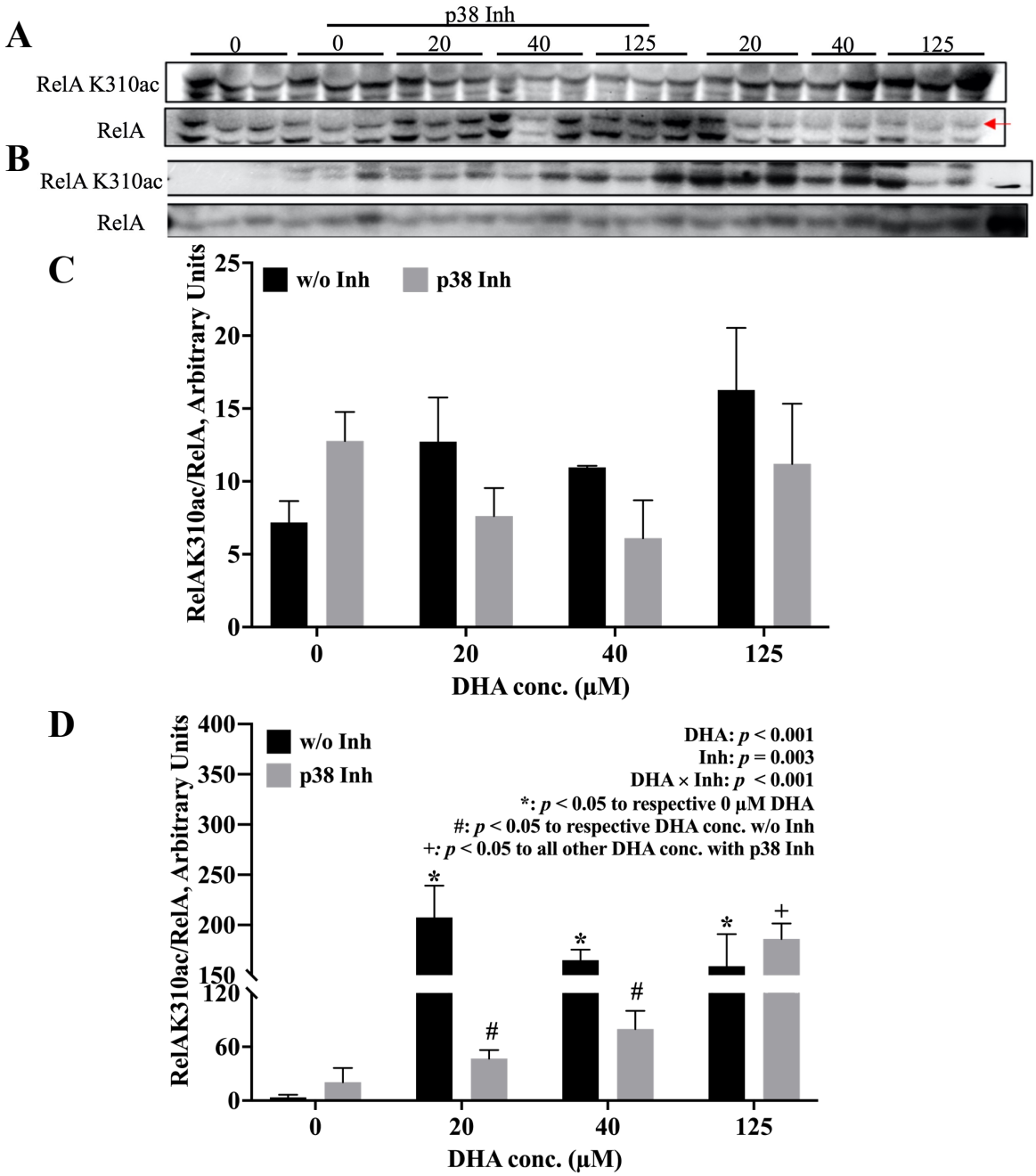

Figure 14. Effect of DHA and p38 MAPK inhibition on RelA acetylation at Lys-310 in endothelial cells.

Growing and quiescent EA.hy926 cells were treated with 0, 20, 40, and 125 μM DHA for 8 h with or without the p38 MAPK inhibitor, SB202190 (1 μM). Western blotting was used to measure RelA K310ac and total RelA. The blots show 3 biological replicates per treatment in growing cells (A) and quiescent cells (B). The band intensities of RelA K310ac were quantified and are graphically presented relative to total RelA band intensity in growing cells (C) and quiescent cells (D). Data are presented as means ± SEM (n=3). Different symbols denote statistical significance ($p < 0.05$) between different treatment conditions as indicated in the graph. Inh: inhibitor.

Apart from directly activating p300 to acetylate RelA [113], p38 MAPK can also induce RelAK310ac via MSK and p-RelA Ser-276: MSK activated by p38 MAPK can directly phosphorylate RelA at Ser-276, which then promotes the binding of CBP/p300 to acetylate RelA at Lys-310 [73,74]. This possibility was explored by examining RelA phosphorylation at Ser-276 and acetylation at Lys-310 in growing (Fig. 15) and quiescent cells (Fig. 16) under combined treatment of MSK inhibition and DHA.

No distinct pattern of band intensities was identified in the blots for growing cells (Fig. 15A), and this is true for DHA-only treatment. No significant effect of DHA was observed on either p-RelA Ser-276 levels (Fig. 15B), nor RelAK310ac (Fig. 15C) levels, consistent with the lack of effect of DHA on RelA acetylation in growing cells as illustrated in Fig. 14C. MSK inhibition was found to suppress both RelA phosphorylation at Ser-276 (Fig. 15B) and RelA acetylation at Lys-310 (Fig. 15C). No significant interaction between DHA and the inhibitor was detected.

Similarly, in quiescent cells, the blots showed no obvious difference in band intensities among different treatments (Fig. 16A), but the quantification revealed more details. When the cells were treated with DHA alone, there was a trend for higher p-RelA Ser-276 levels in 125 μM DHA sample lysates compared to both the 20 μM ($p = 0.052$) and 40 μM ($p = 0.096$) DHA sample lysates as shown in Fig. 16B. When MSK was inhibited, instead of causing suppression as seen in growing cells (Fig. 15B), MSK inhibition significantly elevated p-RelA Ser-276 levels in the presence of 20 and 40 μM DHA (Fig. 16B). Nevertheless, this effect of MSK inhibition was not conveyed to RelAK310ac (Fig. 16C). On the other hand, a trend ($p = 0.075$) for the main effect of DHA concentration was detected for RelA acetylation at Lys-310. And the average RelAK310ac levels with 125 μM DHA were substantially higher compared to those treated with 20 and 40 μM DHA (Fig. 16C). Overall, it was less likely that in quiescent cells, RelAK310ac is stimulated subsequent to p-RelA Ser-276.

In summary, how DHA affects RelA modifications via MSK signaling depends on the endothelial cell growth state. Also, quiescent cells seemed to be more responsive to DHA treatment. However, neither p38 MAPK nor MSK-induced RelA phosphorylation at Ser-276 fully explains the effect of DHA on RelA acetylation at Lys-310. There are therefore other players likely involved.

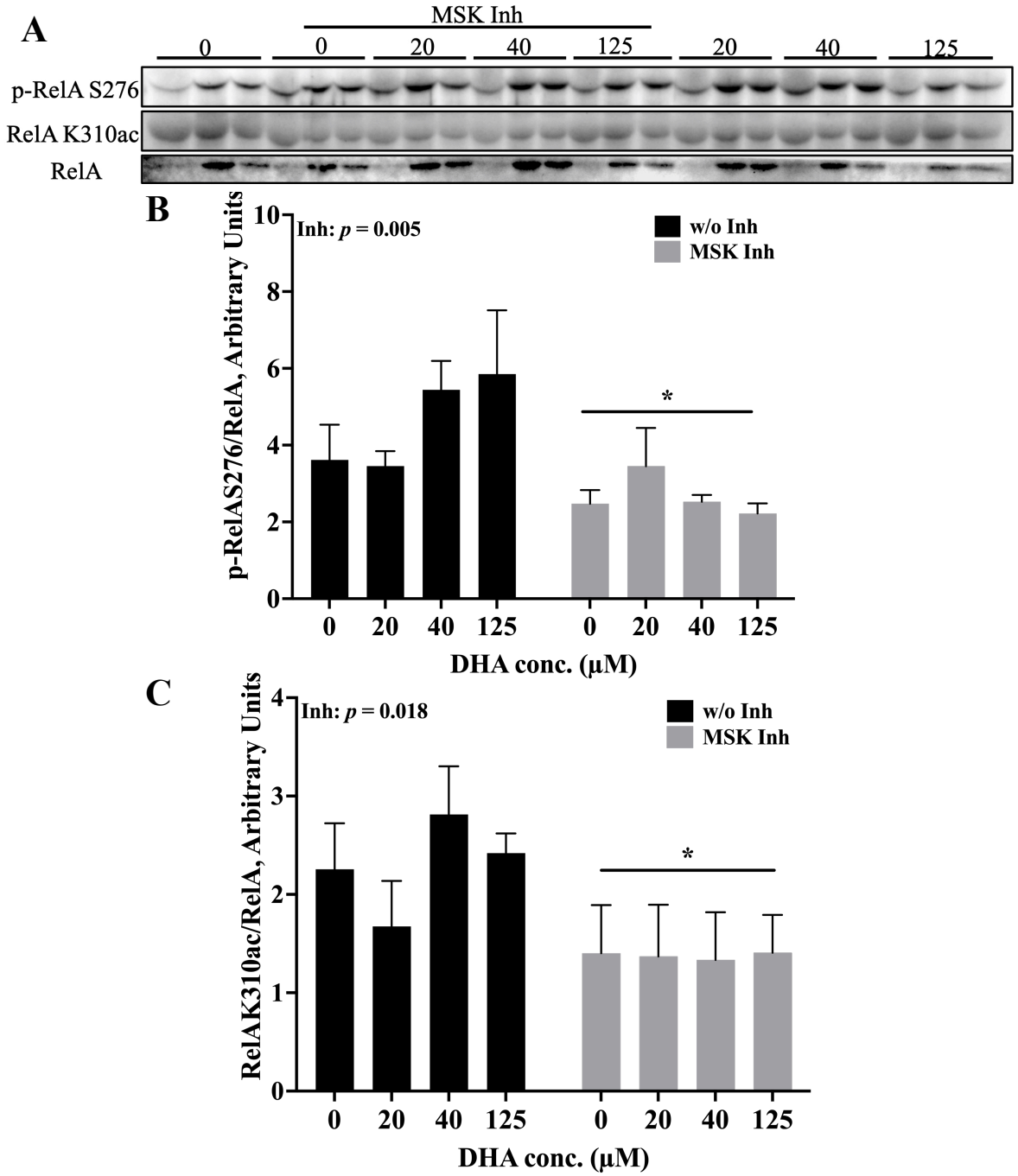

Figure 15. Effect of DHA and MSK inhibition on RelA phosphorylation at Ser-276 and RelA acetylation at Lys-310 in growing cells.

Growing EA.hy926 cells were treated with 0, 20, 40, and 125 μM DHA for 8 h with or without the MSK inhibitor, SB747651A (5 μM). Western blotting was used to measure p-RelA (Ser-276), RelA K310ac, and total RelA. The blots (A) showed 3 biological replicates per treatment. The band intensities of RelA phosphorylation at Ser-276 (B) and acetylation at Lys-310 (C) were quantified and are graphically presented relative to total RelA band intensity. Data are presented as means ± SEM (n=3). The asterisk denotes the statistically significant ($p < 0.05$) main effect of inhibitor. Inh: inhibitor.

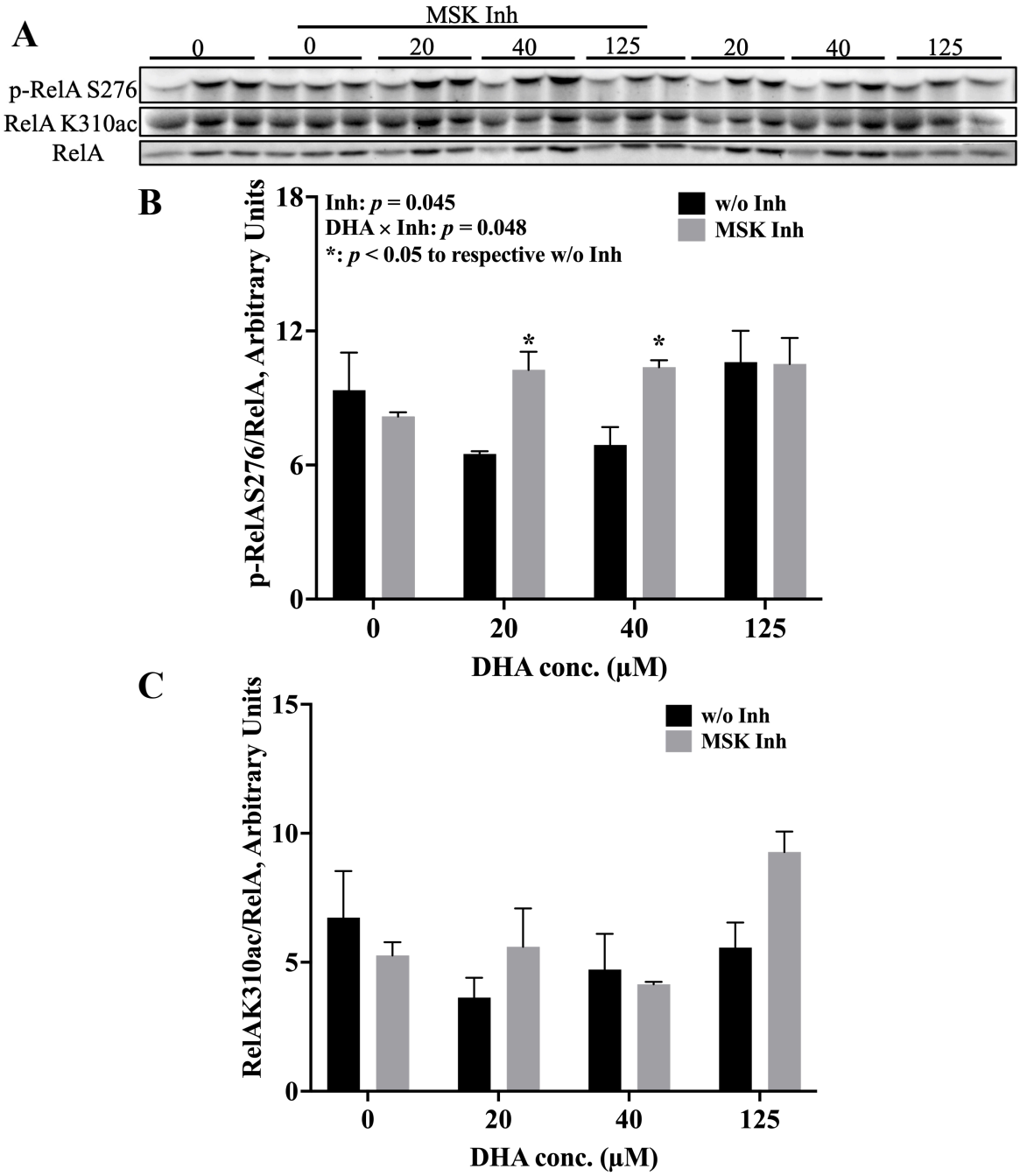

Figure 16. Effect of DHA and MSK inhibition on RelA phosphorylation at Ser-276 and RelA acetylation at Lys-310 in quiescent cells.

Quiescent EA.hy926 cells were treated with 0, 20, 40, and 125 μM DHA for 8 h with or without the MSK inhibitor, SB747651A (5 μM). Western blotting was used to measure p-RelA (Ser-276), RelA K310ac, and total RelA. The blots (A) showed 3 biological replicates per treatment. The band intensities of RelA phosphorylation at Ser-276 (B) and acetylation at Lys-310 (C) were quantified and are graphically presented relative to total RelA band intensity. Data are presented as means ± SEM (n=3). The asterisk denotes statistical significance ($p < 0.05$) between different treatment conditions as indicated in the graph. Inh: inhibitor.

DHA may affect CREB activation and modulate RelA acetylation via CREB/CBP interaction

Another way that CBP can be recruited to acetylate RelA is via an interaction with CREB, which can be activated by MSK. The possible involvement of the CREB/CBP complex in RelA acetylation at Lys-310 was examined using CCII [265].

Visual examination of the Western blots showed that adding CCII to the cells resulted in fainter bands in the presence of DHA compared to the ones without CCII in both growing (Fig. 17A) and quiescent cells (Fig. 17B). Also, concentration-dependent induction of RelAK310ac by DHA can be seen in quiescent cells, together with more intense bands for 0 μM DHA in the presence of CCII when compared to vehicle control without the inhibitor (Fig. 17B). All of these observations were confirmed by quantification (Fig. 17C and D).

In growing cells (Fig. 17C) in the presence of CCII, a high concentration of DHA (125 μM) significantly increased RelAK310ac levels compared to 0 and 20 μM DHA. Furthermore, in the presence of 20 μM DHA, CCII treatment significantly suppressed RelA acetylation at Lys-310 compared to 20 μM DHA alone. In quiescent cells (Fig. 17D), DHA alone induced RelAK310ac in a concentration-dependent manner: DHA significantly increased RelAK310ac levels at 40 and 125 μM, but not 20 μM, compared to the vehicle control. On the other hand, CCII alone significantly induced RelA acetylation at Lys-310, but when DHA was present, CCII curtailed the DHA-increased RelAK310ac levels at 20 and 125 μM DHA. Taken together, DHA may induce RelA acetylation at Lys-30 via CREB/CBP complexes in both growing and quiescent endothelial cells, and this induction is concentration dependent in quiescent cells.

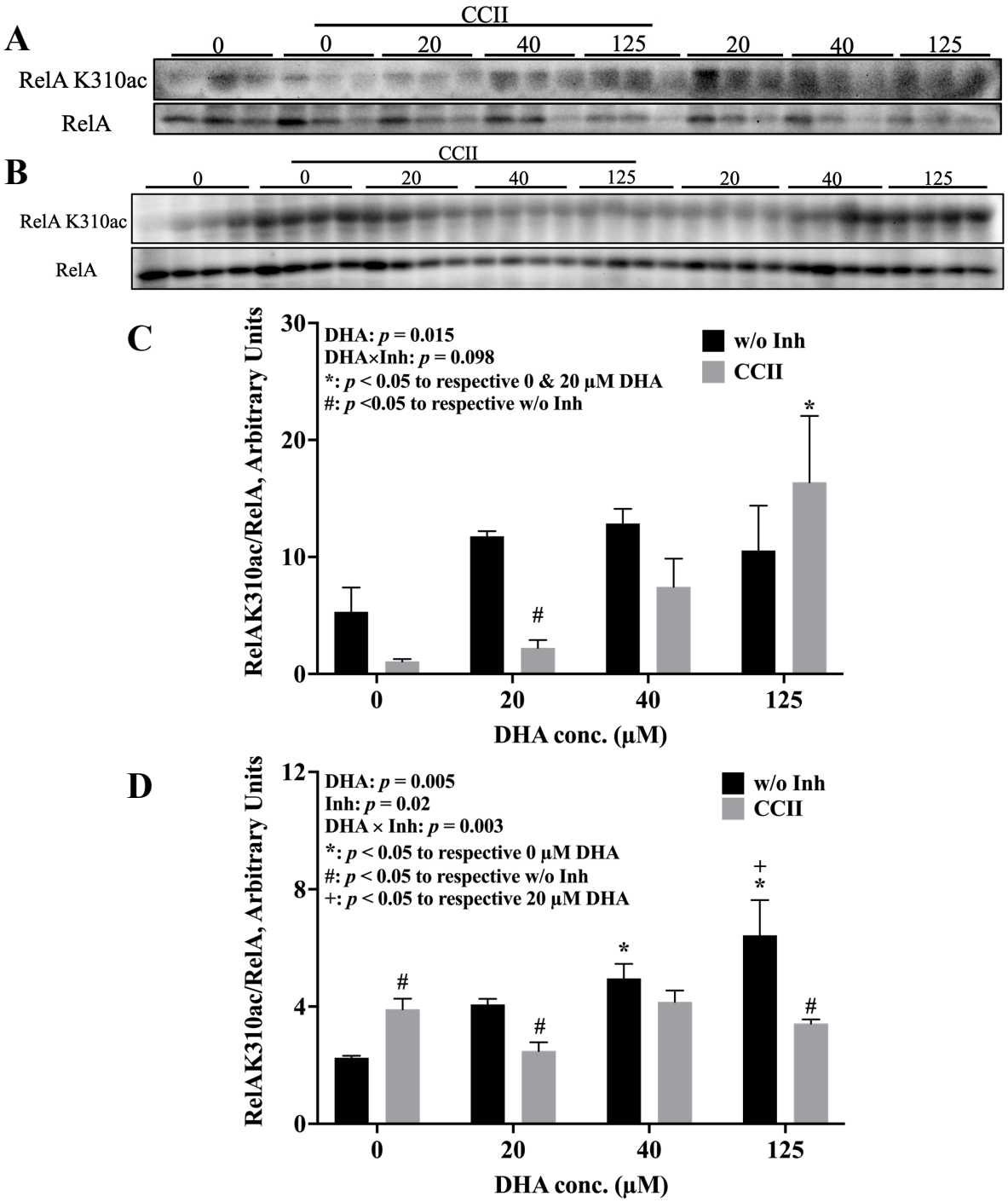

Figure 17. Effect of DHA and CCII on RelA acetylation at Lys-310 in endothelial cells.

Growing and quiescent EA.hy926 cells were treated with 0, 20, and 125 µM DHA for 8 h with or without CCII (20 µM). Western blotting was used to measure RelA K310ac and total RelA. The blots show 3 biological replicates per treatment in growing cells (A) and quiescent cells (B). The band intensities of RelA K310ac were quantified and are graphically presented relative to total RelA band intensity in growing cells (C) and quiescent cells (D). Data are presented as means ± SEM (n=3). Different symbols denote statistical significance ($p < 0.05$) between different treatment conditions as indicated in the graph. Inh: inhibitor.

CREB itself is also an important TF that can modulate the transcription of genes such as *NOS3* [121]. CREB can be activated by phosphorylation at Ser-133 by many kinases including MSK. However, the effect of DHA on CREB activation in endothelial cells has not been studied previously. Whether DHA can modulate CREB activity via MSK was investigated by examining CREB phosphorylation levels at Ser-133 under the combined treatments of DHA and MSK inhibition as illustrated in Fig. 18.

The blots showed that DHA seems to activate CREB in a concentration-dependent manner in growing cells (Fig. 18A), but a concentration-dependent activation was not obvious in quiescent cells except for those treated with 125 μM DHA (Fig. 18B). Also, MSK inhibition substantially reduced the band intensities of p-CREB in both growth states. The quantification analysis agreed with these observations as presented in Fig. 18C and D. Interestingly, in growing cells (Fig. 18C), lower concentrations of DHA (20 and 40 μM) suppressed CREB activation while 125 μM DHA activated CREB compared to vehicle control. These opposite effects of DHA at different concentrations were MSK-dependent, since p-CREB levels were downregulated by MSK inhibition across all DHA treatments. In quiescent cells (Fig. 18D), however, only 125 μM DHA significantly activated CREB compared to all other conditions, while MSK inhibition reduced p-CREB levels compared to cells without inhibitor treatment. Overall, growing cells seems to be more responsive to DHA treatment than quiescent cells, with concentration-dependent differential effects of DHA on p-CREB levels compared to vehicle control. And the CREB phosphorylation was indeed dependent on MSK in both growth states.

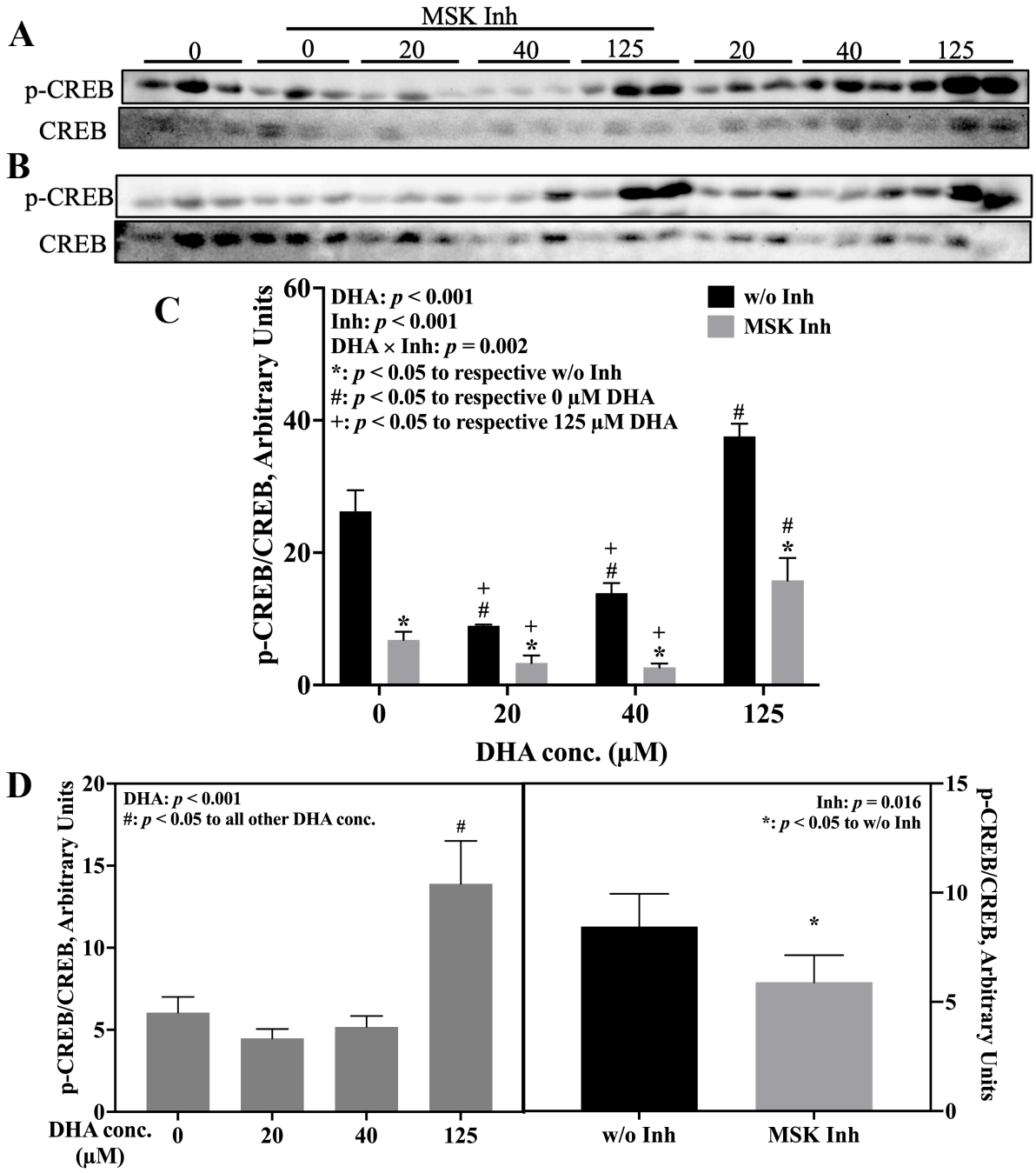

Figure 18. Effect of DHA and MSK inhibition on CREB activation in endothelial cells.

Growing and quiescent EA.hy926 cells were treated with 0, 20, and 125 µM DHA for 8 h with or without the MSK inhibitor, SB747651A (5 µM). Western blotting was used to measure p-CREB (Ser-133) and total CREB in growing cells (A) and quiescent cells (B). The p-CREB (representative of its activation) band intensities were quantified and are graphically presented relative to total CREB band intensity in growing cells (C) and quiescent cells (D). Data are presented as means ± SEM (n=3) in panel C, and for the main effect of DHA concentration (n = 6) and inhibitor (n = 12) in panel D. Different symbols denote statistical significance ($p < 0.05$) between different treatment conditions as indicated in the graph. Inh: inhibitor.

DHA induced histone H3 phosphorylation

Another epigenetic factor that can be regulated by MSK is histone H3 phosphorylation. Histone marks p-H3S10 and p-H3S28, which can be added by MSK, are usually associated with transcriptionally active genes. The effects of DHA on these two histone marks in relation to MSK were examined for both growing cells (Fig 19) and quiescent cells (Fig. 20).

In growing cells, the blots showed that DHA seemed to induce p-H3S10 with no obvious suppression when MSK was inhibited, while p-H3S28 levels seemed to be less affected by either DHA or MSK inhibition except for DHA at 125 μM (Fig. 19A). Quantification confirmed that DHA at 20 and 40 μM significantly increased p-H3S10 levels but not at 125 μM compared to vehicle control, whereas the high concentration (125 μM) of DHA significantly induced p-H3S10 with MSK inhibition compared to all DHA concentrations in the presence of the inhibitor (Fig. 19B). There was a trend ($p = 0.08$) for elevated p-H3S10 levels with MSK inhibition alone, and a trend ($p = 0.061$) for suppression of 20 μM DHA-induced p-H3S10 in the presence of the MSK inhibitor. With respect to H3S28 phosphorylation status (Fig. 19C), 125 μM DHA significantly elevated p-H3S28 levels compared to the other 3 DHA treatments, both in the absence and in the presence of the MSK inhibitor. MSK inhibition further increased p-H3S28 levels in the presence of 40 μM and 125 μM DHA compared to their respective DHA-alone treatment controls. The increasing instead of decreasing H3 phosphorylation caused by MSK inhibition may reflect the involvement of other writers of p-H3S10 and p-H3S28 that respond to DHA at high concentration to compensate for the loss of MSK function. Alternatively, MSK inhibition may suppress the activity of some erasers that can be modulated by DHA.

Similar patterns in the Western blot results were observed in quiescent cells (Fig. 20A) compared to growing cells (Fig. 19A). H3S10 phosphorylation (Fig. 20B) was increased by MSK inhibition and by 20 μM DHA. Also, 125 μM DHA significantly induced p-H3S28, while 40 μM DHA showed a trend ($p = 0.065$) for p-H3S28 induction when compared to vehicle control (Fig. 20C). MSK inhibition did not affect p-H3S28 in quiescent cells. According to these results, DHA and MSK seem to function independently of each other in quiescent cells with respect to the regulation of the two H3 phosphorylation marks.

Taken together, the lower concentration of DHA (20 μM) was found to induce p-H3S10 but not p-H3S28, while the opposite was observed for the high concentration of DHA (125 μM) in both growth states. While only the 20 μM DHA-induced p-H3S10 in growing cells was dependent on MSK, MSK inhibition elevated H3 phosphorylation levels at both Ser-10 and

Ser-28 sites in growing cells when treated with 125 μM DHA, and also elevated p-H3S10 levels in quiescent cells independent of DHA.

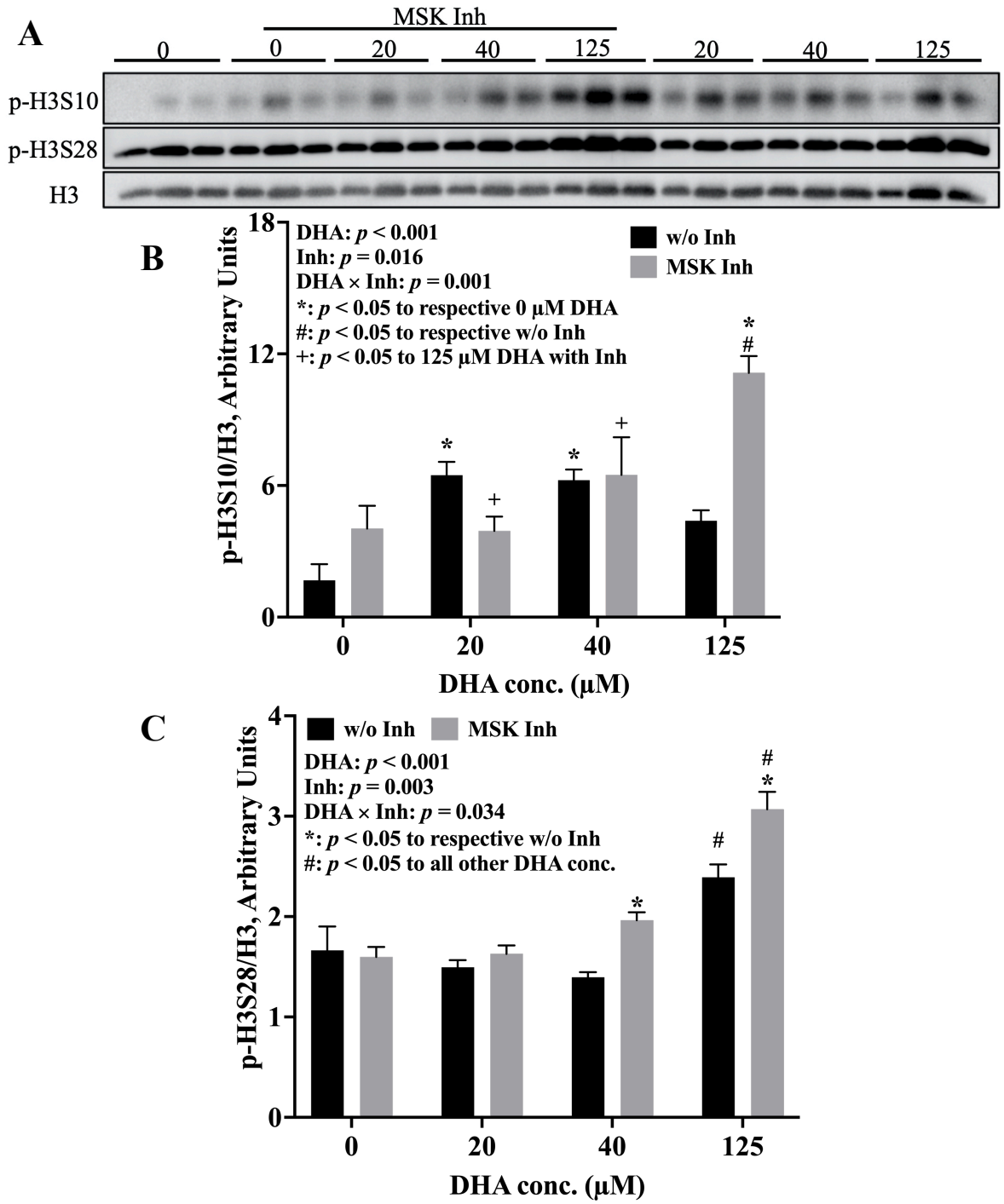

Figure 19. Effect of DHA and MSK inhibition on p-H3S10 and p-H3S28 in growing cells.

Growing EA.hy926 cells were treated with 0, 20, 40, and 125 µM DHA for 8 h with or without the MSK inhibitor, SB747651A (5 µM). Western blotting was used to measure p-H3 (Ser-10), p-H3 (Ser-28), and total H3. The blots (A) showed 3 biological replicates per treatment. The band intensities of p-H3 at Ser-10 (B) and Ser-28 (C) were quantified and are graphically presented relative to total H3 band intensity. Data are presented as means ± SEM (n=3). Different symbols denote statistical significance ($p < 0.05$) between different treatment conditions as indicated in the graph. Inh: inhibitor.

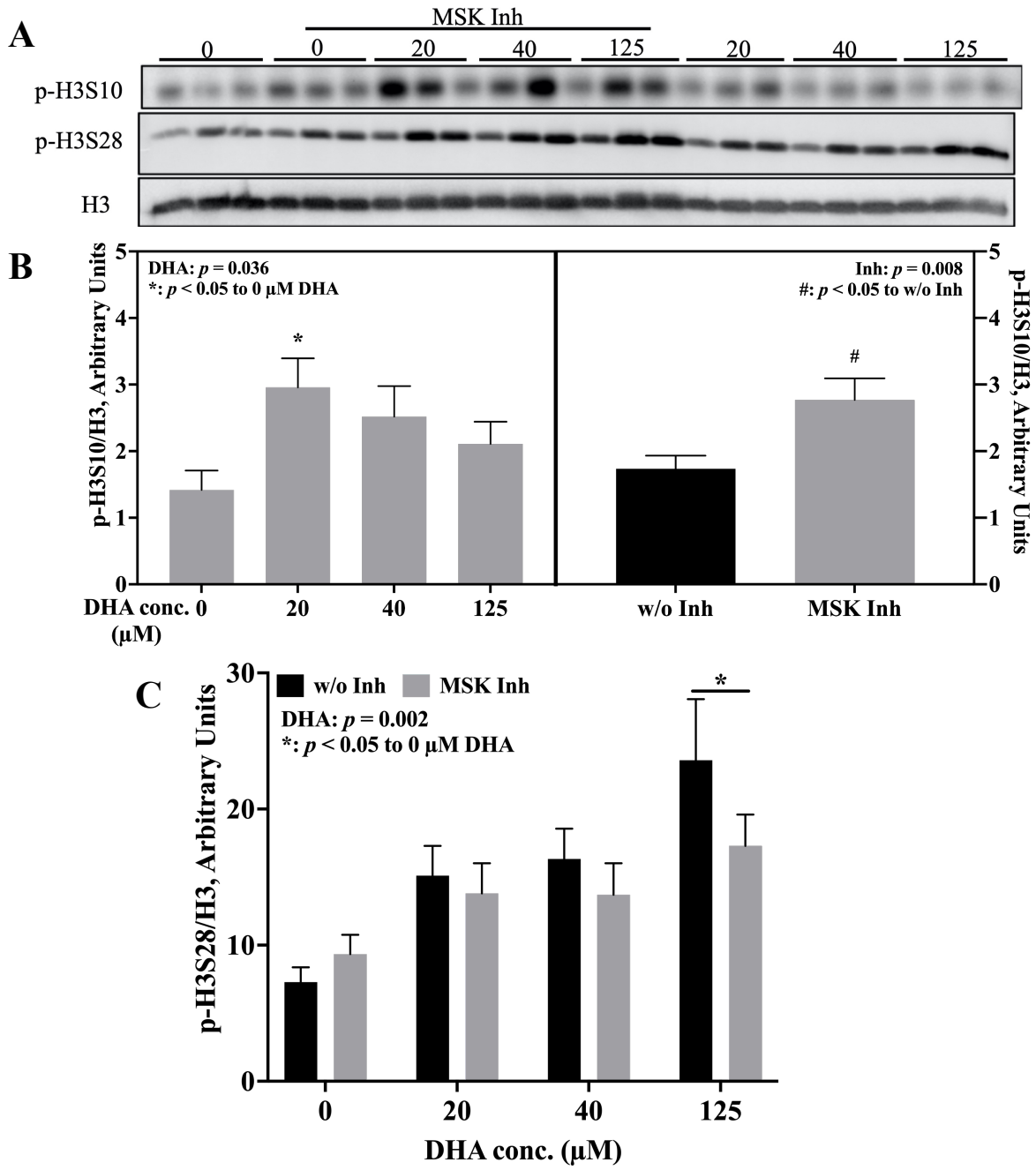

Figure 20. Effect of DHA and MSK inhibition on p-H3S10 and p-H3S28 in quiescent cells.

Quiescent EA.hy926 cells were treated with 0, 20, 40, and 125 µM DHA for 8 h with or without the MSK inhibitor, SB747651A (5 µM). Western blotting was used to measure p-H3 (Ser-10), p-H3 (Ser-28), and total H3. The blots (A) showed 3 biological replicates per treatment. The band intensities of p-H3 at Ser-10 (B) and Ser-28 (C) were quantified and are graphically presented relative to total H3 band intensity. Data are presented as means ± SEM for the main effect of DHA concentration (n= 6) and inhibitor (n = 12) in panel B, and as means ± SEM (n=3) in panel C. Different symbols denote statistical significance ($p < 0.05$) between different treatment conditions as indicated in the graph. Inh: inhibitor

DHA affected cell cycling

There are reports that DHA may cause cell cycle arrest in various cells and thus prevent cell proliferation [211,271–274], a key feature of active endothelial cells. Here, cell cycle analysis was done using flow cytometry with PI staining to assess the possible effects of DHA.

The data in Fig. 21A – D demonstrate that there were clear differences in the cell cycle profiles of the two growth states of EA.hy926 cells. There were fewer cells in the sub G0/G1 phase in quiescent cells (1.88% ± 0.31) compared to growing cells (2.76% ± 0.60, Fig. 21A), with about 10% more cells in the G0/G1 phase in quiescent cells (88.33% ± 0.49) compared to growing cells (71.29% ± 1.55, Fig. 21B). Also, the percentages of cells in S phase (2.26% ± 0.13 vs. 11.45% ± 0.69, Fig. 21C) and G2/M phase (5.77% ± 0.20 vs. 10.68% ± 0.91, Fig. 21D) were much lower in quiescent cells. This indicates that in the quiescent state (day 10), the cells were arrested in the G0/G1 phase and were not actively cycling as in the growing state (day 4). Also, the cells were protected from apoptosis in the quiescent state, based on analysis of the sub G0/G1 phase region which usually denotes apoptosis [275]. In this set of analyses, DHA showed little effect on cell cycle progression, except that 125 μM DHA increased the percentage of cells in the sub G0/G1 phase (Fig. 21A) compared to vehicle control in growing cells but not quiescent cells. Therefore, at high concentrations (125 μM), DHA may induce apoptosis in growing endothelial cells only.

Cell cycle progression can be affected by p38 MAPK via cyclin D1 [58,98], and there was time-dependent activation of p38 MAPK by DHA in quiescent endothelial cells that differed from the p38 MAPK activation pattern in growing cells, as well as the activation patterns of other MAPKs by DHA [6]. This time- and growth-state-dependent p38 MAPK activation pattern in response to DHA is shown in Fig. 3 as well. Therefore, the effects of DHA on the cell cycle profile of quiescent cells were examined closely by treating day 10 (quiescent) cells with 2 different concentrations (20 and 125 μM) DHA for 2 durations (2 and 8 h) as illustrated in Fig. 22. The low concentration of DHA (20 μM) significantly reduced the number of apoptotic cells after 8 h of treatment as indicated by the sub G0/G1 results (Fig. 22A) compared to both vehicle control and 125 μM DHA treatment. There was also a trend (p = 0.058) for a lower percentage of cells in the sub G0/G1 phase with 125 μM DHA at 2 h treatment compared to 8 h treatment time. In S phase (Fig. 22C), there was a lower percentage of cells at 2 h compared to 8 h (1.63% ± 0.21 vs. 2.05% ± 0.11, respectively), regardless of DHA concentration, while the low concentration (20 μM) of DHA had a lower percentage of cells compared to vehicle control, regardless of treatment time. This indicates that 20 μM DHA

may suppress DNA synthesis thus lowering the number of cells in S phase, given that 2 h treatment time may be limited for cell cycle progression. In addition, there was a trend (p = 0.057) for fewer cells in S phase with 125 μM DHA compared to vehicle control, and a trend (p = 0.09) for more cells in S phase with 125 μM DHA compared to 20 μM DHA. No significant difference was observed in G0/G1 phase (Fig. 22B) or G2/M phase (Fig. 22D). Taken together, in quiescent cells, 20 μM DHA may protect cells against apoptosis and may also prevent G1-to-S phase transition and/or suppress DNA synthesis, thus reducing the percentage of cells in S phase. The high concentration (125 μM) of DHA showed a subtle time-dependent effect on apoptosis in quiescent endothelial cells but in general 125 μM DHA did not protect the cells from apoptosis. At this concentration (125 μM), DHA might also affect G1-to-S phase transition and/or DNA synthesis but not as effectively as 20 μM DHA treatment.

Overall, the cell cycle analysis results supported the view that EA.hy926 cells at day 10 resemble the quiescent state. A high concentration of DHA (125 μM) induced apoptosis in growing cells but not quiescent cells when treated for 8 h, while a lower concentration of DHA (20 μM) showed an apoptosis-protective effect in quiescent cells regardless of treatment time. Also, the effect of DHA on cell cycle progression is time- and concentration-dependent in quiescent cells.

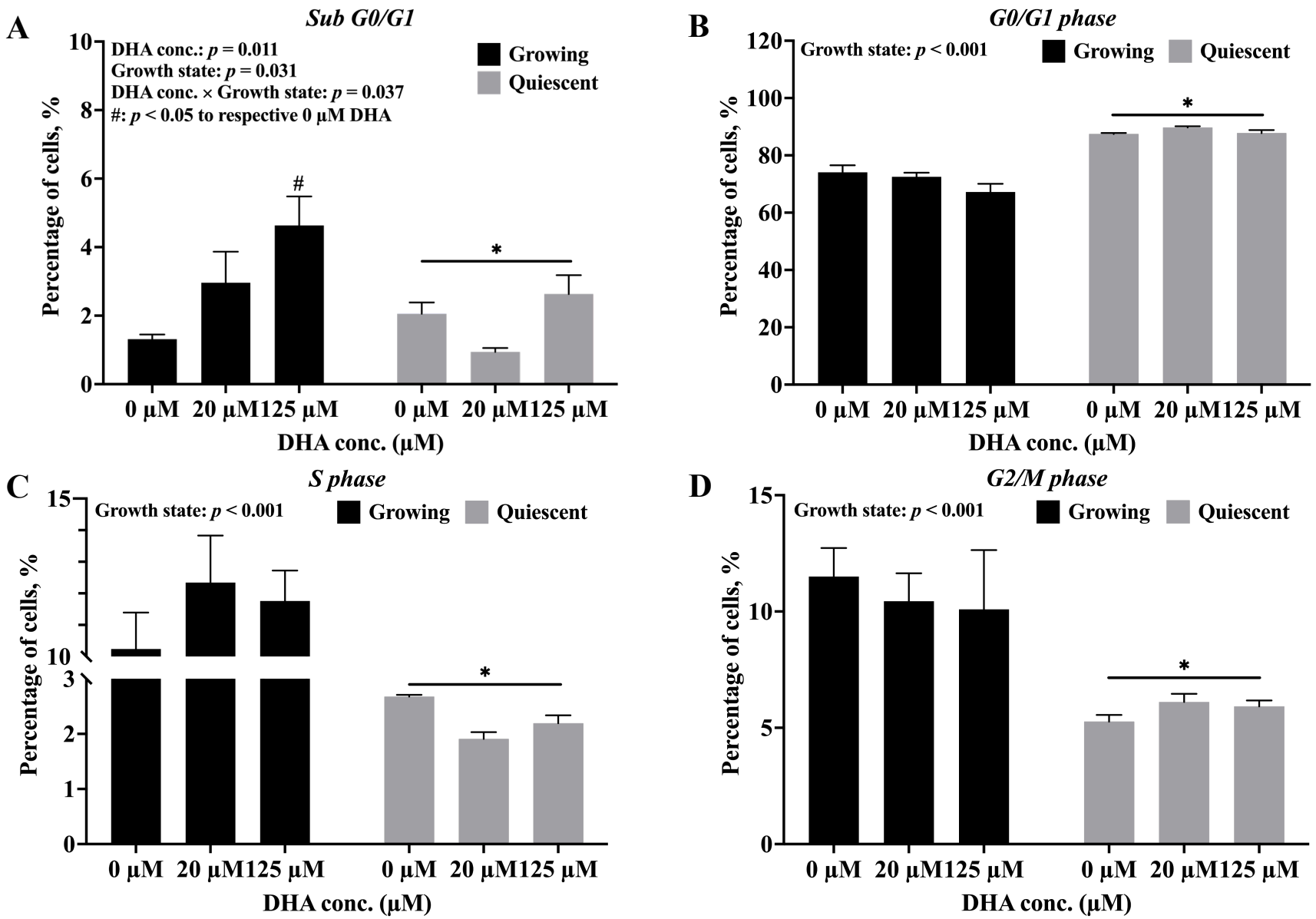
A
Sub G0/G1
DHA conc.: p = 0.011
Growth state: p = 0.031
DHA conc. × Growth state: p = 0.037
#: p < 0.05 to respective 0 μM DHA
Growing
Quiescent
Percentage of cells, %
0 μM 20 μM 125 μM 0 μM 20 μM 125 μM
DHA conc. (μM)
B
G0/G1 phase
Growth state: p < 0.001
Growing
Quiescent
Percentage of cells, %
0 μM 20 μM 125 μM 0 μM 20 μM 125 μM
DHA conc. (μM)
C
S phase
Growth state: p < 0.001
Growing
Quiescent
Percentage of cells, %
0 μM 20 μM 125 μM 0 μM 20 μM 125 μM
DHA conc. (μM)
D
G2/M phase
Growth state: p < 0.001
Growing
Quiescent
Percentage of cells, %
0 μM 20 μM 125 μM 0 μM 20 μM 125 μM
DHA conc. (μM)

Figure 21. Effect of DHA on the cell cycle of growing and quiescent endothelial cells.

Growing and quiescent EA.hy926 cells were treated with 0, 20, and 125 μM DHA for 8 h before fixation with ethanol and analysis by flow cytometry after PI staining. The percentages of cells in the subG0/G1 (A), G0/G1 (B), S (C), and G2/M (D) phases were calculated by the software and are presented graphically. All data are presented as means ± SEM (n=3). The asterisk denotes the statistically significant ($p < 0.05$) main effect of growth state while the pound sign denotes statistical significance ($p < 0.05$) to 0 μM DHA in growing cells.

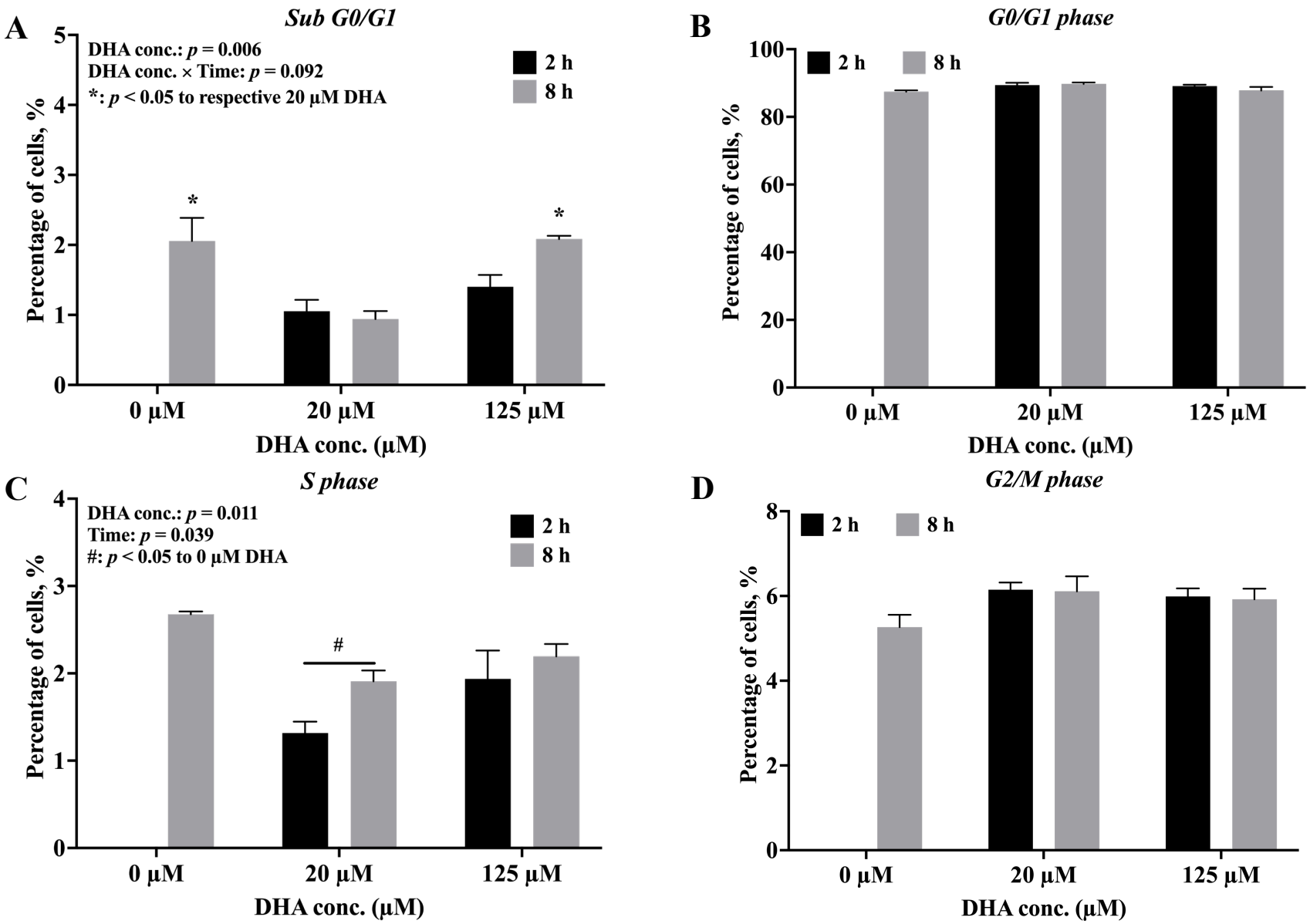
A
Sub G0/G1
DHA conc.: p = 0.006
DHA conc. × Time: p = 0.092
*: p < 0.05 to respective 20 µM DHA
2 h
8 h
Percentage of cells, %
0 µM
20 µM
125 µM
DHA conc. (µM)
B
G0/G1 phase
C
S phase
DHA conc.: p = 0.011
Time: p = 0.039
#: p < 0.05 to 0 µM DHA
D
G2/M phase

Figure 22. Effect of DHA on the cell cycle of growing and quiescent endothelial cells.

Quiescent EA.hy926 cells were treated with 20 or 125 μM DHA for 2 h or 8 h before fixation with ethanol and analysis by flow cytometry after PI staining. The percentages of cells in the subG0/G1 (A), G0/G1 (B), S (C), and G2/M (D) phases were calculated by the software and are presented graphically. All data are presented as means ± SEM (n=3). Different symbols denote statistical significance ($p < 0.05$) between different treatment conditions as indicated in the graph.

Cyclin D can serve as a bridge between extracellular signals and cell cycle progression [92]. Its expression can be suppressed by p38 MAPK [58], in parallel with p38 MAPK promoting cyclin D1 degradation [98]. DHA might regulate the cell cycle as shown previously (Fig. 21) via cyclin D and p38 MAPK. The effects of DHA on cyclin D1 were therefore examined with and without p38 MAPK inhibition (Fig. 23 and 24).

Thr-286 phosphorylation on cyclin D1 dictates its proteasomal degradation. The blots showed that in both growing (Fig. 23A) and quiescent (Fig. 23B) cells, the p-cyclin D1 band intensities of p38 MAPK inhibited sample lysates were higher than those with DHA treatment only, and 125 μM DHA in conjunction with the p38 MAPK inhibitor further increased p-cyclin D1 band intensity. Quantification of the growing cell (Fig. 23C) and quiescent cell (Fig. 23D) results agreed with these observations. DHA-alone treatment had no effect on p-cyclin D1 levels in both growth states. When p38 MAPK was inhibited, however, 125 μM DHA significantly elevated p-cyclin D 1 levels in growing cells. There was even a concentration-dependent increase in cyclin D1 phosphorylation induced by DHA under p38 MAPK inhibition in quiescent cells (Fig. 23D): 40 μM DHA elevated p-cyclin D1 levels compared to 0 and 20 μM but the levels were still significantly lower than those induced by 125 μM DHA.

Cyclin D1 protein levels were analyzed as well (Fig. 24). The expression of cyclin D1 was unchanged in growing cells based on visual examination of the blots (Fig. 24A), while the band intensities of 125 μM DHA treated samples were lower than those treated with other concentrations (0, 20, and 40 μM) of DHA in quiescent cells (Fig. 24B). The quantification results shown in Fig. 24C confirmed that DHA and p38 MAPK had no effect on cyclin D1 protein levels in growing endothelial cells. In quiescent cells, on the other hand, apart from a decrease in cyclin D1 levels with 125 μM DHA, DHA at a lower concentration (20 μM) was found to increase cyclin D1 levels (Fig. 24D). The decrease or increase of cyclin D1 protein levels in response to DHA was greater when p38 MAPK was functional. Also, the effect at 20 μM DHA was found to be p38 MAPK dependent.

In summary, DHA may be able to regulate both cyclin D1 proteasomal-related turnover and its total protein level, and these actions of DHA are dependent on p38 MAPK signaling and DHA concentration.

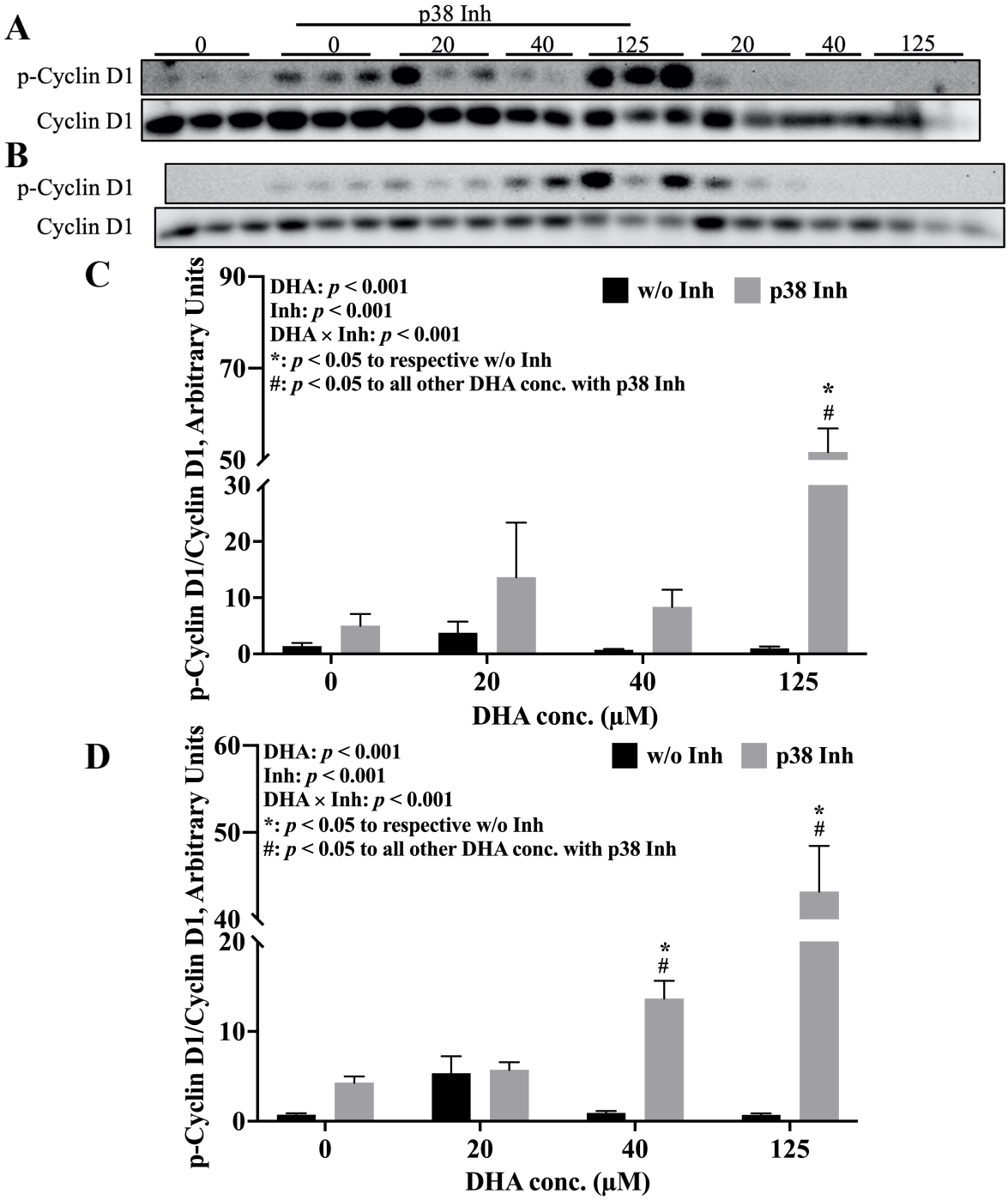

Figure 23. Effect of DHA and p38 MAPK inhibition on p-cyclin D1 in endothelial cells.

Growing and quiescent EA.hy926 cells were treated with 0, 20, 40, and 125 μM DHA for 8 h with or without the p38 MAPK inhibitor, SB202190 (1 μM). Western blotting was used to measure p-cyclin D1 (Thr-286) and total cyclin D1 in growing cells (A) and quiescent cells (B). The band intensities of p-cyclin D1 were quantified and are graphically presented relative to total cyclin D1 band intensity in growing cells (C) and quiescent cells (D). Data are presented as means ± SEM (n=3). Different symbols denote statistical significance ($p < 0.05$) between different treatment conditions as indicated in the graph. Inh: inhibitor.

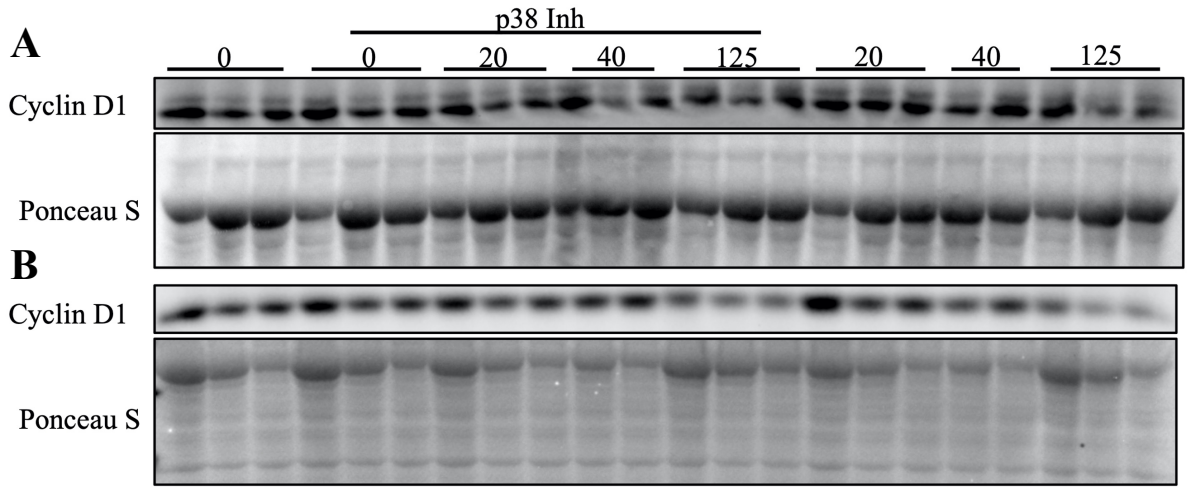
A
p38 Inh
0
0
20
40
125
20
40
125
Cyclin D1
Ponceau S
B
Cyclin D1
Ponceau S

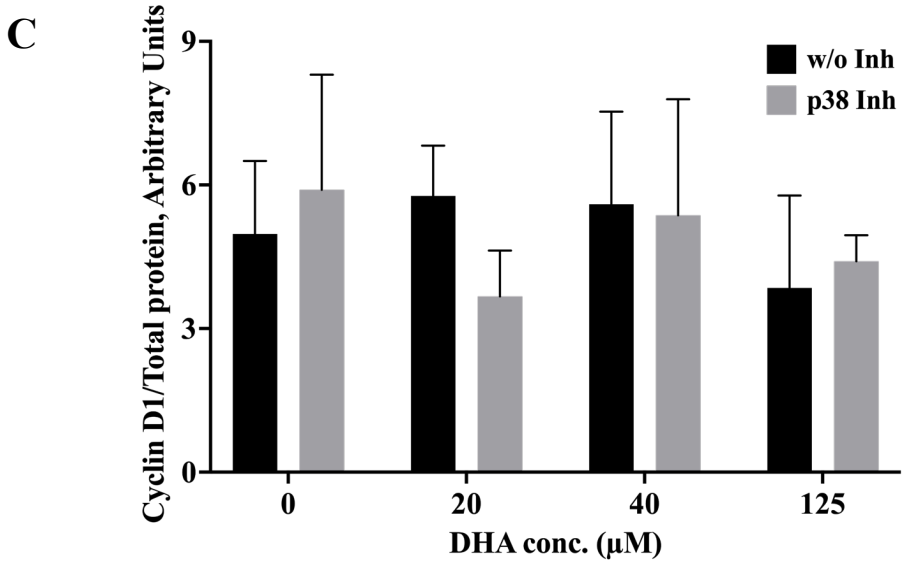
C
Cyclin D1/Total protein, Arbitrary Units
9
6
3
0
w/o Inh
p38 Inh
0
20
40
125
DHA conc. (μM)

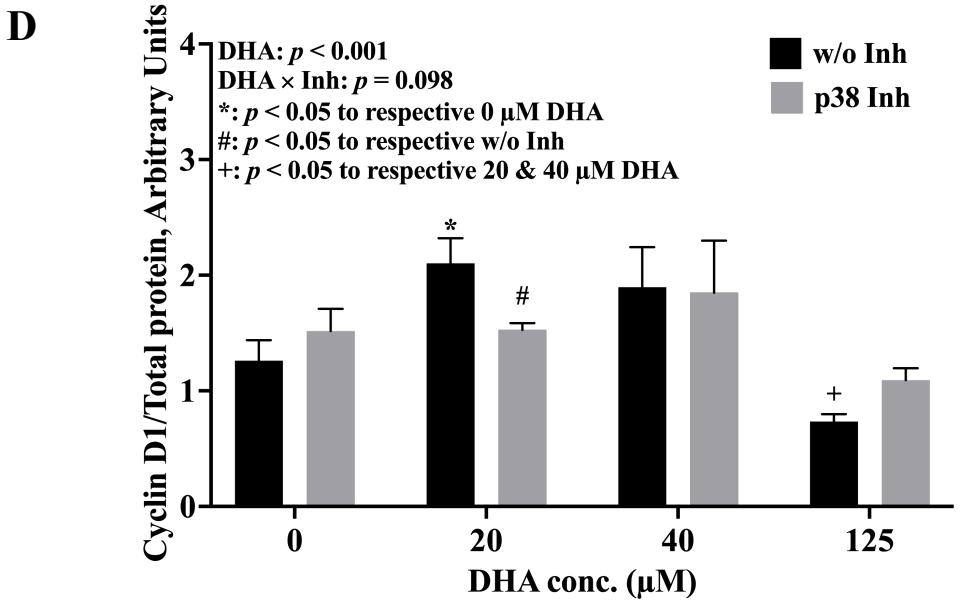
D
Cyclin D1/Total protein, Arbitrary Units
4
3
2
1
0
DHA: p < 0.001
DHA × Inh: p = 0.098
*: p < 0.05 to respective 0 μM DHA
#: p < 0.05 to respective w/o Inh
+: p < 0.05 to respective 20 & 40 μM DHA
w/o Inh
p38 Inh
*
#
+
0
20
40
125
DHA conc. (μM)

Figure 24. Effect of DHA and p38 MAPK inhibition on total cyclin D1 protein levels in endothelial cells.

Growing and quiescent EA.hy926 cells were treated with 0, 20, 40, and 125 μM DHA for 8 h with or without the p38 MAPK inhibitor, SB202190 (1 μM). Western blotting was used to measure total cyclin D1 relative to total protein load (Ponceau S staining). The blots show 3 biological replicates per treatment in growing cells (A) and quiescent cells (B). The total cyclin D1 band intensities were quantified and are graphically presented relative to total protein load in growing cells (C) and quiescent cells (D. Data are presented as means ± SEM (n=3). Different symbols denote statistical significance ($p < 0.05$) between different treatment conditions as indicated in the graph. Inh: inhibitor.

DISCUSSION

This study is the first to explore the potential atheroprotective effect of DHA on endothelial cells in two different growth states. We also studied the possible epigenetic and transcriptional players involved with the aim of identifying plausible mechanisms of action for DHA on endothelial cell properties. In general, DHA was found to activate eNOS, mediate eNOS expression, regulate the transactivation of NF-κB as well as CREB, influence histone H3 phosphorylation status, and affect cell cycling as well as cyclin D1 expression levels. Most of these effects of DHA showed concentration-, treatment time-, and endothelial cell growth state-dependency. Specifically, as summarized in Table 4, after 8 h of DHA treatment, a lower concentration of DHA (20 μM) upregulated both eNOS activation and expression, downregulated the activities of NF-κB and CREB, increased H3 phosphorylation at Ser-10, decreased the number of cells in sub G0/G1 phase and S phase, and increased the amount of cyclin D1 expressed. In contrast, a higher concentration of DHA (125 μM) had mainly the opposite effects, as shown by downregulation of eNOS expression, increased NF-κB and CREB transactivation, more cells in sub G0/G1 phase, lower cyclin D1 expression levels, and induction of H3 phosphorylation at Ser-28.

Table 4. A summary of DHA effects at 20 μM and 125 μM for 8 h in growing and quiescent endothelial cells.[1]

DHA for 8 h	20 μM		125 μM	
	Growing	**Quiescent**	**Growing**	**Quiescent**
p-eNOS	~	up	~	~
eNOS	up	up	down	down
Cell cycle	~	Sub G0/G1 & S down	Sub G0/G1 up	~
Cyclin D1		up		down
RelAS276ph	~	Down[2]	~	~
RelAK310ac	~	~	~	up
p-CREB	down	~	up	up
H3S10ph	up	up	~	~
H3S28ph	~	~	up	up

[1]All changes were significant and compared to respective control conditions unless otherwise stated; "~" means no significant difference observed.

[2]The change was compared to 125 μM DHA with a trend ($p = 0.052$).

Interestingly, according to Table 4, quiescent endothelial cells seem to be slightly more responsive to DHA than growing cells, especially at 20 μM. Modulation of the activities and/or expression of these key proteins by DHA occurred in part via p38 MAPK, with MSK also having a role. But DHA was unlikely to exert its effects on endothelial function through a linked p38 MAPK/MSK signaling pathway.

Effects of DHA on eNOS and cell cycle profile

As described in the Literature Review, eNOS activity and eNOS uncoupling play an important role in ED [3]. Cell proliferation is another critical process that mediates the progression of atherosclerosis [276]. While DHA has been reported to affect eNOS activity [240,254,277] and cell cycling [211,261,278] in various cell models, no study has systematically explored the effects of concentration and treatment time of DHA on both parameters concurrently, let alone in two different endothelial cell growth states.

In this study, we found that DHA may differentially activate eNOS, as measured by eNOS Ser-1177 phosphorylation, depending on time, concentration, and growth state as illustrated in Fig. 3. The maximum effect of DHA on eNOS phosphorylation seemed to occur at 2 - 4 h or 16 - 24 h in growing cells, but 8 h in quiescent cells, after treatment with 20 μM. The data from growing cells match the citrulline assay results obtained by Li et al. [279], which showed, compared to other concentrations (0 - 75 μM), that 25 μM DHA significantly increased the catalytic ability of eNOS almost 2-fold after treatment for 24 h. DHA at a concentration close to 20 μM (12 μM) was found to elevate p-eNOS Ser-1177 levels 48 h after treatment as well [280]. Increased eNOS phosphorylation at this site can also be triggered by treatment with 20 - 80 μM DHA for 24 h in EA.hy926 cells [281]. Although we did not find significant activation of eNOS by DHA lower than 20 μM for the time tested (8 h), longer treatment times of 24 h with 3 and 10 μM of DHA [254] as well as 48 h with 10 μM of DHA [282] were found to increase NO production by the nitrite/nitrate assay. Chronic treatment for 7 days with even lower DHA concentrations (5 and 50 nM) increased both eNOS phosphorylation and NO production [277]. The cell models used in all of these studies were either primary endothelial cell lines like HCAEC, or immortalized ones like EA.hy926, but grown in the absence of an extracellular matrix coating. Under this condition, the cells do not reach quiescence even when they are confluent [5]. Therefore, literature for comparison with the results we obtained with quiescent cells grown on MG is very limited. What is clear is that eNOS exhibited distinct phosphorylation patterns in response to DHA in growing and quiescent cells. While the evidence for low concentrations of DHA activating eNOS is strong, data for

higher DHA concentrations (>100 μM) on eNOS activation are scarce. Only Chao et al. [253] reported that DHA at 100 μM for 8 h may decrease VEGF-induced eNOS phosphorylation, thus reducing cell migration. However, they did not test the effect of DHA alone. This lack of data may be due to the apoptosis-triggering property of DHA at higher concentrations (≥100 μM for ≥8 h) [253,255,263,283]. In addition, our data showed that at those higher concentrations (125 and 150 μM), DHA had a limited effect on eNOS activation in comparison to 20 μM, especially in quiescent cells.

Detecting eNOS phosphorylation, especially at Ser-1177, using Western blotting is the most commonly used method to study eNOS activation, since it is correlated with its NO-producing activity. The importance and physiological relevance of Ser-1177 (human site, corresponding to Ser-1176 in mouse) phosphorylation has been established *in vivo* using transgenic mice expressing either a phosphomimic form (S1176D, serine to aspartate mutation) or a phospho-null form (S1176A, serine to alanine mutation) of eNOS. Mice with the S1176D mutation showed improved endothelial-dependent vasomotor tone, reduced insulin levels and decreased stroke severity, while the ones carrying the S1176A mutant had higher blood pressure, decreased endothelial-dependent vasodilation, and insulin resistance [284–286]. Moreover, *Apoe*$^{-/-}$ mice (an atherosclerotic mouse model) expressing the S1176A mutant demonstrated an increase in atherosclerotic lesions and oxidative stress relative to control *Apoe*$^{-/-}$ mice [287]. This level of *in vivo* evidence has not been seen with other eNOS phosphorylation sites [29]. Therefore, eNOS phosphorylation at Ser-1177 may be used as a marker for eNOS activation and thus an indirect indicator of endothelial health. However, discordance between eNOS phosphorylation status at Ser-1177 and the citrulline assay has been reported [281]. In that study, DHA increased p-eNOS levels but not citrulline production from L-arginine in EA.hy926 cells, while a similar treatment regimen (DHA 20 – 80 μM for 24 h) in HUVEC resulted in increased citrulline production [279]. Eroglu et al. [288] addressed this discordance using a highly sensitive and specific NO biosensor to monitor real-time NO production from live EA.hy926 cells. In that study, certain eNOS-stimuli (VEGF and insulin) failed to raise NO production together with the induced eNOS phosphorylation at Ser-1177, while other stimuli (ATP and histamine) increased both NO and p-eNOS levels. This insulin-stimulated effect agrees with previous reports as well [289,290]. Although Eroglu et al. [288] suspected that phosphorylation at Ser-1177 might be related to superoxide generation by eNOS if not producing NO, others found that insulin also induced Tyr-657 phosphorylation, an inhibitory site on eNOS, resulting in a final reduction of eNOS activity [3]. Therefore, the discordance between p-eNOS at Ser-1177 and NO production by insulin stimulation can be explained. Still,

the atheroprotective effect of DHA via eNOS activation would be more conclusive if data from other eNOS activity assays (e.g. the citrulline assay and the nitrite/nitrate assay) and superoxide production assay supported the phosphorylation results obtained. However, the results for those functional assays are not available yet.

There have been a couple of reports showing DHA had no effect on total eNOS protein levels [277,280], while another paper reported that DHA impeded the decrease in *NOS3* mRNA levels induced by TNFα [240]. The discrepancy in how DHA affects eNOS may be the result of differences in DHA concentrations, as indicated in our study. The first two studies used up to 12 μM DHA, while the latter one used 30 and 50 μM DHA. In our study, 20 μM DHA elevated total eNOS protein levels in both growing cells and quiescent cells (Fig. 5C and 6C), while high concentrations of DHA, reaching 125 μM, may be deleterious by largely reducing eNOS protein levels, irrespective of growth state and/or other co-treatment (Fig. 4B, 5C, 6C, and 9C). It has not been reported previously that quiescent cells have higher protein levels of total eNOS compared to growing cells (Fig. 4B); this observation also validated that our quiescent cell state more closely matches the healthy state *in vivo,* with more eNOS available as compared to the proliferative, dysfunctional state represented by growing cells.

The cell cycle results also support the notion that cells at day 10 are in a quiescent state. In this state, compared to the growing state, there were many more cells in G0/G1 phase, fewer in both S and G2/M phases, and also fewer apoptotic cells (Fig. 21 A - D). All of these are features of the quiescent state, and support the cell proliferation assay results reported previously that day 10 cells had substantially less bromodeoxyuridine incorporated into DNA than day 4 cells in the growing state [5].

The effect of DHA on cell apoptosis, proliferation and cell cycle regulation is well-established, especially in cancer cells where DHA has potential therapeutic uses [272,274]. DHA, especially at higher concentrations as mentioned earlier, was reported to reduce cell viability mostly by inducing apoptosis in endothelial cells [253,255,291], as well as in many other cell types [272,292,293]. Kim et al. [271] also reported that DHA induced apoptosis in growing HUVEC but not confluent cells. This agrees with our results where DHA treatment for 8 h concentration-dependently increased the percentage of cells in sub G0/G1 phase in growing cells (Fig. 21A) but not in quiescent cells (Fig. 22A). However, another paper found that DHA largely induced apoptosis in confluent EA.hy926 cells grown on MG [263]. The discrepancy may be due to differences in concentration and treatment time. Kim et al. [271] treated cells with 20 and 40 μM DHA for 24 h, which may be compared to our 20 μM DHA, 8 h treatment. The other paper [263] used DHA at 125 μM for 24 h, a much higher

concentration than what was used in the paper by Kim et al. [271], and a longer treatment time compared to the 2 h and 8 h used in this study. In our study, only 20 μM DHA protected quiescent cells from apoptosis but not 125 μM treatment when compared to vehicle control (Fig. 22A). Therefore, the effect of DHA on endothelial cell apoptosis depends also on concentration, time, and growth state. Both the apoptosis-inducing effect of DHA in growing cells and the protective effect of low DHA concentration in quiescent cells can be considered as beneficial. On one hand, apoptosis helps to get rid of activated, potentially dysfunctional endothelial cells, without worsening inflammation, while at the same time, it protects healthy endothelial cells from cell death. Also, the induction of apoptosis by DHA at the high concentration (125 μM) may be one of the main reasons for the concentration-dependent responses to different signaling pathways that are going to be discussed later.

There is little controversy that DHA can block cell proliferation, but its effect on cell cycle progression seems diverse in cancer cells [274]. In non-cancer cells, DHA was mainly found to increase the percentage of cells in G1 phase [278,292,293], while only a few reported a decrease in S phase [278] and an alteration in G2/M phase [294]. What is consistent, though, is that DHA can inhibit DNA synthesis [247,261,291,292,294], which may be related to the effect of DHA on S phase. In our results, DHA seemed to modestly decrease the percentage of cells in G1 phase but elevated S phase in growing cells (Fig. 21 B and C), although statistical significance was not reached. This may be contradictory to the literature, but it can also be explained if DHA caused cell cycle arrest at S phase as in Jurkat cells [295] where the proportion of cells in S phase doubled with a concomitant reduction in G1 phase. This also agrees with the inhibitory effect of DHA on DNA synthesis. In quiescent cells, in contrast, the percentage of cells in S phase declined significantly following treatment with 20 μM DHA, and potentially with 125 μM DHA as well (Fig. 22C). This may indicate that DHA at those specific conditions suppressed DNA synthesis in agreement with the literature [247,291]. Another possible explanation is that DHA may have caused cell cycle arrest at G0/G1 phase as reported by several papers [274,278,292,293]. Since the cells were not synchronized prior to DHA treatment, however, those cells already in S or G2/M phase could progress to finish the cell cycle, but those in G1 phase were stalled at this stage. The overall effect resulted in a reduced number of cells in S phase. The limitation associated with not synchronizing cells prior to treatment may be overcome by the strength that different DHA concentrations and treatment durations were compared, as suggested by Newell et al. [274].

Cyclin D1 is one of the major G1 phase markers, and the arrested G1-to-S phase progression can be due to a decrease in cyclin D1 levels [97]. In general, DHA may reduce

cyclin D1 expression in different cell types over a broad concentration range extending from 12.5 μM to 500 μM [247,261,278,296], but few studies have reported the effect of DHA on cyclin D1 phosphorylation and its subsequent turnover. We found that even if not inhibitory, DHA alone at the conditions tested had little effect on cyclin D1 phosphorylation at Thr-286 regardless of cell growth state (Fig. 23). While high concentrations (125 μM) of DHA did decrease the cyclin D1 level in quiescent cells consistent with the literature in other cell types [247,261,278,296], lower DHA concentrations of 20 and 40 μM raised the cyclin D1 protein level instead (Fig. 24D). Overexpression of cyclin D1 was found to inhibit DNA synthesis and thus S phase entry in fibroblasts [297]. This explains the importance of p-cyclin D1 (Thr-286) assisted cyclin D1 nuclear export and subsequent degradation at the G1/S phase boundary for smooth progression into S phase [97,297]. The elevation of cyclin D1 levels by lower concentrations (20 and 40 μM) of DHA may cause the cell cycle to stall at the G1/S boundary in quiescent cells, matching the cell cycle analysis results described above (Fig. 22C).

Involvement of p38 MAPK/NF-κB signaling in the effects of DHA on eNOS and cell cycling

p38 MAPK and its downstream target, NF-κB, have diverse roles in the expression and/or functioning of cyclin D1. It is well established in tumor cells that p38 MAPK can induce overexpression of *CCND1* (the gene encoding cyclin D1) via activation of NF-κB [298], while NF-κB may differentially regulate *CCND1* transcription during different cell cycle phases [299]. Cyclin D1 protein may in turn act as a co-repressor for NF-κB [300], and p38 MAPK can directly phosphorylate cyclin D1, which leads to its degradation [97]. Yet, little is known about the effects of DHA in these signaling pathways. In this study, instead of a reduction, we observed an increase in cyclin D1 phosphorylation when p38α/β MAPK was inhibited (Fig. 23 A and B). In addition, p38 MAPK seemed to hinder the induction of p-cyclin D1 by DHA, and none of the effect was growth-state-dependent. In an engineered HEK293 cell line, co-induction of p-cyclin D1 at Thr-286 by p38 MAPK and ERK1/2 was suggested to delay G1-to-S phase transition of the cells [98]. Unlike p38 MAPK, ERK1/2 can be stimulated by DHA at 8 h in both growing and quiescent endothelial cells [6]. It is then possible to speculate that DHA may promote cyclin D1 phosphorylation via ERK1/2 but not p38 MAPK in endothelial cells; however, this DHA-induced cyclin D1 phosphorylation via ERK1/2 is likely to be inhibited by p38 MAPK. To confirm this speculation, further study focusing on ERK1/2 signaling is needed. This also suggests that apart from its synergistic effects, p38 MAPK can also act contrary to ERK1/2 in cell cycle regulation. Apart from inducing *CCND1* expression,

p38 MAPK was also found to reduce it [58] probably by decreasing the transcriptional activity of the *CCND1* promoter [98]. This dual effect of p38 MAPK on *CCND1* expression might explain the different trends observed in cyclin D1 protein levels after treatment with 20 μM and 125 μM DHA in the presence of the p38 MAPK inhibitor: the inhibition decreased cyclin D1 protein levels with 20 μM DHA but modestly increased it with 125 μM DHA (Fig. 24), especially in quiescent cells. However, the induction pattern of RelA by DHA and p38 MAPK did not match that of the cyclin D1 levels. Thus, it is hard to conclude that NF-κB also plays a role in the modulation of cyclin D1 expression by DHA. Further research, especially including RelA PTM sites reported to be associated with *CCND1* transcription [299], is needed to confirm the involvement of NF-κB. Overall, p38 MAPK, but not NF-κB, may be involved in both DHA-induced cyclin D1 degradation and cyclin D1 expression.

The activity of eNOS can be regulated by DHA [253,254] as well as by p38 MAPK [270]. While the effect of DHA is conditional, as discussed above, p38 MAPK was found to activate eNOS in response to black tea polyphenols [270]. However, Wang et al. [301] reported that specific knockdown of p38α MAPK by siRNA augmented p-eNOS levels, and TNFα-induced p38 MAPK activation was accompanied by a decline in eNOS phosphorylation. In our study, p38 MAPK activation also seemed to be inversely related to p-eNOS levels in response to DHA (Fig. 3G vs. 3H, 3I vs. 3J, 3M vs. 3N). Indeed, p38α/β MAPK inhibition drastically induced eNOS phosphorylation in quiescent cells (Fig. 6B and 7B), in agreement with the p38α-specific siRNA results reported by others [301]. In growing cells, on the other hand, the p38α/β MAPK inhibitor alone decreased p-eNOS levels (Fig. 7B), meaning that normal functioning of p38 MAPK is required for maintaining eNOS activity. Yet, activation of p38 MAPK by DHA at 8 h, as illustrated in Fig. 3H, 3L and 3P, prevented DHA-induced eNOS activation (Fig. 5B). DHA was able to activate PI3K/AKT signaling in EA.hy926 cells [258]. This activation, specifically by a high concentration of DHA (125 μM), but not lower concentration, may lead to eNOS phosphorylation [302], matching our results showing that only 125 μM DHA significantly activates eNOS when p38α/β MAPK is inhibited. Therefore, DHA may induce eNOS phosphorylation via other pathways like PI3K/AKT in growing cells, which can then be inhibited by DHA-activated p38 MAPK.

MSK is an important p38 MAPK substrate that can also be activated by ERK1/2 [66], but a link between MSK and eNOS activation has not been described. We report here for the first time that, in both growing and quiescent endothelial cells, MSK is required for eNOS phospho-activation, although the detailed patterns differ slightly in each growth state. In growing cells, just as we observed with p38 MAPK, MSK was necessary to maintain eNOS

phosphorylation, but DHA showed no effect on eNOS activation (Fig. 8B). In contrast, DHA apparently activates eNOS via MSK at lower concentrations (20 and 40 μM) but not at higher concentrations (125 μM) in quiescent cells (Fig. 9B). At 8 h of treatment, p38 MAPK was only activated by DHA in growing cells and not quiescent cells, but ERK1/2 was activated in both growth states [6]. In growing cells, however, p38 MAPK inhibition did not reduce MSK activation by MAPK (phosphorylation at Thr-581) nor its catalytic ability (phosphorylation at Ser-376) in response to DHA treatment, but increased phosphorylation levels at both sites instead (Fig. 11). In quiescent cells, the eNOS response to p38 MAPK inhibition and to MSK inhibition were fundamentally different as well: when MSK was inhibited, DHA at 125 μM activated eNOS, restoring p-eNOS levels close to that seen in the absence of inhibition. Overall, it is unlikely that the effect of MSK on eNOS activation is modulated by p38 MAPK. Rather, DHA may act via ERK1/2 to activate MSK in both growing and quiescent endothelial cells, which then mediates eNOS phosphorylation, especially at lower DHA concentrations. At high DHA concentration (125 μM), there may be pathways other than MAPK/MSK that DHA can activate to phosphorylate eNOS, such as the postulated PI3K/AKT pathway.

NOS3 expression can also be modulated by DHA [240,255] and p38 MAPK [121,241,301], possibly via the NF-κB binding sites located on the promoter [29]. DHA was found to ameliorate the decrease in *NOS3* mRNA levels caused by TNFα, and this was accompanied by attenuation of TNFα-dependent induction of *MAPK14* and *RELA* expression [239,240]. This differential response of p38 MAPK and eNOS mRNA levels to TNFα and DHA is supported by the finding that p38 MAPK can downregulate *NOS3* promoter activity [241,301]. We observed a subtle increase in eNOS expression in p38 MAPK-inhibited samples compared to control, but statistical significance was not reached (Fig. 7C and 40, and 125 μM DHA results in 5C). However, this relation did not hold in quiescent cells, especially with 20 μM DHA treatment: under this condition, p38 MAPK signaling was required for DHA-induced eNOS expression (Fig. 6C). p38 MAPK is reported to induce *NOS3* expression by activating CREB thus inducing the expression of AP-1 which promotes *NOS3* transcription [121]. Nevertheless, we did not find CREB activation by 20 μM DHA in quiescent cells (Fig. 18D), nor should p38 MAPK be activated under these conditions (Fig. 3N and R). Although NF-κB may also temporarily induce *NOS3* expression in response to LSS [303,304], its general long term effect on *NOS3* mRNA levels is still inhibitory [303,305]. The decrease in eNOS expression caused by 125 μM DHA (Fig. 4B, 6C, and 9C) may be related to an induction of NF-κB transactivation (Fig. 14 - 17) as indicated by RelA Lys-310 acetylation and/or Ser-276

phosphorylation levels. On the other hand, the effect of 20 μM DHA on RelA activity was inconclusive, and a link to elevated eNOS expression is thus unlikely under this condition.

Effects of DHA on epigenetic and transcriptional factors via p38 MAPK signaling

From what is already known, DHA usually inhibits the transcriptional activity of NF-κB via either PPARs [243,244] or FFAR4 [245]. The latter pathway involves ERK1/2 and p38 MAPK. However, we did not observe any effect of DHA on p-RelA Ser-536 levels nor was there an involvement of p38 MAPK (Fig. 13). On the other hand, 125 μM DHA induced RelA acetylation at Lys-310, while the effect of 20 μM DHA was modest and inconclusive (Fig. 14 - 17). RelA phosphorylation at Ser-536 as well as Ser-276 can promote recruitment of CBP/p300 and subsequent acetylation at Lys-310 [74] that is essential for the full transcriptional activity of NF-κB on pro-inflammatory genes [306–308]. MSK is an important kinase that phosphorylates RelA at Ser276 [73]. p38 MAPK has also been found to directly activate p300 with subsequent acetylation of RelA at Lys-310 [113]. The involvement of p38 MAPK in RelA acetylation was confirmed by the decrease in RelAK310ac levels when p38 MAPK is inhibited (Fig. 14D). However, p38 MAPK was only required for RelA acetylation at lower concentrations of DHA (20 and 40 μM) in quiescent endothelial cells. Interestingly, the signal may not be transduced from p38 MAPK to MSK in quiescent cells (Fig. 16C). Moreover, MSK may not be the kinase responsible for phosphorylating the Ser-276 site on RelA, since the presence of the MSK inhibitor increased phosphorylation levels instead (Fig. 16B). Other kinases that can phosphorylate the Ser-276 site include the catalytic subunit of protein kinase A (PKAc) [309,310], protein kinase C α (PKCα) [311], and p90 ribosomal S6 kinases (RSKs) RSK1 and RSK2, but not RSK3 [312]. RSK1 can be inhibited by SB747651A, similar to MSK, while more than 80% of the activity of RSK2 can be inhibited [264]. PKA is a cyclic AMP (cAMP)-dependent protein kinase whose activity is not inhibited to the same degree as MSK by SB747651A at the 5 μM concentration used in this study, while the activity of PKC was not effectively inhibited [264]. The cAMP-induced PKA/NF-κB signaling pathway was found to play a part in VEGF-induced endothelial cell migration [313]. PKAc can also phosphorylate RelA independent of cAMP: inactive PKAc can bind to IκB/NF-κB complexes, and dissociation of IκB also activates PKAc to phosphorylate RelA at Ser-276 in the cytosol [309]. In addition, a recent transcriptomic study revealed that PKA-specific inhibition had an opposite effect on the direction a set of genes was expressed when compared to H89, which inhibits both MSK+PKA [314]. This means that MSK and PKA may function counter to each other, a scenario similar to that seen with RelA Ser-276 phosphorylation

regulation by DHA and SB767451A. PKC, like PKA, belongs to the AGC protein kinase family that responds to cytosolic second messenger concentration changes [315]. Unlike PKA, certain PKCs are responsive to DAG and/or Ca^{2+} [316]. DHA has been reported to increase the cytosolic Ca^{2+} concentration, therefore inducing the activity of PKCγ and -δ but not PKCα or -β [317]. Additionally, PKCα inhibition by PPARγ agonists [318] and PKCε inhibition by DHA (which also has PPARγ agonistic activity) [319] in endothelial cells were both found to suppress the expression of pro-inflammatory cyclooxygenase-2 (COX-2). The latter effect of DHA may possibly occur via ERK1/2 but not p38 MAPK. DHA may also trigger increased cytoplasmic accumulation of cAMP via FFAR4 [320] as well as a Ca^{2+} concentration surge via FFAR1 [321] and phospholipase C (PLC) [317]. PLC also produces DAG from membrane phospholipids. Therefore, elevation of p-RelA Ser-276 levels in response to 20 and 40 μM DHA treatment in the presence of SB747651A may be attributed to the FFAR1 or PLC or PPARγ)/PKC/ERK1/2/MSK signaling pathway or, to a lesser extent, activated PKA via FFAR4 acting in opposition to MSK. The fact that functioning MSK inhibited this process in quiescent cells suggests a requirement for DHA-dependent inhibition of PKC signaling. In growing cells, on the other hand, RelAK310ac correlates with MSK and RelA phosphorylation at Ser 276, judging from the similar activation patterns of the 2 sites following treatment with DHA and the MSK inhibitor (Fig. 15B vs 15C). Another way to recruit CBP/p300 to the chromatin is via an interaction with CREB which cooperates with NF-κB on the same promoters [322]. The CREB/CBP complex may also contribute to DHA-induced RelA acetylation at Lys-310, especially in quiescent cells treated with 125 μM DHA (Fig. 17D), which is not regulated by either p38 MAPK or MSK. This also means that CREB may be activated by DHA to bind CBP via kinases other than MSK, and this is going to be discussed later.

Apart from inducing Lys-310 acetylation on RelA, 125 μM DHA also seemed to modestly elevate Ser-276 phosphorylation (Fig. 15B and 16B), while 20 μM DHA appeared to moderately inhibit RelA phosphorylation at Ser-276, especially in quiescent cells (Fig. 16B). Both Ser-276 phosphorylation and Lys-310 acetylation on RelA are usually associated with pro-inflammatory [323,324] and pro-apoptotic [324–326] responses, thus having deleterious effects on cells. As a TF, NF-κB causes these effects by regulating the expression of target genes. By affecting the transcriptional activity of NF-κB, these 2 PTMs of RelA can act through recruitment of co-factors that aid in chromatin remodeling, transcription induction, and transcription elongation [324]. Recruitment of CBP/p300 by phospho-Ser-276 not only can lead to acetylation of RelA at Lys-310, but can also act on chromatin to acetylate histones [70].

In addition, Ser-276 phosphorylation is necessary to recruit DNA (cytosine-5)-methyltransferase-1 to the promoters of "good" genes such as tumor suppressor genes, therefore silencing the gene via DHA methylation [327]. RelAK310ac can directly bind to bromodomain-containing protein 4 (BRD4) [307,328], which also seems to require phosphorylation at Ser-276 [329,330]. BRD4, as its name suggests, functions as an acetylated lysine residue reader and then recruits other cofactors to the active gene locus [331]. One of the most important cofactors that BRD4 can interact with is the positive transcription elongation factor b (P-TEFb) [332]. P-TEFb, a complex of CDK9 and cyclin T1, is critical in promoting transcription elongation by phosphorylating Pol II, and BRD4 was found to directly bind to CDK9 [331,332]. NF-κB was found to recruit P-TEFb via BRD4 to the promoters of pro-inflammatory genes such as *IL8* and *IL6*, and this recruitment requires Ser-276-phosphorylation-coupled Lys-310 acetylation on RelA [307,324,329,331–334]. In addition, RelAK310ac can also block RelA ubiquitination and subsequent degradation, increase the stability of NF-κB, and prolong its occupation on chromatin for transcription induction [335,336]. Therefore, induction of RelA Ser-276 phosphorylation and Lys-310 acetylation by 125 μM DHA should tend towards a pro-inflammatory state *in vitro*, while 20 μM DHA may lean towards the anti-inflammatory side if it truly inhibits the modification of at least one of the two PTMs. Additional tests to explore the expression profiles of genes downstream of NF-κB that may be differentially modulated by high and low concentrations of DHA may help to confirm this speculation.

We demonstrated here for the first time that DHA may in a concentration-dependent fashion modulate CREB activation in endothelial cells (Fig. 18). CREB is an important TF that controls the transcription of thousands of genes that regulate diverse cellular processes. It can also be activated by various stimuli including cAMP, Ca^{2+}, stress, growth factors, hormones, etc [337]. CREB plays a vital role in neuronal signaling [338,339], circadian rhythm [340–342], cell proliferation and oncogenesis [343,344], as well as inflammation [345,346] and more. CREB exerts its transcriptional activity by engaging co-factors, such as other TFs, DNA methyltransferases [347], and most importantly, CBP [348]. Ser-133 phosphorylation is indispensable for CREB activation, and similar to RelA Ser-276 phosphorylation, the kinases that phosphorylate CREB include MSK, RSK, PKA, and PKC [72,264,348]. The SB747651A treatment results proved that MSK and/or RSK were required for the phospho-activation of CREB in endothelial cells, but it did not explain the full activity. The (ERK1/2 and/or p38 MAPK)/(MSK and/or RSK)/CREB signaling pathway has been well-established in many cell types and tissues [349,350], and this signaling pathway is linked to cardiac fibrosis, VSMC

migration, and pro-inflammatory responses [345,349]. DHA was reported to upregulate CREB signaling in neural cells to induce neurogenesis and improve cell viability in brains [351,352], which was proposed to signal through FFAR1 [353] to also activate PKA and/or PKC. However, activation of CREB by TG-rich lipoproteins in the endothelium was reported to be harmful, accompanied with activation of NF-κB via both ERK1/2 and p38 MAPK, thus leading to increased expression of pro-inflammatory genes and adhesion molecules [354]. By activating CREB in both growing and endothelial cells, high concentrations of DHA (125 μM) may be more pro-inflammatory. The pathway leading to CREB activation by 125 μM DHA may be slightly different in growing cells versus quiescent cells. MSK and/or RSK as well as PKA and/or PKC may participate in both growth states, while p38 MAPK signaling is likely to be only involved in quiescent cells and not growing cells. In growing endothelial cells, ERK1/2 might be the main MAPK that links DHA and MSK according to the DHA-induced MSK activation results with p38 MAPK inhibitor (Fig. 11 and 12). On the other hand, lower concentrations of DHA (20 and 40 μM) suppressed CREB in growing cells, while having only a moderate effect in quiescent cells. It was found in adipocytes that DHA reduced p-CREB levels upon DHA treatment for 1 to 24 h [320]. As discussed above, DHA [319] and PPARγ agonists [318] were reported to inhibit PKC in endothelial cells, both leading to transcriptional inhibition of COX-2, although the PKC isoforms involved in these two studies were different. Downregulation of COX-2 mRNA levels by PPARγ agonists was found to be mediated via CREB suppression (reduced phosphorylation at Ser-133) [318]. Therefore, the reduction of CREB phosphorylation by low concentrations of DHA may be due to inhibition of PKC via the PPARγ/PKC/CREB signaling as in the COX-2 case. This should lead to suppressed expression of those CREB-associated pro-inflammatory genes.

Histone H3 phosphorylation at Ser-10 and Ser-28 via MAPK (ERK1/2 and p38 MAPK)/MSK signaling has been well recognized [77,355–357], and so is their strong association with transcription promotion of immediate-early genes (IEGs) such as *FOS*, *JUN* and *EGR-1* [358]. Although p38 MAPK and ERK1/2 can be activated by DHA (Fig 3 and [6]), their activation patterns at 8 h of DHA treatment differed considerably from the DHA-induced H3 phosphorylation patterns in both growing and quiescent cells (Fig. 19 and 20). Furthermore, MSK inhibition by SB747651A did not attenuate this induction, matching the IEG expression stimulation results obtained in MSK-knockout fibroblasts and H89-treated human primary fibroblasts that were both stimulated with epidermal growth factor or a tumor promoting compound, phorbol 12-myristate 13-acetate [314]. Instead, H3 phosphorylation at these 2 sites both increased under certain treatment conditions in the presence of the MSK inhibitor. This

means that, although MSK can modulate H3 phosphorylation at Ser-10 and Ser-28, the kinase(s) mainly responsible for their modification in response to DHA are likely to be other candidates. Sawicka and Seiser [102] have summarized a list of writers reported for these 2 phospho-sites. Besides MSK, only aurora-B was found to phosphorylate both sites, but during mitosis instead of interphase [102,107]. PKA and AKT are also in this list. Both PKA and AKT may be involved in the alternative signaling pathways that DHA can induce, and that may be able to act against p38 MAPK and/or MSK signaling, as discussed above. However, both PKA and AKT were only reported to promote H3 phosphorylation on Ser-10 [102]. The plausible counteracting effect of MSK and PKA [314] as mentioned above might be able to explain the general increase in p-H3S10 levels after MSK inhibition in quiescent cells (Fig. 20B). Another kinase that was shown to phosphorylate H3 at both Ser-10 and Ser-28 sites is Ca^{2+}/CaM-dependent protein kinase II (CaMKII) [359,360]. It plays an important role in the pathology of heart failure [361] as well as atherosclerosis [362,363], and as its name suggests, CaMKII is activated by Ca^{2+}/calmodulin. Although DHA was found to trigger cytoplasmic Ca^{2+} accumulation [317] that may activate CaMKII, inhibition of CaMKII by DHA at greater than 50 μM was recently reported in a pancreatic carcinoma cell line [364]. DHA inactivated CaMKII at higher concentrations (100 and 150 μM) but not lower ones (25 and 50 μM) and this may explain the induction pattern of H3 Ser-10 phosphorylation by DHA: lower concentrations of DHA (20 and/or 40 μM) increased Ser-10 phosphorylation on H3 in both growing and quiescent cells, while 125 μM DHA did not (Fig. 19B and 20B). If MSK can also inhibit DHA/CaMKII signaling, then this may be able to justify SB767451A-induced H3 Ser-10 phosphorylation by 125 μM DHA in growing cells. Nevertheless, the induction of H3 Ser-28 phosphorylation by higher concentrations (125 and/or 40 μM) of DHA only (Fig. 19C and 20C) cannot be rationalized this way. The differential phosphorylation patterns after DHA treatment and possibly distinct pathways leading to these both support the previous findings by Dyson et al. [77] and Dunn and Davie [355] that H3S10 and H3S28 are phosphorylated independently on different chromatin loci. The associations of H3S10 or H3S28 with other H3 PTMs such as acetylation as well as other co-factors (CBP/p300) were also found to differ [355,357,365,366]. For instance, HDAC inhibition was found to promote H3 phosphorylation on Ser-28 but not Ser-10 [77,367]. And DHA may serve as a HDAC inhibitor and lead to upregulation of histone acetylation on H3 [147,368]. This may clarify the increased p-H3S28 levels by higher concentrations of DHA but not p-H3S10. Also, this process may be modulated by MSK in growing endothelial cells but not in quiescent ones, since MSK inhibition elevated H3 Ser-28 phosphorylation in growing cells only (Fig. 19C vs 20C).

Unlike histone acetylation, the effect of DHA on histone phosphorylation is not well documented, especially outside the brain. Here, we demonstrated for the first time that DHA may be able to induce H3 phosphorylation in endothelial cells and this effect was concentration- and site-specific but less dependent on growth state. Although H3 phosphorylation events on Ser-10 and Ser-28 share similar signaling pathways in some cases, they should be induced via different mechanisms by DHA in endothelial cells as discussed above. Also, these two phospho-events were found to act separately in promoting transcription. Ser-28 phosphorylation on H3 is proposed to be more associated with transcriptionally active promoters [369] and trigger transcription initiation [370] as well as elongation especially for IEGs [358] and stress-induced genes [356]. The upregulation of IEG expression can also be related to inflammation [371,372], so the increased p-H3S28 levels seen with higher concentrations (125 and/or 40 μM) of DHA might indicate that the cells were in a stressed, pro-inflammatory state. Although H3 Ser-10 phosphorylation is also associated with IEG expression during interphase, this process was found to be MSK-dependent [102,373], which is not consistent with our results for MSK-independent p-H3S10 induction by lower concentrations (20 and 40 μM) of DHA. Another important and special role of H3 Ser-10 (also for H3 Ser-28 to some extent) phosphorylation is its association with chromatin condensation, especially during mitosis [107,374]. This phospho-site is proposed to serve as a flag/mark for cell cycle checkpoints so that chromatin can be correctly processed during G2/M phase, and if p-H3S10 was induced in interphase, chromosome condensation may happen before the cells enter M phase [107]. This might lead to cell cycle disruption and probably genome instability [374] that could result in slower and/or partial replication of chromatin at the condensed area [375]. This might provide the basis for DHA-attenuated DNA synthesis (discussed above) and the lower proportion of cells in S phase after treatment with 20 μM DHA but not 125 μM DHA (Fig. 21E). However, this cannot explain why the cell cycle results were only observed in quiescent cells while H3 Ser-10 phosphorylation induction was observed in both growth states.

As mentioned, CaMKII is an important kinase in cardiovascular signaling. It is not only able to phosphorylate histone H3 as discussed, but also able to modulate the activity of eNOS [376–378], NF-κB [379,380], and CREB [381–383]. CaMKII was reported to be responsible for eNOS phospho-activation at the Ser-1177 site, which is dependent on the dephosphorylation of an inhibitory site, Thr-497 [378]. While the involvement of CaMKII in NO-dependent endothelial function *in vivo* remains debatable [377], it has been confirmed to induce *NOS3* transcription [384,385], phosphorylate eNOS and upregulate NO production *in vitro* [376,377] and *ex vivo* [376]. In addition, eNOS activation by CaMKII was found to be

less dependent on a Ca^{2+} surge, but was proposed to be mediated via signal transduction along a few CaMKII-downstream kinases such as AKT and ERK1/2 [376]. CaMKII was also found to upregulate NF-κB nuclear translocation and transcriptional activity [379,380,386], together with increased IKK activation [386] and RelA phosphorylation at Ser-536 [387,388]. Unlike the activation effect on eNOS and NF-κB, CaMKII was found to prevent CREB activation by PKA via phosphorylation of an inhibitory site on CREB, Ser-142 [381]. Although CaMKII can also phosphorylate CREB at Ser-133, this action of CaMKII occurs in neurons only, via CaMKIIα and -β isoforms [381,389] or CaMKIV [383]. CaMKII isoforms demonstrate a tissue-specific expression profile: α and β isoforms are largely restricted to neurons and central nervous system-associated cells, while γ and δ isoforms are mainly in other tissues [362,390]. CaMKIIδ is the major isoform in muscle cells and endothelial cells [362,390,391]. It was reported that CaMKIIδ decreased the transcriptional activity of CREB by phosphorylating it at Ser-142 probably via ERK1/2 activation and it did not affect CREB Ser-133 phosphorylation levels in VSMC [382]. Moreover, CaMKII was found to affect cell cycle progression and associate with cyclin D1 expression [362,392]. Given that CaMKII was found to be responsive to DHA [364,393,394], it is possible that CaMKII may also play a role in DHA-regulated eNOS activation, RelA phosphorylation at Ser-536, CREB inactivation indicated by decreasing Ser-133 phosphorylation levels, and/or altered cell cycle progression. In addition, CaMKII possesses a wide range of splice variants from the 4 isoforms, whose expression can be differentially regulated in response to a stimulus [392,395,396] and whose signaling pathways were found to be distinct as well [362,386], which may lead to phenotype switching of VSMC [397]. Therefore, if CaMKII contributes to those DHA-stimulated signaling events as just mentioned, the differences in various splice variants of CaMKII might be able to explain the growth-state-dependent effects of DHA. These speculations about the involvement of CaMKII in the effect of DHA on endothelial cells need to be addressed experimentally.

Based on the above discussion, the possible signaling pathways that DHA can adopt under different scenarios are summarized in Fig. 25. Further studies are required to validate the involvement of the proposed enzymes. It is clear, however, that the growth-state-dependent differential activation of p38 MAPK by DHA only played a small part in the DHA mediated growth-state- and concentration-dependent effects on endothelial cells.

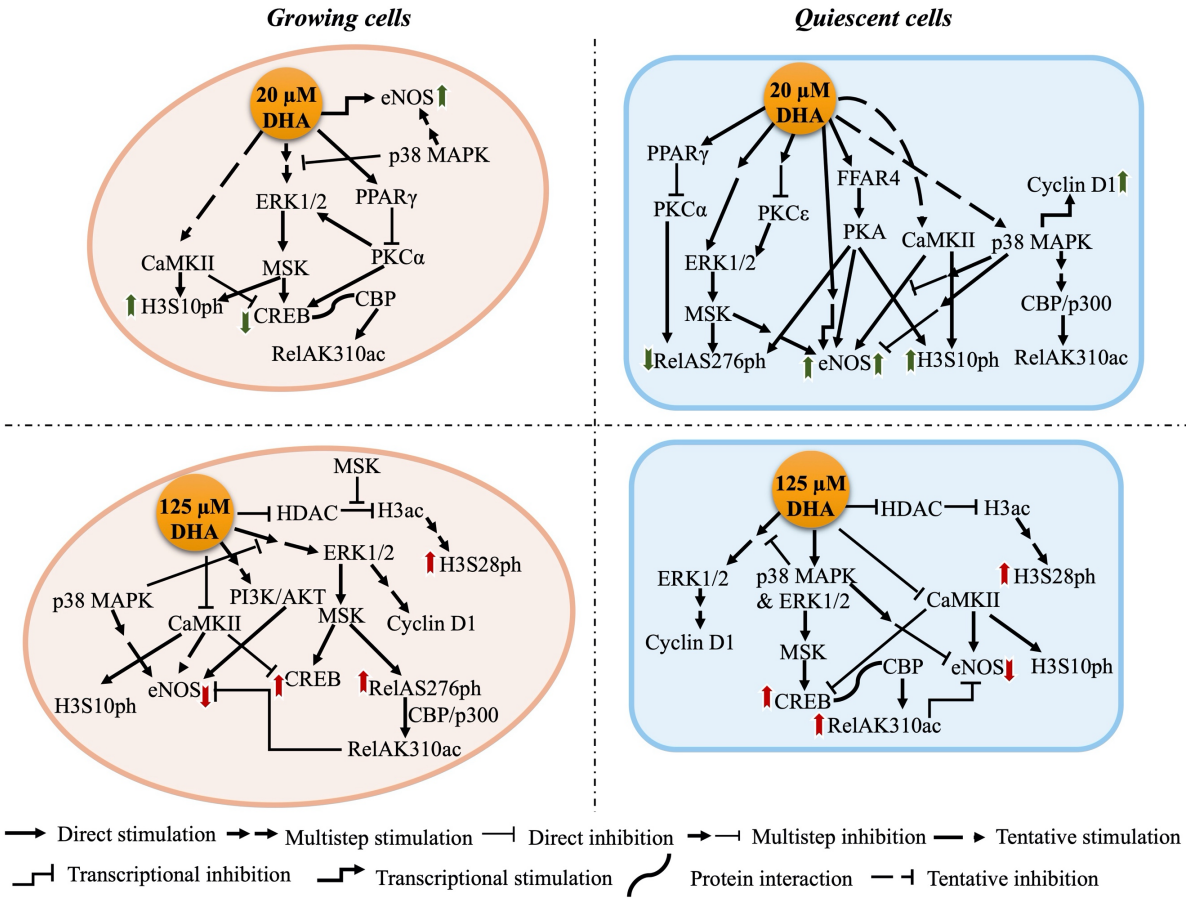

Figure 25. Proposed mechanisms of action of DHA in growing and quiescent endothelial cells at low (20 µM) and high (125 µM) DHA concentrations.

The involvement of PKC, PKA, PI3K/AKT, CaMKII and HDAC is based on information taken from the literature. Upwards or downwards colored arrows beside the protein name stand for observed results exhibiting significant upregulation or downregulation, respectively. Green arrows indicate potential beneficial outcomes, while red ones represent possible deleterious effects. Arrows to the left of the protein name stand for regulations of activity, and arrows to the right of the protein name represent regulation of expression.

Effects of DHA are affected by growth state, concentration, and other factors

As summarized in Fig. 25 and Table 4, the distinct effects of DHA on effectors related to ED and the possible mechanisms underlying their actions were dependent upon both concentration and cell growth state. Treatment time is another factor that may affect how DHA influences endothelial cells as illustrated in Fig. 3: the phosphorylation levels of eNOS, p38 MAPK, and NF-κB in response to DHA fluctuated as a function of treatment time. For the effect of concentration, generally speaking, 20 μM DHA may possess beneficial effects via induction of eNOS expression and activation, prevention of cell proliferation and apoptosis (as indicated by the cell cycle profile and possibly p-H3S10-induced DNA replication delay), and downregulation of NF-κB- and CREB-associated inflammatory responses. In contrast, high concentrations (125 μM) of DHA appeared to be more pro-inflammatory and deleterious through inhibition of eNOS expression and promotion of NF-κB, CREB, and p-H3S28 associated inflammatory and stress responses. Also, quiescent cells seemed to be more responsive to 20 μM DHA compared to growing ones, while the effects of DHA at 125 μM were similar in growing and quiescent cells.

As noted earlier, the growing and quiescent states of EA.hy926 cells may represent the active, dysfunctional vs. healthy, inactive states, respectively, *in vivo*. Therefore, the differential effects of DHA at 20 μM in these two cell growth states may imply that the beneficial DHA dose for humans is different for healthy individuals compared to patients with ED. This may partially explain the contradictory FMD results obtained from different studies summarized in Table 1: increased FMD after DHA supplementation was observed in children [223] but not in hypertensive older adults (40 -75 years old) with type 2 diabetes [222]. Although Singhal et al. [224] observed no effect of DHA supplementation on FMD in female participants and even a DHA-dependent decrease in FMD in male participants, this may be caused by the high saturated fat and omega-6 fatty acid content of the carrier oil for DHA compared to olive oil as the control [224]. The different responsiveness of growing and quiescent cells to 20 μM DHA may also partly explain the discrepancies between the consistently observed cardioprotective effects of DHA and EPA in observational and epidemiological studies versus the controversial results from large-scale clinical trials examining the effects of intervention with DHA+EPA. Most of those clinical trials focused on secondary prevention, while only two primary prevention trials, ASCEND (A Study of Cardiovascular Events in Diabetes) [398] and VITAL (Vitamin D and Omega-3 Trial) [399], are available to date. Although neither of these two primary prevention trials found significant

differences between the treatment and placebo groups in their primary outcomes, further analysis did reveal significant beneficial effects of n3 PUFA towards CVD protection such as reduced MI and coronary heart disease [400]. This may suggest the potential of DHA and EPA in primary CVD prevention [217], although the evidence is weak due to the paucity of these kinds of studies. Also, the study populations in ASCEND and VITAL were elderly and/or diabetic patients who likely had impaired endothelial function at the time of the study, and thus may not fully match the quiescent cell state in our study. More clinical trials focusing on primary prevention of CVD, especially those using endothelial function as one of the inclusion criteria or a confounding factor in the analyses, are needed to strengthen the evidence for better devising primary care strategies for CVD prevention.

Currently, a commonly used clinical indication of someone's DHA status is the measurement of total plasma fatty acid concentrations (usually in μM) and it may be reported as percentage of total lipids/fatty acids. A cross-sectional study analyzed plasma total fatty acid concentrations in generally healthy Canadians in their 20s from 2004 to 2009 (n = 826) [201]. It was discovered that the plasma DHA concentrations were highly variable in the study population, spanning a range from 7.2 μM to 237.5 μM with 90% between 47.8 μM to 138.0 μM. While the overall mean plasma DHA content was reported to be 88.8 μM, it was significantly higher in females than in males (93.6 ± 38.8 μM vs. 81.0 ± 31.8 μM, $p < 0.01$). This sex effect on plasma DHA content is well recognized and can be attributed to the effect of estrogen [401] and the higher conversion rate from ALA in females [402]. Also, the sex difference may affect changes in plasma DHA content [200] and plasma oxylipin accumulation [198] after n3 PUFA supplementation, and lead to different FMD responses between men and women during DHA-only supplementation [224]. Other factors that may affect the plasma concentration of DHA (and/or its metabolites) and/or its response to supplementation are age [403], type of supplemented n3 PUFA (ALA or EPA or DHA) [196–199], duration of supplementation (study length) [198,404], dose [405], and probably genetics [200]. However, the specified relationships between plasma DHA concentration and membrane-incorporated DHA content in various tissues and cells has received limited attention. And DHA cleaved from the membrane phospholipids can have a significant and profound impact on cell signaling [165]. DHA incorporation into the membranes of cells is affected by DHA treatment concentration, time, and type of cells treated *in vitro* [279,281,282]. Therefore, given the treatment duration, the membrane-incorporated form may be the source of DHA triggering the late activation of MAPK and other proposed signaling pathways such as the (PLC and/or PPARγ)/PKC/(NF-κB and/or CREB) pathways described in this thesis and in previous studies

by our group [6,165]. In addition, it will be useful to understand what the optimal DHA concentration *in vitro* means for membrane DHA content in endothelial cells, and how this links to plasma DHA concentration and dietary DHA intake as well. Individual differences regarding those confounding factors should be considered carefully for this topic.

Apart from acting through different signaling pathways, DHA may also convey its differential mechanisms of action in endothelial cells via the wide range of bioactive lipid mediators it can generate. As just discussed, oxylipin concentrations can be affected by the same factors that affect plasma DHA content and may differ in different body compartments [406]. Furthermore, different oxylipins were found to have different pharmacokinetics and final concentrations at the end of a study [198,199,404,405]. Oxylipins, including specialized pro-resolving mediators (SPM), are generated enzymatically via oxygenation of PUFA, and contribute intimately to the physiological actions of DHA in inflammation, thrombosis, immunity and more [165,406]. They also play an important role in modulating endothelial function [407]. For instance, resolvin D1, a SPM derived from DHA, was found to mitigate stress-induced NF-κB signaling [408]. Therefore, the different effects and mechanisms of action observed for DHA under different treatment conditions and cell growth states may be due to different oxylipins produced from DHA under these conditions. Then, those oxylipins can trigger different signaling pathways depending on their variety and concentration.

Overall, according to our results, the potential atheroprotective effects of DHA on endothelial cells depend on many factors, such as cell growth state, DHA concentration, and treatment time. If these factors were extrapolated to an *in vivo* situation, it would mean that the effect of DHA on CVD prevention is affected by the health status of the individual, and factors that influence the amount of DHA in plasma as well as DHA incorporated into the endothelial cell membrane. In addition, the effect of DHA is also likely affected by the various metabolites originating from DHA. The differential pharmacokinetics of different DHA metabolites might be one of the explanations for the complex mechanisms of action of DHA under different treatment situations, as discussed in the previous section.

STRENGTHS

- The EA.hy926 cell line is a widely used permanent macrovascular endothelial cell line with most of key characteristics of primary endothelial cells.
- MG used for cell culture is similar to ECM components *in vivo*, and the ability to culture EA.hy926 cells to quiescence on MG-coated surfaces has been examined previously, which was further validated via the cell cycle results in this study.
- DHA was delivered to the cell cultures with FA-free BSA trying to mimic the non-esterified FA in circulation.
- Appropriate vehicle controls were used in each set of treatments for more accurate comparison of results.
- Samples from 3 independent experiments (instead of 3 biological replicates from one experiment) were run on the same gel for Western blotting. This minimized technical errors during image acquisition and quantification.
- The specificity of most phospho-specific antibodies used was validated.
- Total protein load was used for Western blotting normalization when applicable, instead of normalizing to a housekeeping protein.
- The effects of DHA on growing and quiescent endothelial cells was compared closely for the first time.
- Concentration, time, and growth state dependency of DHA treatments on eNOS and cell cycling were systematically evaluated.
- The effect of DHA on various key RelA PTMs were evaluated instead of only the Ser-536 site. And the possible mechanisms of DHA-induced RelAK310ac were extensively examined.

LIMITATIONS

- The EA.hy926 cell line is derived from HUVEC, which is of fetal origin. It is not 100% physiologically comparable to adult endothelial cells, especially those from arteries.
- Genetically, EA.hy926 cells are not normal diploid cells since they were generated by fusion with A546 carcinoma cells, and they are of male HUVEC origin. The effects of sex and genetic differences on the results are unknown.
- EA.hy926 cells have different expression patterns of certain cytokines as well as adhesion molecules and inflammatory responses to certain stimuli compared to HUVEC. This may indicate that the cellular signaling pathways in EA.hy926 cells are not the same as primary cells.
- The cells were examined under culture conditions lacking flow. This is not equivalent to the blood flow environment *in vivo*.
- The chemical inhibitors used are not 100% specific, causing ambiguity in deriving possible mechanisms and may pose unknown effects on other signalling pathways.
- No functional assay was performed for eNOS activity and the transcriptional activities of those TFs tested to validate the Western blotting results.
- The variations (most likely due to cells from different cell passages) among the 3 independent samples for Western blotting in some cases may affect the significance analysis.
- The DHA treatment may not be 100% representative to the situation *in vivo* with the presence of esterified DHA in the bloodstream.

FUTURE RESEARCH

- Perform functional assays for eNOS activity, ROS production, and transcriptional activities of NF-κB and CREB.
- Validate and explore the involvement of those pathways proposed in Fig. 25.
- Validate the effects of DHA using primary endothelial cells.
- Validate the involvement of p38 MAPK and MSK using genetic approaches for much higher specificity than chemical inhibitors used in this study.
- Explore the downstream effector genes of DHA in the two growth states of EA.hy926 cells with Whole Genome Sequencing methods.
- Investigate the different receptors for DHA in endothelial cells that may connect to various signaling pathways.
- Validate the growth-state- and concentration-dependent effects of DHA in animal models and even human clinical trials.
- Explore what 20 and 125 μM of DHA *in vitro* might mean in relation to the *in vivo* situation, which may help to determine the dietary refence intakes of DHA, especially the tolerable upper intake limit, and recommended doses for supplementation.

CONCLUSIONS AND SIGNIFICANCE

The effects of DHA on endothelial cells are growth-state-, concentration-, and time-dependent. The lower concentration of DHA (20 μM) is most likely to be atheroprotective based on the responses of eNOS, cell cycle profiles, and epigenetic factors. Specifically, 20 μM DHA induced eNOS activation and expression, reduced proliferation and apoptosis, and downregulated transactivation of NF-κB and CREB. On the other hand, judging from the same factors, 125 μM DHA may be deleterious to endothelial cells by reducing eNOS expression, inducing apoptosis, and promoting inflammation via transactivation of NF-κB and CREB as well as an increase of H3S28 phosphorylation. While p38 MAPK was involved in all these responses to DHA, p38 MAPK signaling only played a small part based on the p38 MAPK inhibition results and the deduced signaling pathways as illustrated in Fig. 25. And DHA may act through many other pathways that collectively lead to the final outcomes we observed. MSK was also partially involved in the DHA-mediated differential responses of NF-κB, CREB, and even eNOS, but MSK acted independently of p38 MAPK in the majority of those responses. In addition, MSK was found to be essential for eNOS activation in both endothelial growth states, which has not been reported yet. Surprisingly, however, MSK is not likely to be the kinase for histone H3 phosphorylation at Ser-10 and Ser-28 sites in endothelial cells. This study is the first to report that DHA may modulate the transcriptional activities of CREB via Ser-133 phosphorylation and NF-κB by differentially regulating various PTMs on RelA, as well as induce H3 phosphorylation in endothelial cells. These epigenetic changes would cause differences in gene expression profiles such as *NOS3*, through which DHA exerts its effects on endothelial cells. It was also found, for the first time, that eNOS was expressed more in quiescent endothelial cells than in growing cells, based on the evidence showing the relative protein levels were about 1.5-fold higher in quiescent cells compared to that in growing cells.

This study emphasized the importance of growth state for the effects of DHA on endothelial cells. The quiescent endothelial cells seem to be more responsive to 20 μM DHA than the growing cells, implying that DHA might be more effective in primary prevention of CVD for healthy individuals compared to patients already with impaired endothelial functions. In addition, the contradictory effects of DHA at different concentrations brings up concerns for DHA intakes, and recommendation for both dietary intake and supplementation. Better and more refined intake recommendations are needed catering to different subpopulations, especially based on their health status, striving to achieve optimal plasma DHA levels. Also, by exploring the specific factors, either intermediate between different pathways or

downstream of those epigenetic factors, we may be able to identify potential therapeutic targets and/or diagnostic markers for endothelial cell functions and atherosclerosis.

REFERENCES

1. World Health Organization. The top 10 causes of death [Internet]. 2020 [cited 2021 Sep 17]. Available from: https://www.who.int/news-room/fact-sheets/detail/the-top-10-causes-of-death
2. Anderson TJ, Gerhard MD, Meredith IT, Charbonneau F, Delagrange D, Creager MA, et al. Systemic nature of endothelial dysfunction in atherosclerosis. Am J Cardiol. 1995 Feb;75(6):71B-74B.
3. Siragusa M, Fleming I. The eNOS signalosome and its link to endothelial dysfunction. Pflugers Arch Eur J Physiol. 2016;468(7):1125–37.
4. Saravanan P, Davidson NC, Schmidt EB, Calder PC. Cardiovascular effects of marine omega-3 fatty acids. Lancet. 2010;376(9740):540–50.
5. Du Y, Taylor CG, Aukema HM, Zahradka P. Importance of extracellular matrix and growth state for the EA.hy926 endothelial cell response to polyunsaturated fatty acids. PLoS One. 2018;13(5):1–21.
6. Du Y. Effects of Dietary Polyunsaturated Fatty Acids and Oxylipins on Human EA.hy926 Endothelial Cells. University of Manitoba; 2018.
7. Alberts B, Johnson A, Lewis J, Raff M, Roberts K, Walter P. Blood Vessels and Endothelial Cells. In: Molecular Biology of the Cell. 4th ed. New York: Garland Science; 2002.
8. Michiels C. Endothelial cell functions. J Cell Physiol. 2003;196(3):430–43.
9. Sturtzel C. Endothelial Cells. Adv Exp Med Biol. 2017;1003:71–91.
10. Pearson JD, Carleton JS, Gordon JL. Metabolism of adenine nucleotides by ectoenzymes of vascular endothelial and smooth-muscle cells in culture. Biochem J. 1980 Aug;190(2):421–9.
11. Moncada S, Gryglewski R, Bunting S, Vane JR. An enzyme isolated from arteries transforms prostaglandin endoperoxides to an unstable substance that inhibits platelet aggregation. Nature. 1976 Oct;263(5579):663–5.
12. Cines DB, Pollak ES, Buck CA, Loscalzo J, Zimmerman GA, McEver RP, et al. Endothelial cells in physiology and in the pathophysiology of vascular disorders. Blood. 1998 May;91(10):3527–61.
13. de Graaf JC, Banga JD, Moncada S, Palmer RM, de Groot PG, Sixma JJ. Nitric oxide functions as an inhibitor of platelet adhesion under flow conditions. Circulation. 1992 Jun;85(6):2284–90.

14. Emeis JJ. The Control of tPA and PAI-1 Secretion from the Vessel Wall. Vasc Med Rev. 1995 May 1;vmr-6(2):153–66.
15. Stern DM, Esposito C, Gerlach H, Gerlach M, Ryan J, Handley D, et al. Endothelium and regulation of coagulation. Diabetes Care. 1991 Feb;14(2):160–6.
16. Esmon CT. The endothelial cell protein C receptor. Thromb Haemost. 2000 May;83(5):639–43.
17. Gross PL, Aird WC. The endothelium and thrombosis. Semin Thromb Hemost. 2000;26(5):463–78.
18. Zimmerman GA, McIntyre TM, Mehra M, Prescott SM. Endothelial cell-associated platelet-activating factor: a novel mechanism for signaling intercellular adhesion. J Cell Biol. 1990 Feb;110(2):529–40.
19. Palmer RM, Ferrige AG, Moncada S. Nitric oxide release accounts for the biological activity of endothelium-derived relaxing factor. Nature. 1987 Jun;327(6122):524–6.
20. Rubanyi GM, Botelho LH. Endothelins. FASEB J. 1991 Sep;5(12):2713–20.
21. Hikmet F, Méar L, Edvinsson Å, Micke P, Uhlén M, Lindskog C. The protein expression profile of ACE2 in human tissues. Mol Syst Biol. 2020;16(7):1–16.
22. Ghafouri-Fard S, Noroozi R, Omrani MD, Branicki W, Pośpiech E, Sayad A, et al. Angiotensin converting enzyme: A review on expression profile and its association with human disorders with special focus on SARS-CoV-2 infection. Vascul Pharmacol. 2020/05/11. 2020 Jul;130:106680.
23. Collins T, Read MA, Neish AS, Whitley MZ, Thanos D, Maniatis T. Transcriptional regulation of endothelial cell adhesion molecules: NF-kappa B and cytokine-inducible enhancers. FASEB J Off Publ Fed Am Soc Exp Biol. 1995 Jul;9(10):899–909.
24. Pober JS, Sessa WC. Evolving functions of endothelial cells in inflammation. Nat Rev Immunol. 2007;7(10):803–15.
25. Toya T, Sara JD, Corban MT, Taher R, Godo S, Herrmann J, et al. Assessment of peripheral endothelial function predicts future risk of solid-tumor cancer. Eur J Prev Cardiol. 2020 Apr;27(6):608–18.
26. Bonetti PO, Lerman LO, Lerman A. Endothelial dysfunction: A marker of atherosclerotic risk. Arterioscler Thromb Vasc Biol. 2003;23(2):168–75.
27. Ludmer PL, Selwyn AP, Shook TL, Wayne RR, Mudge GH, Alexander RW, et al. Paradoxical vasoconstriction induced by acetylcholine in atherosclerotic coronary arteries. N Engl J Med. 1986;315:1046–51.
28. Endemann DH, Schiffrin EL. Endothelial dysfunction. J Am Soc Nephrol.

2004;15(8):1983–92.
29. Garcia V, Sessa WC. Endothelial NOS: perspective and recent developments. Br J Pharmacol. 2019;176(2):189–96.
30. McCabe TJ, Fulton D, Roman LJ, Sessa WC. Enhanced electron flux and reduced calmodulin dissociation may explain "calcium-independent" eNOS activation by phosphorylation. J Biol Chem. 2000 Mar;275(9):6123–8.
31. Tousoulis D, Kampoli A-M, Papageorgiou N, Stefanadis C. The Role of Nitric Oxide on Endothelial Function. Curr Vasc Pharmacol. 2012;10(1):4–18.
32. Vanhoutte PM, Shimokawa H, Feletou M, Tang EHC. Endothelial dysfunction and vascular disease – a 30th anniversary update. Acta Physiol. 2017;219(1):22–96.
33. Davignon J, Ganz P. Role of endothelial dysfunction in atherosclerosis. Circulation. 2004;109(23 SUPPL.):III-27-III–32.
34. Deanfield JE, Halcox JP, Rabelink TJ. Endothelial function and dysfunction: Testing and clinical relevance. Circulation. 2007;115(10):1285–95.
35. Bouïs D, Hospers GAP, Meijer C, Molema G, Mulder NH. Endothelium in vitro: A review of human vascular endothelial cell lines for blood vessel-related research. Angiogenesis. 2001;4(2):91–102.
36. Chi JT, Chang HY, Haraldsen G, Jahnsen FL, Troyanskaya OG, Chang DS, et al. Endothelial cell diversity revealed by global expression profiling. Proc Natl Acad Sci U S A. 2003;100(19):10623–8.
37. Edgell CJS, McDonald CC, Graham JB. Permanent cell line expressing human factor VIII-related antigen established by hybridization. Proc Natl Acad Sci U S A. 1983;80(12 I):3734–7.
38. Unger RE, Krump-Konvalinkova V, Peters K, James Kirkpatrick C. In vitro expression of the endothelial phenotype: Comparative study of primary isolated cells and cell lines, including the novel cell line HPMEC-ST1.6R. Microvasc Res. 2002;64(3):384–97.
39. Warner FJ, Lew RA, Smith AI, Lambert DW, Hooper NM, Turner AJ. Angiotensin-converting enzyme 2 (ACE2), but not ACE, is preferentially localized to the apical surface of polarized kidney cells. J Biol Chem. 2005;280(47):39353–62.
40. Ahn K, Pan S, Beningo K, Hupe D. A permanent human cell line (EA.hy926) preserves the characteristics of endothelin converting enzyme from primary human umbilical vein endothelial cells. Life Sci. 1995;56(26):2331–41.
41. Reiterer M, Branco CM. Endothelial cells and organ function: applications and

implications of understanding unique and reciprocal remodelling. FEBS J. 2020;287(6):1088–100.

42. Anderson TJ, Grégoire J, Pearson GJ, Barry AR, Couture P, Dawes M, et al. 2016 Canadian Cardiovascular Society Guidelines for the Management of Dyslipidemia for the Prevention of Cardiovascular Disease in the Adult. Can J Cardiol. 2016;32(11):1263–82.
43. Bentzon JF, Otsuka F, Virmani R, Falk E. Mechanisms of plaque formation and rupture. Circ Res. 2014;114(12):1852–66.
44. National Heart Lung and Blood Institute. Atherosclerosis [Internet]. U.S. Department of Health and Human Services, National Institutes of Health. [cited 2019 Jan 26]. Available from: https://www.nhlbi.nih.gov/health-topics/atherosclerosis.
45. Perrault R, Zahradka P. Molecular Defects in Cardiovascular Disease. In: Dhalla NS, Nagano M, Ostadal, editors. Molecular Defects in Cardiovascular Disease. Springer Science+Business Media, LLC; 2011. p. 283–303.
46. The AIM-HIGH Investigators. Niacin in Patients with Low HDL Cholesterol Levels Receiving Intensive Statin Therapy. N Engl J Med. 2011 Nov 15;365(24):2255–67.
47. Kastelein JJP, Akdim F, Stroes ESG, Zwinderman AH, Bots ML, Stalenhoef AFH, et al. Simvastatin with or without Ezetimibe in Familial Hypercholesterolemia. N Engl J Med. 2008 Apr 3;358(14):1431–43.
48. Zhou R, Stouffer GA, Smith SC. Targeting the Cholesterol Paradigm in the Risk Reduction for Atherosclerotic Cardiovascular Disease: Does the Mechanism of Action of Pharmacotherapy Matter for Clinical Outcomes? J Cardiovasc Pharmacol Ther. 2021;
49. Stone NJ, Robinson JG, Lichtenstein AH, Bairey Merz CN, Blum CB, Eckel RH, et al. 2013 ACC/AHA guideline on the treatment of blood cholesterol to reduce atherosclerotic cardiovascular risk in adults: A report of the american college of cardiology/american heart association task force on practice guidelines. Circulation. 2014;129(25 SUPPL. 1):1–45.
50. Gajecki D, Gawrys J, Szahidewicz-Krupska E, Doroszko A. Novel Molecular Mechanisms of Pulmonary Hypertension: A Search for Biomarkers and Novel Drug Targets-From Bench to Bed Site. Oxid Med Cell Longev. 2020;2020.
51. Rikitake Y, Liao JK. Rho GTPases, statins, and nitric oxide. Circ Res. 2005;97(12):1232–5.
52. Xu S, Pelisek J, Jin ZG. Atherosclerosis Is an Epigenetic Disease. Vol. 29, Trends in

Endocrinology and Metabolism. 2018. p. 739–42.
53. Khyzha N, Alizada A, Wilson MD, Fish JE. Epigenetics of Atherosclerosis: Emerging Mechanisms and Methods. Trends Mol Med. 2017;23(4):332–47.
54. Greally JM. A user's guide to the ambiguous word "epigenetics." Nat Rev Mol Cell Biol. 2018;19(4):207–8.
55. Cuadrado A, Nebreda AR. Mechanisms and functions of p38 MAPK signalling. Biochem J. 2010;429(3):403–17.
56. Cuenda A, Rousseau S. p38 MAP-Kinases pathway regulation, function and role in human diseases. Biochim Biophys Acta - Mol Cell Res. 2007;1773(8):1358–75.
57. Zarubin T, Han J. Activation and signaling of the p38 MAP kinase pathway. Cell Res. 2005;15(1):11–8.
58. Thornton TM, Rincon M. Non-classical p38 map kinase functions: Cell cycle checkpoints and survival. Int J Biol Sci. 2009;5(1):44–52.
59. Lluís F, Ballestar E, Suelves M, Esteller M, Muñoz-Cánoves P. E47 phosphorylation by p38 MAPK promotes MyoD/E47 association and muscle-specific gene transcription. EMBO J. 2005;24(5):974–84.
60. Simone C, Forcales SV, Hill DA, Imbalzano AN, Latella L, Puri PL. p38 pathway targets SWI-SNF chromatin-remodeling complex to muscle-specific loci. Nat Genet. 2004;36(7):738–43.
61. Rousseau S, Houle F, Landry J, Huot J. P38 MAP kinase activation by vascular endothelial growth factor mediates actin reorganization and cell migration in human endothelial cells. Oncogene. 1997;15(18):2169–77.
62. Hedges JC, Dechert MA, Yamboliev IA, Martin JL, Hickey E, Weber LA, et al. A role for p38(MAPK)/HSP27 pathway in smooth muscle cell migration. J Biol Chem. 1999;274(34):24211–9.
63. Rousseau S, Dolado I, Beardmore V, Shpiro N, Marquez R, Nebreda AR, et al. CXCL12 and C5a trigger cell migration via a PAK1/2-p38alpha MAPK-MAPKAP-K2-HSP27 pathway. Cell Signal. 2006 Nov;18(11):1897–905.
64. Trempolec N, Dave-Coll N, Nebreda AR. SnapShot: P38 MAPK substrates. Cell. 2013;152(4):924-924.e1.
65. Moens U, Kostenko S, Sveinbjørnsson B. The role of mitogen-activated protein kinase-activated protein kinases (MAPKAPKs) in inflammation. Genes (Basel). 2013;4(2):101–33.
66. Duda K, Frödin M. Stimuli That Activate MSK in Cells and the Molecular Mechanism

of Activation. Madame Curie Biosci Database. 2012;2:1–29.
67. McCoy CE, Campbell DG, Deak M, Bloomberg GB, Arthur JSC. MSK1 activity is controlled by multiple phosphorylation sites. Biochem J. 2005;387(2):507–17.
68. Tomás-Zuber M, Mary JL, Lesslauer W. Control sites of ribosomal S6 kinase B and persistent activation through tumor necrosis factor. J Biol Chem. 2000;275(31):23549–58.
69. Sands WA, Palmer TM. Regulating gene transcription in response to cyclic AMP elevation. Cell Signal. 2008 Mar;20(3):460–6.
70. Dancy BM, Cole PA. Protein lysine acetylation by p300/CBP. Chem Rev. 2015;115(6):2419–52.
71. Kalkhoven E. CBP and p300: HATs for different occasions. Biochem Pharmacol. 2004;68(6):1145–55.
72. Vermeulen L, Berghe W Vanden, Beck IME, De Bosscher K, Haegeman G. The versatile role of MSKs in transcriptional regulation. Trends Biochem Sci. 2009;34(6):311–8.
73. Vermeulen L, De Wilde G, Van Damme P, Vanden Berghe W, Haegeman G. Transcriptional activation of the NF-κB p65 subunit by mitogen- and stress-activated protein kinase-1 (MSK1). EMBO J. 2003;22(6):1313–24.
74. Chen L-F, Williams SA, Mu Y, Nakano H, Duerr JM, Buckbinder L, et al. NF-κB RelA Phosphorylation Regulates RelA Acetylation. Mol Cell Biol. 2005;25(18):7966–75.
75. Quivy V, Van Lint C. Regulation at multiple levels of NF-κB-mediated transactivation by protein acetylation. Biochem Pharmacol. 2004;68(6):1221–9.
76. Ning Z, Zheng Z, Hao W, Duan C, Li W, Wang Y, et al. The N Terminus of Orf Virus-Encoded Protein 002 Inhibits Acetylation of NF-κB p65 by Preventing Ser276 Phosphorylation. PLoS One. 2013;8(3):1–10.
77. Dyson MH, Thomson S, Inagaki M, Goto H, Arthur SJ, Nightingale K, et al. MAP kinase-mediated phosphorylation of distinct pools of histone H3 at S10 or S28 via mitogen- and stress-activated kinase 1/2. J Cell Sci. 2005;118(10):2247–59.
78. Zhong ZX, Feng SS, Chen SZ, Chen ZM, Chen XW. Inhibition of MSK1 Promotes Inflammation and Apoptosis and Inhibits Functional Recovery After Spinal Cord Injury. J Mol Neurosci. 2019;68(2):191–203.
79. Williams LM, Gilmore TD. Looking Down on NF-κB. Mol Cell Biol. 2020 Jul 14;40(15):ε00104-20.

80. Hayden MS, Ghosh S. Shared Principles in NF-κB Signaling. Cell. 2008;132(3):344–62.
81. Gilmore TD. Introduction to NF-κB: Players, pathways, perspectives. Oncogene. 2006;25(51):6680–4.
82. Zhang Q, Lenardo MJ, Baltimore D. 30 Years of NF-κB: A Blossoming of Relevance to Human Pathobiology. Cell. 2017;168(1–2):37–57.
83. Perkins ND. Post-translational modifications regulating the activity and function of the nuclear factor kappa B pathway. Oncogene. 2006;25(51):6717–30.
84. Christian F, Smith E, Carmody R. The Regulation of NF-κB Subunits by Phosphorylation. Cells. 2016;5(1):12.
85. Oeckinghaus A, Ghosh S. The NF-κB Family of Transcription Factors and Its Regulation. Cold Spring Harb Perspect Biol. 2009 Oct 1;1(4):a000034.
86. Liu T, Zhang L, Joo D, Sun SC. NF-κB signaling in inflammation. Signal Transduct Target Ther. 2017;2(March).
87. Hou Y, Moreau F, Chadee K. PPARγ is an E3 ligase that induces the degradation of NFκB/p65. Nat Commun. 2012;3:1–11.
88. Scirpo R, Fiorotto R, Villani A, Amenduni M, Spirli C, Strazzabosco M. Stimulation of nuclear receptor peroxisome proliferator-activated receptor-γ limits NF-κB-dependent inflammation in mouse cystic fibrosis biliary epithelium. Hepatology. 2015;62(5):1551–62.
89. Ricote M, Glass CK. PPARs and molecular mechanisms of transrepression. Biochim Biophys Acta - Mol Cell Biol Lipids. 2007;1771(8):926–35.
90. Bordoni A, Di Nunzio M, Danesi F, Biagi PL. Polyunsaturated fatty acids: From diet to binding to ppars and other nuclear receptors. Genes Nutr. 2006;1(2):95–106.
91. Quandt E, Ribeiro MPC, Clotet J. Atypical cyclins: the extended family portrait. Cell Mol Life Sci. 2020;77(2):231–42.
92. Hydbring P, Malumbres M, Sicinski P. Non-canonical functions of cell cycle cyclins and cyclin-dependent kinases. Nat Rev Mol Cell Biol. 2016;17(5):280–92.
93. Martínez-Alonso D, Malumbres M. Mammalian cell cycle cyclins. Semin Cell Dev Biol. 2020;107(March):28–35.
94. Morgan DO. The Cell Cycle: Principles of Control. Lawrence E, editor. London: New Science Press; 2007.
95. Malumbres M, Barbacid M. Cell cycle, CDKs and cancer: A changing paradigm. Nat Rev Cancer. 2009;9(3):153–66.

96. Beroukhim R, Mermel CH, Porter D, Wei G, Raychaudhuri S, Donovan J, et al. The landscape of somatic copy-number alteration across human cancers. Nature. 2010 Feb;463(7283):899–905.
97. Tchakarska G, Sola B. The double dealing of cyclin D1. Cell Cycle. 2020;19(2):163–78.
98. Densham RM, Todd DE, Balmanno K, Cook SJ. ERK1/2 and p38 cooperate to delay progression through G1 by promoting cyclin D1 protein turnover. Cell Signal. 2008;20(11):1986–94.
99. Annunziato AT. DNA Packaging: Nucleosomes and Chromatin. Nat Educ. 2008;1(1):26.
100. Gibney ER, Nolan CM. Epigenetics and gene expression. Heredity (Edinb). 2010;105(1):4–13.
101. Adams J. The complexity of gene expression, protein interaction, and cell differentiation. Nat Educ. 2008;1(1):110.
102. Sawicka A, Seiser C. Histone H3 phosphorylation - A versatile chromatin modification for different occasions. Biochimie. 2012;94(11):2193–201.
103. Clancy S. DNA transcription. Nat Educ. 2008;1(1):41.
104. Fry CJ, Peterson CL. Transcription. Unlocking the gates to gene expression. Science. 2002 Mar;295(5561):1847–8.
105. Hoopes L. Introduction to the gene expression and regulation topic room. Nat Educ. 2008;1(1):160.
106. Thomas MC, Chiang CM. The general transcription machinery and general cofactors. Crit Rev Biochem Mol Biol. 2006;41(3):105–78.
107. Prigent C, Dimitrov S. Phosphorylation of serine 10 in histone H3, what for? J Cell Sci. 2003;116(18):3677–85.
108. Kheirandish-Gozal L, Khalyfa A, Gozal D, Bhattacharjee R, Wang Y. Endothelial dysfunction in children with obstructive sleep apnea is associated with epigenetic changes in the eNOS gene. Chest. 2013 Apr;143(4):971–7.
109. Fish JE, Yan MS, Matouk CC, St. Bernard R, Ho JJD, Gavryushova A, et al. Hypoxic repression of endothelial nitric-oxide synthase transcription is coupled with eviction of promoter histones. J Biol Chem. 2010;285(2):810–26.
110. Li D, Wang C, Li N, Zhang LI. Propofol selectively inhibits nuclear factor-κB activity by suppressing p38 mitogen-activated protein kinase signaling in human EA.hy926 endothelial cells during intermittent hypoxia/reoxygenation. Mol Med Rep.

2014;9(4):1460–6.

111. Hu C, Lu KT, Mukohda M, Davis DR, Faraci FM, Sigmund CD. Interference with PPARγ in endothelium accelerates angiotensin II-induced endothelial dysfunction. Physiol Genomics. 2016;48(2):124–34.

112. Wang S, Awad KS, Elinoff JM, Dougherty EJ, Ferreyra GA, Wang JY, et al. G protein-coupled receptor 40 (GPR40) and peroxisome proliferator-activated receptor γ (PPARγ): An integrated two-receptor signaling pathway. J Biol Chem. 2015;290(32):19544–57.

113. Saha RN, Jana M, Pahan K. MAPK p38 Regulates Transcriptional Activity of NF-κB in Primary Human Astrocytes via Acetylation of p65. J Immunol. 2007;179(10):7101–9.

114. Fang F, Yang Y, Yuan Z, Gao Y, Zhou J, Chen Q, et al. Myocardin-related transcription factor A mediates OxLDL-induced endothelial injury. Circ Res. 2011 Apr;108(7):797–807.

115. Nicorescu I, Dallinga GM, de Winther MPJ, Stroes ESG, Bahjat M. Potential epigenetic therapeutics for atherosclerosis treatment. Atherosclerosis. 2019;281(September 2018):189–97.

116. Pandey D, Sikka G, Bergman Y, Kim JH, Ryoo S, Romer L, et al. Transcriptional regulation of endothelial arginase 2 by histone deacetylase 2. Arterioscler Thromb Vasc Biol. 2014 Jul;34(7):1556–66.

117. El-Osta A, Brasacchio D, Yao D, Pocai A, Jones PL, Roeder RG, et al. Transient high glucose causes persistent epigenetic changes and altered gene expression during subsequent normoglycemia. J Exp Med. 2008;205(10):2409–17.

118. Chen S, Feng B, George B, Chakrabarti R, Chen M, Chakrabarti S. Transcriptional coactivator p300 regulates glucose-induced gene expression in endothelial cells. Am J Physiol Endocrinol Metab. 2010 Jan;298(1):E127-37.

119. Wort SJ, Ito M, Chou P-C, Mc Master SK, Badiger R, Jazrawi E, et al. Synergistic induction of endothelin-1 by tumor necrosis factor alpha and interferon gamma is due to enhanced NF-kappaB binding and histone acetylation at specific kappaB sites. J Biol Chem. 2009 Sep;284(36):24297–305.

120. Chiu J-J, Chien S. Effects of disturbed flow on vascular endothelium: pathophysiological basis and clinical perspectives. Physiol Rev. 2011 Jan;91(1):327–87.

121. Illi B, Nanni S, Scopece A, Farsetti A, Biglioli P, Capogrossi MC, et al. Shear stress-

mediated chromatin remodeling provides molecular basis for flow-dependent regulation of gene expression. Circ Res. 2003 Jul;93(2):155–61.

122. Xia N, Strand S, Schlufter F, Siuda D, Reifenberg G, Kleinert H, et al. Role of SIRT1 and FOXO factors in eNOS transcriptional activation by resveratrol. Nitric oxide Biol Chem. 2013 Aug;32:29–35.
123. Man AWC, Li H, Xia N. The role of sirtuin1 in regulating endothelial function, arterial remodeling and vascular aging. Front Physiol. 2019;10(SEP):1–11.
124. Kauppinen A, Suuronen T, Ojala J, Kaarniranta K, Salminen A. Antagonistic crosstalk between NF-κB and SIRT1 in the regulation of inflammation and metabolic disorders. Cell Signal. 2013 Oct;25(10):1939–48.
125. Fang Z, Wang X, Sun X, Hu W, Miao QR. The Role of Histone Protein Acetylation in Regulating Endothelial Function. Front Cell Dev Biol. 2021;9(April):1–20.
126. Olmos Y, Sánchez-Gómez FJ, Wild B, García-Quintans N, Cabezudo S, Lamas S, et al. SirT1 regulation of antioxidant genes is dependent on the formation of a FoxO3a/PGC-1α complex. Antioxid Redox Signal. 2013 Nov;19(13):1507–21.
127. Fish JE, Matouk CC, Rachlis A, Lin S, Tai SC, D'Abreo C, et al. The expression of endothelial nitric-oxide synthase is controlled by a cell-specific histone code. J Biol Chem. 2005;280(26):24824–38.
128. Yan MS, Marsden PA. Epigenetics in the vascular endothelium: Looking from a different perspective in the epigenomics era. Arterioscler Thromb Vasc Biol. 2015;35:2297–306.
129. Ohtani K, Vlachojannis GJ, Koyanagi M, Boeckel J-N, Urbich C, Farcas R, et al. Epigenetic regulation of endothelial lineage committed genes in pro-angiogenic hematopoietic and endothelial progenitor cells. Circ Res. 2011 Nov;109(11):1219–29.
130. Andreou I, Sun X, Stone PH, Edelman ER, Feinberg MW. miRNAs in atherosclerotic plaque initiation, progression, and rupture. Trends Mol Med. 2015;21(5):307–18.
131. Liu Y, Zheng L, Wang Q, Hu YW. Emerging roles and mechanisms of long noncoding RNAs in atherosclerosis. Int J Cardiol. 2017;228(2017):570–82.
132. Skuratovskaia D, Vulf M, Komar A, Kirienkova E, Litvinova L. Promising directions in atherosclerosis treatment based on epigenetic regulation using microRNAs and long noncoding RNAs. Biomolecules. 2019;9(6).
133. Mohar DS, Malik S. The Sirtuin System: The Holy Grail of Resveratrol? J Clin Exp Cardiolog. 2012 Nov;3(11).
134. Jiang X, Yang Z, Chandrakala AN, Pressley D, Parthasarathy S. Oxidized low density

lipoproteins--do we know enough about them? Cardiovasc drugs Ther. 2011 Oct;25(5):367–77.

135. Lapointe A, Couillard C, Lemieux S. Effects of dietary factors on oxidation of low-density lipoprotein particles. J Nutr Biochem. 2006 Oct;17(10):645–58.
136. Jang H, Serra C. Nutrition, Epigenetics, and Diseases. Clin Nutr Res. 2014;3(1):1.
137. Crider KS, Yang TP, Berry RJ, Bailey LB. Folate and DNA methylation: A review of molecular mechanisms and the evidence for Folate's role. Adv Nutr. 2012;3(1):21–38.
138. Rochtus A, Jansen K, Van Geet C, Freson K. Nutri-epigenomic Studies Related to Neural Tube Defects: Does Folate Affect Neural Tube Closure Via Changes in DNA Methylation? Mini Rev Med Chem. 2015;15(13):1095–102.
139. Vickers MH. Early life nutrition, epigenetics and programming of later life disease. Nutrients. 2014;6(6):2165–78.
140. Indrio F, Martini S, Francavilla R, Corvaglia L, Cristofori F, Mastrolia SA, et al. Epigenetic matters: The link between early nutrition, microbiome, and long-term health development. Front Pediatr. 2017;5(August):1–14.
141. Greco EA, Lenzi A, Migliaccio S, Gessani S. Epigenetic Modifications Induced by Nutrients in Early Life Phases: Gender Differences in Metabolic Alteration in Adulthood. Front Genet. 2019;10(September):1–8.
142. van Otterdijk SD, Michels KB. Transgenerational epigenetic inheritance in mammals: how good is the evidence? FASEB J Off Publ Fed Am Soc Exp Biol. 2016 Jul;30(7):2457–65.
143. Jump DB. Nutrients as Regulators of Gene Expression. In: Scientific Advances in Animal Nutrition: Promise for the New Century: Proceedings of a symposium. Washington, D.C.: National Academies Press; 2001.
144. Lakatos A, Jobst K. Kinetics of histone protein glycation. Acta Biochim Biophys Hung. 26(1–4):33–8.
145. Friso S, Udali S, De Santis D, Choi S-W. One-carbon metabolism and epigenetics. Mol Aspects Med. 2017 Apr;54:28–36.
146. Bradshaw PC. Acetyl-CoA Metabolism and Histone Acetylation in the Regulation of Aging and Lifespan. Antioxidants (Basel, Switzerland). 2021 Apr;10(4).
147. Sadli N, Ackland ML, De Mel D, Sinclair AJ, Suphioglu C. Effects of zinc and DHA on the epigenetic regulation of human neuronal cells. Cell Physiol Biochem. 2012;29(1–2):87–98.
148. Jiang L-L, Zhou S-J, Zhang X-M, Chen H-Q, Liu W. Sulforaphane suppresses in vitro

and in vivo lung tumorigenesis through downregulation of HDAC activity. Biomed Pharmacother. 2016 Mar;78:74–80.

149. Lee JH, Friso S, Choi SW. Epigenetic mechanisms underlying the link between non-alcoholic fatty liver diseases and nutrition. Nutrients. 2014;6(8):3303–25.
150. Bishop KS, Ferguson LR. The interaction between epigenetics, nutrition and the development of cancer. Nutrients. 2015;7(2):922–47.
151. Kalea AZ, Drosatos K, Buxton JL. Nutriepigenetics and cardiovascular disease. Curr Opin Clin Nutr Metab Care. 2018;21(4):252–9.
152. Amatruda M, Ippolito G, Vizzuso S, Vizzari G, Banderali G, Verduci E. Epigenetic effects of n-3 LCPUFAs: A role in pediatric metabolic syndrome. Int J Mol Sci. 2019;20(9).
153. Perfilyev A, Dahlman I, Gillberg L, Rosqvist F, Iggman D, Volkov P, et al. Impact of polyunsaturated and saturated fat overfeeding on the DNA-methylation pattern in human adipose tissue: A randomized controlled trial. Am J Clin Nutr. 2017;105(4):991–1000.
154. Ma Y, Ordovas JM. The integration of epigenetics and genetics in nutrition research for CVD risk factors. Proc Nutr Soc. 2017;76(3):333–46.
155. Chen X, He Y, Fu W, Sahebkar A, Tan Y, Xu S, et al. Histone Deacetylases (HDACs) and Atherosclerosis: A Mechanistic and Pharmacological Review. Front Cell Dev Biol. 2020;8(November).
156. Byrne MM, Murphy RT, Ryan AW. Epigenetic modulation in the treatment of atherosclerotic disease. Front Genet. 2014;5(OCT):1–7.
157. National Institutes of Health. Omega-3 Fatty Acids-Fact sheet for health professionals [Internet]. 2021 [cited 2021 Oct 30]. Available from: https://ods.od.nih.gov/factsheets/Omega3FattyAcids-HealthProfessional/#en30
158. Burdge GC, Jones AE, Wootton SA. Eicosapentaenoic and docosapentaenoic acids are the principal products of alpha-linolenic acid metabolism in young men*. Br J Nutr. 2002 Oct;88(4):355–63.
159. Burdge GC, Wootton SA. Conversion of alpha-linolenic acid to eicosapentaenoic, docosapentaenoic and docosahexaenoic acids in young women. Br J Nutr. 2002 Oct;88(4):411–20.
160. Global Organisation for EPA and DHA. Global Recommendations for EPA and DHA Intake [Internet]. International Society for the Study of Fatty Acids and Lipids. 2014 [cited 2021 Oct 30]. Available from: https://www.issfal.org/goed-recommendations-

for-epa-dha
161. Goyens PLL, Spilker ME, Zock PL, Katan MB, Mensink RP. Conversion of α-linolenic acid in humans is influenced by the absolute amounts of α-linolenic acid and linoleic acid in the diet and not by their ratio. Am J Clin Nutr. 2006;84(1):44–53.
162. Shahidi F, Ambigaipalan P. Omega-3 Polyunsaturated Fatty Acids and Their Health Benefits. Annu Rev Food Sci Technol. 2018;9:345–81.
163. Yasuda T, Ishida T, Rader DJ. Update on the role of endothelial lipase in high-density lipoprotein metabolism, reverse cholesterol transport, and atherosclerosis. Circ J. 2010;74(11):2263–70.
164. Pi X, Xie L, Patterson C. Emerging roles of vascular endothelium in metabolic homeostasis. Circ Res. 2018;123(4):477–94.
165. Calder PC. Docosahexaenoic acid. Ann Nutr Metab. 2016;69(1):8–21.
166. Ghosh A, Gao L, Thakur A, Siu PM, Lai CWK. Role of free fatty acids in endothelial dysfunction. J Biomed Sci. 2017;24(1):1–15.
167. Sarafidis PA, Bakris GL. Non-esterified fatty acids and blood pressure elevation: a mechanism for hypertension in subjects with obesity/insulin resistance? J Hum Hypertens. 2007;21(1):12–9.
168. Carlsson M, Wessman Y, Almgren P, Groop L. High Levels of Nonesterified Fatty Acids Are Associated With Increased Familial Risk of Cardiovascular Disease. Arterioscler Thromb Vasc Biol. 2000 Jun 1;20(6):1588–94.
169. Oppedisano F, Macrì R, Gliozzi M, Musolino V, Carresi C, Maiuolo J, et al. The anti-inflammatory and antioxidant properties of n-3 PUFAs: Their role in cardiovascular protection. Biomedicines. 2020;8(9).
170. Calder PC. Omega-3 fatty acids and inflammatory processes. Nutrients. 2010;2(3):355–74.
171. Calder PC. N-3 Fatty acids, inflammation and immunity: New mechanisms to explain old actions. Proc Nutr Soc. 2013;72(3):326–36.
172. Dyerberg J, Bang HO. Haemostatic function and platelet polyunsaturated fatty acids in Eskimos. Lancet. 1979 Sep;2(8140):433–5.
173. Kagawa Y, Nishizawa M, Suzuki M, Miyatake T, Hamamoto T, Goto K, et al. Eicosapolyenoic acids of serum lipids of Japanese islanders with low incidence of cardiovascular diseases. J Nutr Sci Vitaminol (Tokyo). 1982;28(4):441–53.
174. Kromhout D, Bosschieter EB, de Lezenne Coulander C. The inverse relation between fish consumption and 20-year mortality from coronary heart disease. N Engl J Med.

1985 May;312(19):1205–9.

175. Dolecek TA. Epidemiological evidence of relationships between dietary polyunsaturated fatty acids and mortality in the multiple risk factor intervention trial. Proc Soc Exp Biol Med Soc Exp Biol Med (New York, NY). 1992 Jun;200(2):177–82.

176. Kromhout D, Feskens EJ, Bowles CH. The protective effect of a small amount of fish on coronary heart disease mortality in an elderly population. Int J Epidemiol. 1995 Apr;24(2):340–5.

177. Albert CM, Hennekens CH, O'Donnell CJ, Ajani UA, Carey VJ, Willett WC, et al. Fish consumption and risk of sudden cardiac death. JAMA. 1998 Jan;279(1):23–8.

178. Renier G, Skamene E, DeSanctis J, Radzioch D. Dietary n-3 polyunsaturated fatty acids prevent the development of atherosclerotic lesions in mice. Modulation of macrophage secretory activities. Arterioscler Thromb a J Vasc Biol. 1993 Oct;13(10):1515–24.

179. Daviglus ML, Stamler J, Orencia AJ, Dyer AR, Liu K, Greenland P, et al. Fish consumption and the 30-year risk of fatal myocardial infarction. N Engl J Med. 1997 Apr;336(15):1046–53.

180. Goodfellow J, Bellamy MF, Ramsey MW, Jones CJ, Lewis MJ. Dietary supplementation with marine omega-3 fatty acids improve systemic large artery endothelial function in subjects with hypercholesterolemia. J Am Coll Cardiol. 2000 Feb;35(2):265–70.

181. Thies F, Garry JMC, Yaqoob P, Rerkasem K, Williams J, Shearman CP, et al. Association of n-3 polyunsaturated fatty acids with stability of atherosclerotic plaques: a randomised controlled trial. Lancet (London, England). 2003 Feb;361(9356):477–85.

182. von Schacky C, Angerer P, Kothny W, Theisen K, Mudra H. The effect of dietary omega-3 fatty acids on coronary atherosclerosis. A randomized, double-blind, placebo-controlled trial. Ann Intern Med. 1999 Apr;130(7):554–62.

183. Siasos G, Tousoulis D, Oikonomou E, Zaromitidou M, Verveniotis A, Plastiras A, et al. Effects of Ω-3 fatty acids on endothelial function, arterial wall properties, inflammatory and fibrinolytic status in smokers: a cross over study. Int J Cardiol. 2013 Jun;166(2):340–6.

184. Wiest EF, Walsh-Wilcox MT, Walker MK. Omega-3 Polyunsaturated Fatty Acids Protect Against Cigarette Smoke-Induced Oxidative Stress and Vascular Dysfunction.

Toxicol Sci. 2017 Mar;156(1):300–10.

185. Skulas-Ray AC, Wilson PWF, Harris WS, Brinton EA, Kris-Etherton PM, Richter CK, et al. Omega-3 Fatty Acids for the Management of Hypertriglyceridemia: A Science Advisory from the American Heart Association. Circulation. 2019;140(12):E673–91.
186. Bhatt DL, Steg PG, Miller M, Brinton EA, Jacobson TA, Ketchum SB, et al. Cardiovascular Risk Reduction with Icosapent Ethyl for Hypertriglyceridemia. N Engl J Med. 2018 Nov 10;380(1):11–22.
187. Yokoyama M, Origasa H, Matsuzaki M, Matsuzawa Y, Saito Y, Ishikawa Y, et al. Effects of eicosapentaenoic acid on major coronary events in hypercholesterolaemic patients (JELIS): a randomised open-label, blinded endpoint analysis. Lancet (London, England). 2007 Mar;369(9567):1090–8.
188. Ferrari R, Censi S, Cimaglia P. The journey of omega-3 fatty acids in cardiovascular medicine. Eur Hear Journal, Suppl. 2020;22:J49–53.
189. Nicholls SJ, Lincoff AM, Garcia M, Bash D, Ballantyne CM, Barter PJ, et al. Effect of High-Dose Omega-3 Fatty Acids vs Corn Oil on Major Adverse Cardiovascular Events in Patients at High Cardiovascular Risk: The STRENGTH Randomized Clinical Trial. JAMA - J Am Med Assoc. 2020;324(22):2268–80.
190. Jacobson TA, Ito MK, Maki KC, Orringer CE, Bays HE, Jones PH, et al. National Lipid Association recommendations for patient-centered management of dyslipidemia: Part 1 - Full report. J Clin Lipidol. 2015;9(2):129–69.
191. USDA ARS. Usual Nutrient Intake from Food and Beverages, by Gender and Age, What We Eat in America, NHANES 2015-2018. 2021.
192. Zhang Z, Fulgoni VL, Kris-Etherton PM, Mitmesser SH. Dietary intakes of EPA and DHA omega-3 fatty acids among US childbearing-age and pregnant women: An analysis of NHANES 2001–2014. Nutrients. 2018;10(4).
193. European Food Safety Authority. Scientific Opinion on Dietary Reference Values for fats, including saturated fatty acids, polyunsaturated fatty acids, monounsaturated fatty acids, trans fatty acids, and cholesterol. EFSA J. 2010 Mar;8(3).
194. Forsyth S, Gautier S, Salem N. Global estimates of dietary intake of docosahexaenoic acid and arachidonic acid in developing and developed countries. Ann Nutr Metab. 2016;68(4):258–67.
195. Aranceta J, Pérez-Rodrigo C. Recommended dietary reference intakes, nutritional goals and dietary guidelines for fat and fatty acids: A systematic review. Br J Nutr. 2012;107(SUPPL. 2).

196. Grimsgaard S, Bonaa KH, Hansen JB, Nordøy A. Highly purified eicosapentaenoic acid and docosahexaenoic acid in humans have similar triacylglycerol-lowering effects but divergent effects on serum fatty acids. Am J Clin Nutr. 1997 Sep 1;66(3):649–59.
197. Mori TA, Burke V, Puddey IB, Watts GF, O'Neal DN, Best JD, et al. Purified eicosapentaenoic and docosahexaenoic acids have differential effects on serum lipids and lipoproteins, LDL particle size, glucose, and insulin in mildly hypedipidemic men. Am J Clin Nutr. 2000;71(5):1085–94.
198. Gabbs M, Zahradka P, Taylor CG, Aukema HM. Time Course and Sex Effects of α-Linolenic Acid-Rich and DHA-Rich Supplements on Human Plasma Oxylipins: A Randomized Double-Blind Crossover Trial. J Nutr. 2021;151(3):513–22.
199. Pauls SD, Rodway LR, Sidhu KK, Winter T, Sidhu N, Aukema HM, et al. Oils Rich in α-Linolenic Acid or Docosahexaenoic Acid Have Distinct Effects on Plasma Oxylipin and Adiponectin Concentrations and on Monocyte Bioenergetics in Women with Obesity. J Nutr. 2021;1–14.
200. Metherel AH, Irfan M, Klingel SL, Mutch DM, Bazinet RP. Higher Increase in Plasma DHA in Females Compared to Males Following EPA Supplementation May Be Influenced by a Polymorphism in ELOVL2: An Exploratory Study. Lipids. 2021;56(2):211–28.
201. Abdelmagid SA, Clarke SE, Nielsen DE, Badawi A, El-Sohemy A, Mutch DM, et al. Comprehensive profiling of plasma fatty acid concentrations in young healthy canadian adults. PLoS One. 2015;10(2):1–16.
202. Lauritzen L, Brambilla P, Mazzocchi A, Harsløf LBS, Ciappolino V, Agostoni C. DHA Effects in Brain Development and Function. Nutrients. 2016 Jan;8(1).
203. Kim H-Y, Huang BX, Spector AA. Phosphatidylserine in the brain: metabolism and function. Prog Lipid Res. 2014 Oct;56:1–18.
204. Kosti RI, Kasdagli MI, Kyrozis A, Orsini N, Lagiou P, Taiganidou F, et al. Fish intake, n-3 fatty acid body status, and risk of cognitive decline: a systematic review and a dose-response meta-analysis of observational and experimental studies. Nutr Rev. 2021 Oct;
205. Mazereeuw G, Lanctôt KL, Chau SA, Swardfager W, Herrmann N. Effects of ω-3 fatty acids on cognitive performance: a meta-analysis. Neurobiol Aging. 2012 Jul;33(7):1482.e17-29.
206. van der Wurff ISM, Meyer BJ, de Groot RHM. Effect of Omega-3 Long Chain Polyunsaturated Fatty Acids (n-3 LCPUFA) Supplementation on Cognition in

Children and Adolescents: A Systematic Literature Review with a Focus on n-3 LCPUFA Blood Values and Dose of DHA and EPA. Nutrients. 2020 Oct;12(10).

207. McNamara RK, Jandacek R, Tso P, Dwivedi Y, Ren X, Pandey GN. Lower docosahexaenoic acid concentrations in the postmortem prefrontal cortex of adult depressed suicide victims compared with controls without cardiovascular disease. J Psychiatr Res. 2013 Sep;47(9):1187–91.
208. McNamara RK, Hahn C-G, Jandacek R, Rider T, Tso P, Stanford KE, et al. Selective deficits in the omega-3 fatty acid docosahexaenoic acid in the postmortem orbitofrontal cortex of patients with major depressive disorder. Biol Psychiatry. 2007 Jul;62(1):17–24.
209. SanGiovanni JP, Chew EY. The role of omega-3 long-chain polyunsaturated fatty acids in health and disease of the retina. Prog Retin Eye Res. 2005 Jan;24(1):87–138.
210. Zhong Y, Wang K, Jiang L, Wang J, Zhang X, Xu J, et al. Dietary fatty acid intake, plasma fatty acid levels, and the risk of age-related macular degeneration (AMD): a dose-response meta-analysis of prospective cohort studies. Eur J Nutr. 2021 Sep;60(6):3013–27.
211. Peng Y, Zheng Y, Zhang Y, Zhao J, Chang F, Lu T, et al. Different effects of omega-3 fatty acids on the cell cycle in C2C12 myoblast proliferation. Mol Cell Biochem. 2012;367(1–2):165–73.
212. Huang Y-H, Chiu W-C, Hsu Y-P, Lo Y-L, Wang Y-H. Effects of Omega-3 Fatty Acids on Muscle Mass, Muscle Strength and Muscle Performance among the Elderly: A Meta-Analysis. Nutrients. 2020 Dec;12(12).
213. Zhang H-J, Gao X, Guo X-F, Li K-L, Li S, Sinclair AJ, et al. Effects of dietary eicosapentaenoic acid and docosahexaenoic acid supplementation on metabolic syndrome: A systematic review and meta-analysis of data from 33 randomized controlled trials. Clin Nutr. 2021 Jul;40(7):4538–50.
214. Oliver C, Watson H. Omega-3 fatty acids for cystic fibrosis. Cochrane database Syst Rev. 2016 Jan 5;2016(1):CD002201–CD002201.
215. Garić D, Dumut DC, Shah J, De Sanctis JB, Radzioch D. The role of essential fatty acids in cystic fibrosis and normalizing effect of fenretinide. Cell Mol Life Sci. 2020 Nov;77(21):4255–67.
216. Ma Y, Lindsey ML, Halade G V. DHA derivatives of fish oil as dietary supplements: a nutrition-based drug discovery approach for therapies to prevent metabolic cardiotoxicity. Expert Opin Drug Discov. 2012/06/24. 2012 Aug;7(8):711–21.

217. Bernasconi AA, Wiest MM, Lavie CJ, Milani R V., Laukkanen JA. Effect of Omega-3 Dosage on Cardiovascular Outcomes: An Updated Meta-Analysis and Meta-Regression of Interventional Trials. Mayo Clin Proc. 2021;96(2):304–13.
218. Khan SU, Lone AN, Khan MS, Virani SS, Blumenthal RS, Nasir K, et al. Effect of omega-3 fatty acids on cardiovascular outcomes: A systematic review and meta-analysis. EClinicalMedicine. 2021;38:100997.
219. Bernasconi AA, Lavie CJ, Milani R V., Laukkanen JA. Omega-3 Benefits Remain Strong Post-STRENGTH. Mayo Clin Proc. 2021;96(5):1371–2.
220. Abdelhamid AS, Brown TJ, Brainard JS, Biswas P, Thorpe GC, Moore HJ, et al. Omega-3 fatty acids for the primary and secondary prevention of cardiovascular disease. Cochrane Database Syst Rev. 2020 Feb 29;2020(3).
221. Casula M, Olmastroni E, Gazzotti M, Galimberti F, Zambon A, Catapano AL. Omega-3 polyunsaturated fatty acids supplementation and cardiovascular outcomes: do formulation, dosage, and baseline cardiovascular risk matter? An updated meta-analysis of randomized controlled trials. Pharmacol Res. 2020;160(July):105060.
222. Woodman RJ, Mori TA, Burke V, Puddey IB, Barden A, Watts GF, et al. Effects of purified eicosapentaenoic acid and docosahexaenoic acid on platelet, fibrinolytic and vascular function in hypertensive type 2 diabetic patients. Atherosclerosis. 2003;166(1):85–93.
223. Engler MM, Engler MB, Malloy M, Chiu E, Besio D, Paul S, et al. Docosahexaenoic acid restores endothelial function in children with hyperlipidemia: Results from the early study. Int J Clin Pharmacol Ther. 2004;42(12):672–9.
224. Singhal A, Lanigan J, Storry C, Low S, Birbara T, Lucas A, et al. Docosahexaenoic acid supplementation, vascular function and risk factors for cardiovascular disease: a randomized controlled trial in young adults. J Am Heart Assoc. 2013;2(4):1–11.
225. Mori TA, Bao DQ, Burke V, Puddey IB, Beilin LJ. Docosahexaenoic Acid but Not Eicosapentaenoic Acid Lowers Ambulatory Blood Pressure and Heart Rate in Humans. Hypertension. 1999;34:253–60.
226. Kelley DS, Siegel D, Fedor DM, Adkins Y, Mackey BE. DHA supplementation decreases serum C-reactive protein and other markers of inflammation in hypertriglyceridemic men. J Nutr. 2009;139(3):495–501.
227. Allaire J, Couture P, Leclerc M, Charest A, Marin J, Lépine MC, et al. A randomized, crossover, head-to-head comparison of eicosapentaenoic acid and docosahexaenoic acid supplementation to reduce inflammation markers in men and women: The

Comparing EPA to DHA (ComparED) Study. Am J Clin Nutr. 2016;104(2):280–7.
228. Woodman RJ, Mori TA, Burke V, Puddey IB, Watts GF, Beilin LJ. Effects of purified eicosapentaenoic and docosahexaenoic acids on glycemic control, blood pressure, and serum lipids in type 2 diabetic patients with treated hypertension. Am J Clin Nutr. 2002;76(5):1007–15.
229. Kelley DS, Siegel D, Vemuri M, Mackey BE. Docosahexaenoic acid supplementation improves fasting and postprandial lipid profiles in hypertriglyceridemic men. Am J Clin Nutr. 2007;86(2):324–33.
230. Jones PJH, Senanayake VK, Pu S, Jenkins DJA, Connelly PW, Lamarche B, et al. DHA-enriched high-oleic acid canola oil improves lipid profile and lowers predicted cardiovascular disease risk in the canola oil multicenter randomized controlled trial. Am J Clin Nutr. 2014 Jul;100(1):88–97.
231. Sniderman AD, Furberg CD, Keech A, Roeters van Lennep JE, Frohlich J, Jungner I, et al. Apolipoproteins versus lipids as indices of coronary risk and as targets for statin treatment. Lancet. 2003;361:777–80.
232. Pichler G, Amigo N, Tellez-Plaza M, Pardo-Cea MA, Dominguez-Lucas A, Marrachelli VG, et al. LDL particle size and composition and incident cardiovascular disease in a South-European population: The Hortega-Liposcale Follow-up Study. Int J Cardiol. 2018 Aug 1;264:172–8.
233. Woodman RJ, Mori TA, Burke V, Puddey IB, Watts GF, Best JD, et al. Docosahexaenoic Acid But Not Eicosapentaenoic Acid Increases LDL Particle Size in Treated Hypertensive Type 2 Diabetic Patients. Diabetes Care. 2003;26(1):253.
234. Allaire J, Vors C, Tremblay AJ, Marin J, Charest A, Tchernof A, et al. High-dose DHA has more profound effects on LDL-related features than high-dose EPA: The ComparED study. J Clin Endocrinol Metab. 2018;103(8):2909–17.
235. Rizos EC, Ntzani EE, Bika E, Michael S. Kostapanos, Elisaf MS. Association Between Omega-3 Fatty Acid Supplementation and Risk of Major Cardiovascular Disease Events. JAMA - J Am Med Assoc. 2012;308(10):1024–33.
236. Aung T, Halsey J, Kromhout D, Gerstein HC, Marchioli R, Tavazzi L, et al. Associations of omega-3 fatty acid supplement use with cardiovascular disease risks meta-analysis of 10 trials involving 77 917 individuals. JAMA Cardiol. 2018;3(3):225–34.
237. Mori TA, Watts GF, Burke V, Hilme E, Puddey IB, Beilin LJ. Differential Effects of Eicosapentaenoic Acid and Docosahexaenoic Acid on Vascular Reactivity of the

Forearm Microcirculation in Hyperlipidemic, Overweight Men. Circulation. 2000;102:1264–9.

238. Kelley DS, Siegel D, Vemuri M, Chung GH, Mackey BE. Docosahexaenoic acid supplementation decreases remnant-like particle-cholesterol and increases the (n-3) index in hypertriglyceridemic men. J Nutr. 2008;138(1):30–5.
239. Wang TM, Chen CJ, Lee TS, Chao HY, Wu WH, Hsieh SC, et al. Docosahexaenoic acid attenuates VCAM-1 expression and NF-κB activation in TNF-α-treated human aortic endothelial cells. J Nutr Biochem. 2011;22(2):187–94.
240. Yamagata K, Suzuki S, Tagami M. Docosahexaenoic acid prevented tumor necrosis factor alpha-induced endothelial dysfunction and senescence. Prostaglandins Leukot Essent Fat Acids. 2016;104:11–8.
241. Xing F, Jiang Y, Liu J, Zhao K, Mo Y, Liu Z, et al. Downregulation of human endothelial nitric oxide synthase promoter activity by p38 mitogen-activated protein kinase activation. Biochem Cell Biol. 2006;84(5):780–8.
242. Chen H, Li D, Chen J, Roberts GJ, Saldeen T, Mehta JL. EPA and DHA attenuate ox-LDL-induced expression of adhesion molecules in human coronary artery endothelial cells via protein kinase B pathway. J Mol Cell Cardiol. 2003;35(7):769–75.
243. Massaro M, Scoditti E, Carluccio MA, De Caterina R. Basic mechanisms behind the effects of n-3 fatty acids on cardiovascular disease. Prostaglandins Leukot Essent Fat Acids. 2008;79(3–5):109–15.
244. Lin HC, Lii CK, Lin AH, Li CC, Tsai CH, Pan SK, et al. Docosahexaenoic acid inhibits TNFα-induced ICAM-1 expression by activating PPARα and autophagy in human endothelial cells. Food Chem Toxicol. 2019;134(June):110811.
245. Liu KL, Yang YC, Yao HT, Chia TW, Lu CY, Li CC, et al. Docosahexaenoic acid inhibits inflammation via free fatty acid receptor FFA4, disruption of TAB2 interaction with TAK1/TAB1 and downregulation of ERK-dependent Egr-1 expression in EA.hy926 cells. Mol Nutr Food Res. 2016;60(2):430–43.
246. Gareus R, Kotsaki E, Xanthoulea S, van der Made I, Gijbels MJJ, Kardakaris R, et al. Endothelial Cell-Specific NF-κB Inhibition Protects Mice from Atherosclerosis. Cell Metab. 2008;8(5):372–83.
247. Kim HJ, Ohk B, Yoon HJ, Kang WY, Seong SJ, Kim SY, et al. Docosahexaenoic acid signaling attenuates the proliferation and differentiation of bone marrow-derived osteoclast precursors and promotes apoptosis in mature osteoclasts. Cell Signal. 2017;29:226–32.

248. Yang S, Yuan HQ, Hao YM, Ren Z, Qu SL, Liu LS, et al. Macrophage polarization in atherosclerosis. Clin Chim Acta. 2020;501(September 2019):142–6.
249. Si TL, Liu Q, Ren YF, Li H, Xu XY, Li EH, et al. Enhanced anti-inflammatory effects of DHA and quercetin in lipopolysaccharide-induced RAW264.7 macrophages by inhibiting NF-κB and MAPK activation. Mol Med Rep. 2016;14(1):499–508.
250. Chang HY, Lee HN, Kim W, Surh YJ. Docosahexaenoic acid induces M2 macrophage polarization through peroxisome proliferator-activated receptor γ activation. Life Sci. 2015;120:39–47.
251. Yamagata K, Tusruta C, Ohtuski A, Tagami M. Docosahexaenoic acid decreases TNF-α-induced lectin-like oxidized low-density lipoprotein receptor-1 expression in THP-1 cells. Prostaglandins Leukot Essent Fat Acids. 2014;90(4):125–32.
252. Kattoor AJ, Goel A, Mehta JL. LOX-1: Regulation, signaling and its role in atherosclerosis. Antioxidants. 2019;8(7):1–15.
253. Chao C-Y, Lii C-K, Ye S-Y, Li C-C, Lu C-Y, Lin A-H, et al. Docosahexaenoic Acid Inhibits Vascular Endothelial Growth Factor (VEGF)-Induced Cell Migration via the GPR120/PP2A/ERK1/2/eNOS Signaling Pathway in Human Umbilical Vein Endothelial Cells. J Agric Food Chem. 2014 May 7;62(18):4152–8.
254. Jung SB, Kwon SK, Kwon M, Nagar H, Jeon BH, Irani K, et al. Docosahexaenoic acid improves vascular function via up-regulation of SIRT1 expression in endothelial cells. Biochem Biophys Res Commun. 2013;437(1):114–9.
255. Novinbahador T, Nourazarian A, Asgharzadeh M, Rahbarghazi R, Avci ÇB, Bagca BG, et al. Docosahexaenoic acid attenuates the detrimental effect of palmitic acid on human endothelial cells by modulating genes from the atherosclerosis signaling pathway. J Cell Biochem. 2018;119(12):9752–63.
256. Jiang WC, Chen CM, Hamdin CD, Orekhov AN, Sobenin IA, Layne MD, et al. Therapeutic potential of heme oxygenase-1 in aneurysmal diseases. Antioxidants. 2020;9(11):1–21.
257. Idriss NK, Blann AD, Lip GYH. Hemoxygenase-1 in Cardiovascular Disease. J Am Coll Cardiol. 2008;52(12):971–8.
258. Yang YC, Lii CK, Wei YL, Li CC, Lu CY, Liu KL, et al. Docosahexaenoic acid inhibition of inflammation is partially via cross-talk between Nrf2/heme oxygenase 1 and IKK/NF-κB pathways. J Nutr Biochem. 2013;24(1):204–12.
259. Stulnig G, Frisch MT, Crnkovic S, Stiegler P, Sereinigg M, Stacher E, et al. Docosahexaenoic acid (DHA)-induced heme oxygenase-1 attenuates cytotoxic effects

of DHA in vascular smooth muscle cells. Atherosclerosis. 2013;230(2):406–13.
260. Altenburg JD, Siddiqui RA. Docosahexaenoic acid downregulates interferon gamma-induced expression of CXCL16 in human aortic smooth muscle cells. Biochem Biophys Res Commun. 2010;391(1):609–14.
261. Bousserouel S, Raymondjean M, Brouillet A, Béréziat G, Andréani M. Modulation of cyclin D1 and early growth response factor-1 gene expression in interleukin-1β-treated rat smooth muscle cells by n-6 and n-3 polyunsaturated fatty acids. Eur J Biochem. 2004;271(22):4462–73.
262. Oeckinghaus A, Hayden MS, Ghosh S. Crosstalk in NF-κB signaling pathways. Nat Immunol. 2011;12(8):695–708.
263. Du Y, Taylor CG, Aukema HM, Zahradka P. Regulation of docosahexaenoic acid-induced apoptosis of confluent endothelial cells : Contributions of MAPKs and caspases. BBA - Mol Cell Biol Lipids. 2021;1866(5):158902.
264. Naqvi S, Macdonald A, Mccoy CE, Darragh J, Reith AD, Arthur JSC. Characterization of the cellular action of the MSK inhibitor SB-747651A. Biochem J. 2012;441(1):347–57.
265. Perrault R, Molnar P, Poole J, Zahradka P. PDGF-BB-mediated activation of CREB in vascular smooth muscle cells alters cell cycling via Rb, FoxO1 and p27kip1. Exp Cell Res. 2021;404(1):112612.
266. Taylor SC, Posch A. The design of a quantitative western blot experiment. Biomed Res Int. 2014;2014.
267. Sabbir MG, Taylor CG, Zahradka P. Hypomorphic CAMKK2 in EA.hy926 endothelial cells causes abnormal transferrin trafficking, iron homeostasis and glucose metabolism. Biochim Biophys Acta - Mol Cell Res. 2020;1867(10):118763.
268. Darzynkiewicz Z, Juan G, Bedner E. Determining cell cycle stages by flow cytometry. Curr Protoc cell Biol. 2001 May;Chapter 8:Unit 8.4.
269. Tate EH, Wilder ME, Cram LS, Wharton W. A method for staining 3T3 cell nuclei with propidium iodide in hypotonic solution. Cytometry. 1983;4(3):211–5.
270. Anter E, Chen K, Shapira OM, Karas RH, Keaney JF. p38 mitogen-activated protein kinase activates eNOS in endothelial cells by an estrogen receptor α-dependent pathway in response to black tea polyphenols. Circ Res. 2005;96(10):1072–8.
271. Kim HJ, Vosseler CA, Weber PC, Erl W. Docosahexaenoic acid induces apoptosis in proliferating human endothelial cells. J Cell Physiol. 2005;204(3):881–8.
272. Newell M, Brun M, Field CJ. Treatment with DHA Modifies the Response of MDA-

MB-231 Breast Cancer Cells and Tumors from nu/nu Mice to Doxorubicin through Apoptosis and Cell Cycle Arrest. J Nutr. 2019;149(1):46–56.

273. Maillard V, Desmarchais A, Durcin M, Uzbekova S, Elis S. Docosahexaenoic acid (DHA) effects on proliferation and steroidogenesis of bovine granulosa cells. Reprod Biol Endocrinol. 2018;16(1):1–18.
274. Newell M, Baker K, Postovit LM, Field CJ. A critical review on the effect of docosahexaenoic acid (Dha) on cancer cell cycle progression. Int J Mol Sci. 2017;18(8):1–14.
275. Blizard Institute of Cell and Molecular Science, Warnes G. DNA fragmentation. Uses of flow cytometry. 2019.
276. Shafi O. Switching of vascular cells towards atherogenesis, and other factors contributing to atherosclerosis: a systematic review. Thromb J. 2020;18(1):1–18.
277. Stebbins CL, Stice JP, Hart CM, Mbai FN, Knowlton AA. Effects of dietary decosahexaenoic acid (DHA) on eNOS in human coronary artery endothelial cells. J Cardiovasc Pharmacol Ther. 2008;13(4):261–8.
278. Wang CC, Liu W Bin, Cao XF, Huang YY, Wang X, Xiao K, et al. Excess DHA Induces Cell Cycle Arrest by Activating the P53/Cycling Pathway in Blunt Snout Bream (Megalobrama amblycephala). Front Mar Sci. 2020;7(May):1–13.
279. Li Q, Zhang Q, Wang M, Liu F, Zhao S, Ma J, et al. Docosahexaenoic acid affects endothelial nitric oxide synthase in caveolae. Arch Biochem Biophys. 2007;466(2):250–9.
280. Vu TT, Dieterich P, Vu TT, Deussen A. Docosahexaenoic acid reduces adenosine triphosphate-induced calcium influx via inhibition of store-operated calcium channels and enhances baseline endothelial nitric oxide synthase phosphorylation in human endothelial cells. Korean J Physiol Pharmacol. 2019;23(5):345–56.
281. Gousset-Dupont A, Robert V, Grynberg A, Lacour B, Tardivel S. The effect of n-3 PUFA on eNOS activity and expression in Ea hy 926 cells. Prostaglandins Leukot Essent Fat Acids. 2007;76(3):131–9.
282. Matesanz N, Park G, McAllister H, Leahey W, Devine A, Mcveigh GE, et al. Docosahexaenoic acid improves the nitroso-redox balance and reduces VEGF-mediated angiogenic signaling in microvascular endothelial cells. Investig Ophthalmol Vis Sci. 2010;51(12):6815–25.
283. Baker EJ, Valenzuela CA, De Souza CO, Yaqoob P, Miles EA, Calder PC. Comparative anti-inflammatory effects of plant- and marine-derived omega-3 fatty

acids explored in an endothelial cell line. Biochim Biophys Acta - Mol Cell Biol Lipids. 2020;1865(6):158662.

284. Atochin DN, Wang A, Liu VWT, Critchlow JD, Dantas AP V, Looft-Wilson R, et al. The phosphorylation state of eNOS modulates vascular reactivity and outcome of cerebral ischemia in vivo. J Clin Invest. 2007 Jul;117(7):1961–7.
285. Li Q, Atochin D, Kashiwagi S, Earle J, Wang A, Mandeville E, et al. Deficient eNOS phosphorylation is a mechanism for diabetic vascular dysfunction contributing to increased stroke size. Stroke. 2013 Nov;44(11):3183–8.
286. Kashiwagi S, Atochin DN, Li Q, Schleicher M, Pong T, Sessa WC, et al. eNOS phosphorylation on serine 1176 affects insulin sensitivity and adiposity. Biochem Biophys Res Commun. 2013 Feb;431(2):284–90.
287. Park K, Mima A, Li Q, Rask-Madsen C, He P, Mizutani K, et al. Insulin decreases atherosclerosis by inducing endothelin receptor B expression. JCI Insight. 2016;1(6).
288. Eroglu E, Saeedi Saravi SS, Sorrentino A, Steinhorn B, Michel T. Discordance between eNOS phosphorylation and activation revealed by multispectral imaging and chemogenetic methods. Proc Natl Acad Sci U S A. 2019;116(40):20210–7.
289. Fleming I, Schulz C, Fichtlscherer B, Kemp BE, Fisslthaler B, Busse R. AMP-activated protein kinase (AMPK) regulates the insulin-induced activation of the nitric oxide synthase in human platelets. Thromb Haemost. 2003;90(11):863–71.
290. Randriamboavonjy V, Schrader J, Busse R, Fleming I. Insulin Induces the Release of Vasodilator Compounds From Platelets by a Nitric Oxide–G Kinase–VAMP-3–dependent Pathway . J Exp Med. 2004 Jan 26;199(3):347–56.
291. Pakala R, Pakala R, Radcliffe JD, Benedict CR. Serotonin-induced endothelial cell proliferation is blocked by omega-3 fatty acids. Prostaglandins Leukot Essent Fat Acids. 1999;60(2):115–23.
292. Crnkovic S, Riederer M, Lechleitner M, Hallström S, Malli R, Graier WF, et al. Docosahexaenoic acid-induced unfolded protein response, cell cycle arrest, and apoptosis in vascular smooth muscle cells are triggered by Ca 2+-dependent induction of oxidative stress. Free Radic Biol Med. 2012;52(9):1786–95.
293. He J, Hong B, Bian M, Jin H, Chen J, Shao J, et al. Docosahexaenoic acid inhibits hepatic stellate cell activation to attenuate liver fibrosis in a PPARγ-dependent manner. Int Immunopharmacol. 2019;75(July):105816.
294. Insua MF, Garelli A, Rotstein NP, German OL, Arias A, Politi LE. Cell cycle regulation in retinal progenitors by glia-derived neurotrophic factor and

docosahexaenoic acid. Investig Ophthalmol Vis Sci. 2003;44(5):2235–44.

295. Siddiqui RA, Jenski LJ, Harvey KA, Wiesehan JD, Stillwell W, Zaloga GP. Cell-cycle arrest in Jurkat leukaemic cells: a possible role for docosahexaenoic acid. Biochem J. 2003 Apr 15;371(Pt 2):621–9.
296. Chen ZY, Istfan NW. Docosahexaenoic acid, a major constituent of fish oil diets, prevents activation of cyclin-dependent kinases and S-phase entry by serum stimulation in HT-29 cells. Prostaglandins Leukot Essent Fat Acids. 2001;64(1):67–73.
297. Alao JP. The regulation of cyclin D1 degradation: Roles in cancer development and the potential for therapeutic invention. Mol Cancer. 2007;6:1–16.
298. Lin N, Uchi H, Moroi Y, Fukiwake N, Dainichi T, Takeuchi S, et al. Expression of the p38 MAPK, NF-κB and cyclin D1 in extramammary Paget's disease. J Dermatol Sci. 2007;45(3):187–92.
299. Witzel II, Koh LF, Perkins ND. Regulation of cyclin D1 gene expression. Biochem Soc Trans. 2010;38(1):217–22.
300. Rubio MF, Fernandez PNL, Alvarado C V., Panelo LC, Grecco MR, Colo GP, et al. Cyclin D1 is a NF-κB corepressor. Biochim Biophys Acta - Mol Cell Res. 2012;1823(6):1119–31.
301. Wang B, Xing F, Liu N, Chen D, Li Z, Liu J. P38α subtype is a potential target to inhibit eNOS activity and NO production in human endothelial cells. Microvasc Res. 2014;91:58–65.
302. Chiu SC, Chiang EPI, Tsai SY, Wang FY, Pai MH, Syu JN, et al. Eicosapentaenoic acid induces neovasculogenesis in human endothelial progenitor cells by modulating c-kit protein and PI3-K/Akt/eNOS signaling pathways. J Nutr Biochem. 2014;25(9):934–45.
303. Searles CD. Transcriptional and posttranscriptional regulation of endothelial nitric oxide synthase expression. Am J Physiol - Cell Physiol. 2006;291(5).
304. Cheriyan VT, Alfaidi M, Jorgensen AN, Alam MA, Abdullah CS, Kolluru GK, et al. Neurogranin regulates eNOS function and endothelial activation. Redox Biol. 2020;34(February):101487.
305. Lee KS, Kim J, Kwak SN, Lee KS, Lee DK, Ha KS, et al. Functional role of NF-κB in expression of human endothelial nitric oxide synthase. Biochem Biophys Res Commun. 2014;448(1):101–7.
306. Chen L feng, Mu Y, Greene WC. Acetylation of RelA at discrete sites regulates

distinct nuclear functions of NF-κB. EMBO J. 2002;21(23):6539–48.
307. Huang B, Yang X-D, Zhou M-M, Ozato K, Chen L-F. Brd4 Coactivates Transcriptional Activation of NF-κB via Specific Binding to Acetylated RelA. Mol Cell Biol. 2009;29(5):1375–87.
308. Greene WC, Chen L. Regulation of NF-kappaB action by reversible acetylation. Novartis Found Symp. 2004;259:208–25.
309. Zhong H, SuYang H, Erdjument-Bromage H, Tempst P, Ghosh S. The transcriptional activity of NF-κB is regulated by the IκB- associated PKAc subunit through a cyclic AMP-independent mechanism. Cell. 1997;89(3):413–24.
310. Gao N, Hibi Y, Cueno M, Asamitsu K, Okamoto T. A-kinase-interacting protein 1 (AKIP1) acts as a molecular determinant of PKA in NF-kappaB signaling. J Biol Chem. 2010 Sep;285(36):28097–104.
311. Wang Y, Mo X, Piper MG, Wang H, Parinandi NL, Guttridge D, et al. M-CSF induces monocyte survival by activating NF-κB p65 phosphorylation at Ser276 via protein kinase C. PLoS One. 2011;6(12).
312. Wang H, Moreau F, Hirota CL, MacNaughton WK. Proteinase-activated receptors induce interleukin-8 expression by intestinal epithelial cells through ERK/RSK90 activation and histone acetylation. FASEB J. 2010;24(6):1971–80.
313. Lu Q, Tong B, Luo Y, Sha L, Chou G, Wang Z, et al. Norisoboldine suppresses VEGF-induced endothelial cell migration via the cAMP-PKA-NF-κB/Notch1 pathway. PLoS One. 2013;8(12).
314. Sharma KL, Jia S, Beacon TH, Adewumi I, López C, Hu P, et al. Mitogen-induced transcriptional programming in human fibroblasts. Gene. 2021;800(July).
315. Turnham RE, Scott JD. Protein kinase A catalytic subunit isoform PRKACA; History, function and physiology. Gene. 2016;577(2):101–8.
316. Rosse C, Linch M, Kermorgant S, Cameron AJM, Boeckeler K, Parker PJ. PKC and the control of localized signal dynamics. Nat Rev Mol Cell Biol. 2010;11(2):103–12.
317. Aires V, Hichami A, Filomenko R, Plé A, Rébé C, Bettaieb A, et al. Docosahexaenoic acid induces increases in [Ca2+]i via inositol 1,4,5-triphosphate production and activates protein kinase Cγ and -δ via phosphatidylserine binding site: Implication in apoptosis in U937 cells. Mol Pharmacol. 2007;72(6):1545–56.
318. Scoditti E, Massaro M, Carluccio MA, Distante A, Storelli C, De Caterina R. PPAR γ agonists inhibit angiogenesis by suppressing PKCα-and CREB-mediated COX-2 expression in the human endothelium. Cardiovasc Res. 2010;86(2):302–10.

319. Massaro M, Habib A, Lubrano L, Del Turco S, Lazzerini G, Bourcier T, et al. The omega-3 fatty acid docosahexaenoate attenuates endothelial cyclooxygenase-2 induction through both NADP(H) oxidase and PKCε inhibition. Proc Natl Acad Sci U S A. 2006;103(41):15184–9.
320. Hilgendorf KI, Johnson CT, Mezger A, Rice SL, Norris AM, Demeter J, et al. Omega-3 Fatty Acids Activate Ciliary FFAR4 to Control Adipogenesis. Cell. 2019;179(6):1289-1305.e21.
321. Hauge M, Vestmar MA, Husted AS, Ekberg JP, Wright MJ, Di Salvo J, et al. GPR40 (FFAR1) - Combined Gs and Gq signaling invitro is associated with robust incretin secretagogue action ex vivo and in vivo. Mol Metab. 2015;4(1):3–14.
322. Nakayama K. cAMP-response element-binding protein (CREB) and NF-κB transcription factors are activated during prolonged hypoxia and cooperatively regulate the induction of matrix metalloproteinase MMP1. J Biol Chem. 2013 Aug;288(31):22584–95.
323. Chandrakesan P, Ahmed I, Anwar T, Wang Y, Sarkar S, Singh P, et al. Novel changes in NF-κB activity during progression and regression phases of hyperplasia: Role of MEK, ERK, and p38. J Biol Chem. 2010;285(43):33485–98.
324. Diamant G, Dikstein R. Transcriptional Control by NF-κB: Elongation in Focus. Biochim Biophys Acta - Gene Regul Mech. 2013;1829(9):937–45.
325. Lanzillotta A, Sarnico I, Ingrassia R, Boroni F, Branca C, Benarese M, et al. The acetylation of RelA in Lys310 dictates the NF-κB-dependent response in post-ischemic injury. Cell Death Dis. 2010;1(11):1–8.
326. Schiaffino L, Bonafede R, Scambi I, Parrella E, Pizzi M, Mariotti R. Acetylation state of RelA modulated by epigenetic drugs prolongs survival and induces a neuroprotective effect on ALS murine model. Sci Rep. 2018;8(1):1–13.
327. Liu Y, Mayo MW, Nagji AS, Smith PW, Ramsey CS, Li D, et al. Phosphorylation of RelA/p65 promotes DNMT-1 recruitment to chromatin and represses transcription of the tumor metastasis suppressor gene BRMS1. Oncogene. 2012 Mar;31(9):1143–54.
328. Zou Z, Huang B, Wu X, Zhang H, Qi J, Bradner J, et al. Brd4 maintains constitutively active NF-κB in cancer cells by binding to acetylated RelA. Oncogene. 2014 May 20;33(18):2395–404.
329. Nowak DE, Tian B, Jamaluddin M, Boldogh I, Vergara LA, Choudhary S, et al. RelA Ser276 phosphorylation is required for activation of a subset of NF-kappaB-dependent genes by recruiting cyclin-dependent kinase 9/cyclin T1 complexes. Mol Cell Biol.

2008 Jun;28(11):3623–38.

330. Tian B, Zhao Y, Sun H, Zhang Y, Yang J, Brasier AR. BRD4 mediates NF-κB-dependent epithelial-mesenchymal transition and pulmonary fibrosis via transcriptional elongation. Am J Physiol Lung Cell Mol Physiol. 2016 Dec;311(6):L1183–201.
331. Wang N, Wu R, Tang D, Kang R. The BET family in immunity and disease. Signal Transduct Target Ther. 2021;6(1).
332. Yang J, Tian B, Brasier AR. Targeting Chromatin Remodeling in Inflammation and Fibrosis. 1st ed. Vol. 107, Advances in Protein Chemistry and Structural Biology. Elsevier Inc.; 2017. 1–36 p.
333. Barboric M, Nissen RM, Kanazawa S, Jabrane-Ferrat N, Peterlin BM. NF-kappaB binds P-TEFb to stimulate transcriptional elongation by RNA polymerase II. Mol Cell. 2001 Aug;8(2):327–37.
334. Brasier AR, Tian B, Jamaluddin M, Kalita MK, Garofalo RP, Lu M. RelA Ser276 phosphorylation-coupled Lys310 acetylation controls transcriptional elongation of inflammatory cytokines in respiratory syncytial virus infection. J Virol. 2011 Nov;85(22):11752–69.
335. Yang X-D, Tajkhorshid E, Chen L-F. Functional Interplay between Acetylation and Methylation of the RelA Subunit of NF-κB. Mol Cell Biol. 2010;30(9):2170–80.
336. Li H, Wittwer T, Weber A, Schneider H, Moreno R, Maine GN, et al. Regulation of NF-B activity by competition between RelA acetylation and ubiquitination. Oncogene. 2012;31(5):611–23.
337. Andrisani OM. CREB-mediated transcriptional control. Crit Rev Eukaryot Gene Expr. 1999;9(1):19–32.
338. Carlezon WA, Duman RS, Nestler EJ. The many faces of CREB. Trends Neurosci. 2005;28(8):436–45.
339. Sharma VK, Singh TG. CREB: A Multifaceted Target for Alzheimer's Disease. Curr Alzheimer Res. 2020;17(14):1280–93.
340. Maurer C, Winter T, Chen S, Hung H-C, Weber F. The CREB-binding protein affects the circadian regulation of behaviour. Vol. 590, FEBS letters. England; 2016. p. 3213–20.
341. Davis BT 4th, Voigt RM, Shaikh M, Forsyth CB, Keshavarzian A. CREB Protein Mediates Alcohol-Induced Circadian Disruption and Intestinal Permeability. Alcohol Clin Exp Res. 2017 Dec;41(12):2007–14.

342. Wheaton KL, Hansen KF, Aten S, Sullivan KA, Yoon H, Hoyt KR, et al. The Phosphorylation of CREB at Serine 133 Is a Key Event for Circadian Clock Timing and Entrainment in the Suprachiasmatic Nucleus. J Biol Rhythms. 2018 Oct;33(5):497–514.
343. Sapio L, Salzillo A, Ragone A, Illiano M, Spina A, Naviglio S. Targeting creb in cancer therapy: A key candidate or one of many? an update. Cancers (Basel). 2020;12(11):1–23.
344. Shankar DB, Sakamoto KM. The role of cyclic-AMP binding protein (CREB) in leukemia cell proliferation and acute leukemias. Leuk Lymphoma. 2004 Feb;45(2):265–70.
345. Newton K, Dixit VM. Signaling in innate immunity and inflammation. Cold Spring Harb Perspect Biol. 2012;4(3).
346. Li G, Jiang Q, Xu K. CREB family: A significant role in liver fibrosis. Biochimie. 2019;163:94–100.
347. Hervouet E, Vallette FM, Cartron P-F. Dnmt3/transcription factor interactions as crucial players in targeted DNA methylation. Epigenetics. 2009 Oct;4(7):487–99.
348. Steven A, Friedrich M, Jank P, Heimer N, Budczies J, Denkert C, et al. What turns CREB on? And off? And why does it matter? Cell Mol Life Sci. 2020;77(20):4049–67.
349. Koga Y, Tsurumaki H, Aoki-Saito H, Sato M, Yatomi M, Takehara K, et al. Roles of cyclic AMP response element binding activation in the ERK1/2 and p38 MAPK signalling pathway in central nervous system, cardiovascular system, osteoclast differentiation and mucin and cytokine production. Int J Mol Sci. 2019;20(6):1–23.
350. Dong Q, Jie Y, Ma J, Li C, Xin T, Yang D. Renal tubular cell death and inflammation response are regulated by the MAPK-ERK-CREB signaling pathway under hypoxia-reoxygenation injury. J Recept Signal Transduct. 2019;39(5–6):383–91.
351. Alvarez-Nölting R, Arnal E, Barcia JM, Miranda M, Romero FJ. Protection by DHA of early hippocampal changes in diabetes: Possible role of CREB and NF-κB. Neurochem Res. 2012;37(1):105–15.
352. Zhao WN, Hylton NK, Wang J, Chindavong PS, Alural B, Kurtser I, et al. Activation of WNT and CREB signaling pathways in human neuronal cells in response to the Omega-3 fatty acid docosahexaenoic acid (DHA). Mol Cell Neurosci. 2019;99(June):103386.
353. Yamashima T. PUFA-GPR40-CREB signaling hypothesis for the adult primate

neurogenesis. Prog Lipid Res. 2012;51(3):221–31.
354. Botham KM, Wheeler-Jones CPD. Postprandial lipoproteins and the molecular regulation of vascular homeostasis. Prog Lipid Res. 2013;52(4):446–64.
355. Dunn KL, Davie JR. Stimulation of the Ras-MAPK pathway leads to independent phosphorylation of histone H3 on serine 10 and 28. Oncogene. 2005;24(21):3492–502.
356. Sawicka A, Hartl D, Goiser M, Pusch O, Stocsits RR, Tamir IM, et al. H3S28 phosphorylation is a hallmark of the transcriptional response to cellular stress. Genome Res. 2014;24(11):1808–20.
357. Adewumi I, López C, Davie JR. Mitogen and stress- activated protein kinase regulated gene expression in cancer cells. Adv Biol Regul. 2019;71(August 2018):147–55.
358. Drobic B, Pérez-Cadahía B, Yu J, Kung SKP, Davie JR. Promoter chromatin remodeling of immediate-early genes is mediated through H3 phosphorylation at either serine 28 or 10 by the MSK1 multi-protein complex. Nucleic Acids Res. 2010;38(10):3196–208.
359. Awad S, Al-Haffar KMA, Marashly Q, Quijada P, Kunhi M, Al-Yacoub N, et al. Control of histone H3 phosphorylation by CaMKII. in response to haemodynamic cardiac stress. J Pathol. 2015;235(4):606–18.
360. Saadatmand AR, Sramek V, Weber S, Finke D, Dewenter M, Sticht C, et al. CaM kinase II regulates cardiac hemoglobin expression through histone phosphorylation upon sympathetic activation. Proc Natl Acad Sci U S A. 2019;116(44):22282–7.
361. Veitch CR, Power AS, Erickson JR. CaMKII Inhibition is a Novel Therapeutic Strategy to Prevent Diabetic Cardiomyopathy. Front Pharmacol. 2021;12:695401.
362. Ebenebe O V., Heather A, Erickson JR. CaMKII in Vascular Signalling: “Friend or Foe”? Hear Lung Circ. 2018;27(5):560–7.
363. Maione AS, Cipolletta E, Sorriento D, Borriello F, Soprano M, Rusciano MR, et al. Cellular subtype expression and activation of CaMKII regulate the fate of atherosclerotic plaque. Atherosclerosis. 2017;256:53–61.
364. Syu JN, Lee DY, Hung HC, Li CY, Lin HY, Chiang EPI, et al. Docosahexaenoic acid inhibits cell proliferation through a suppression of c-myc protein in pancreatic ductal adenocarcinoma cells. Antioxidants. 2021;10(11).
365. Cai W, Wang C, Li Y, Yao C, Shen L, Liu S, et al. Genome-wide analysis of regulation of gene expression and H3K9me2 distribution by JIL-1 kinase mediated histone H3S10 phosphorylation in Drosophila. Nucleic Acids Res. 2014 May 14;42(9):5456–67.

366. Khan DH, Healy S, He S, Lichtensztejn D, Klewes L, Sharma KL, et al. Mitogen-induced distinct epialleles are phosphorylated at either H3S10 or H3S28, depending on H3K27 acetylation. Mol Biol Cell. 2017;28(6):817–24.
367. Soloaga A, Thomson S, Wiggin GR, Rampersaud N, Dyson MH, Hazzalin CA, et al. MSK2 and MSK1 mediate the mitogen- and stress-induced phosphorylation of histone H3 and HMG-14. EMBO J. 2003;22(11):2788–97.
368. Pham TX, Bae M, Lee Y, Park Y-K, Lee J-Y. Transcriptional and posttranscriptional repression of histone deacetylases by docosahexaenoic acid in macrophages. J Nutr Biochem. 2018 Jul;57:162–9.
369. Sun JM, Chen HY, Espino PS, Davie JR. Phosphorylated serine 28 of histone H3 is associated with destabilized nucleosomes in transcribed chromatin. Nucleic Acids Res. 2007;35(19):6640–7.
370. Lau PNI, Cheung P. Histone code pathway involving H3 S28 phosphorylation and K27 acetylation activates transcription and antagonizes polycomb silencing. Proc Natl Acad Sci. 2011 Feb 15;108(7):2801 LP – 2806.
371. Lantz M, Vondrichova T, Parikh H, Frenander C, Ridderstråle M, Asman P, et al. Overexpression of immediate early genes in active Graves' ophthalmopathy. J Clin Endocrinol Metab. 2005 Aug;90(8):4784–91.
372. Novo S, Shihan MH, Wang Y, Duncan MK. Immediate early genes as drivers of inflammation and posterior capsular opacification following cataract surgery. Invest Ophthalmol Vis Sci. 2019 Jul 22;60(9):6447.
373. Healy S, Khan P, He S, Davie JR. Histone H3 phosphorylation, immediate-early gene expression, and the nucleosomal response: A historical perspective. Biochem Cell Biol. 2012;90(1):39–54.
374. Castellano-Pozo M, Santos-Pereira J, Rondón AG, Barroso S, Andújar E, Pérez-Alegre M, et al. R loops are linked to histone H3 S10 phosphorylation and chromatin condensation. Mol Cell. 2013;52(4):583–90.
375. Skourti-Stathaki K, Proudfoot NJ. Histone 3 S10 Phosphorylation: "Caught in the R Loop!" Mol Cell. 2013;52(4):470–2.
376. Kobayashi T, Nemoto S, Ishida K, Taguchi K, Matsumoto T, Kamata K. Involvement of CaM kinase II in the impairment of endothelial function and eNOS activity in aortas of Type 2 diabetic rats. Clin Sci. 2012;123(6):375–86.
377. Murthy S, Koval OM, Ramiro Diaz JM, Kumar S, Nuno D, Scott JA, et al. Endothelial CaMKII as a regulator of eNOS activity and NO-mediated vasoreactivity. PLoS One.

2017;12(10):1–23.

378. Fleming I, Fisslthaler B, Dimmeler S, Kemp BE, Busse R. Phosphorylation of Thr495 Regulates Ca2+/Calmodulin-Dependent Endothelial Nitric Oxide Synthase Activity. Circ Res. 2001 Jun 8;88(11):e68–75.
379. Kashiwase K, Higuchi Y, Hirotani S, Yamaguchi O, Hikoso S, Takeda T, et al. CaMKII activates ASK1 and NF-kappaB to induce cardiomyocyte hypertrophy. Biochem Biophys Res Commun. 2005 Feb;327(1):136–42.
380. Ling H, Gray CBB, Zambon AC, Grimm M, Gu Y, Dalton N, et al. Ca2+/Calmodulin-dependent protein kinase II δ mediates myocardial ischemia/reperfusion injury through nuclear factor-κB. Circ Res. 2013 Mar;112(6):935–44.
381. Sun P, Enslen H, Myung PS, Maurer RA. Differential activation of CREB by Ca2+/calmodulin-dependent protein kinases type II and type IV involves phosphorylation of a site that negatively regulates activity. Genes Dev. 1994;8(21):2527–39.
382. Liu Y, Sun LY, Singer D V., Ginnan R, Singer HA. CaMKIIδ-dependent inhibition of cAMP-response elementbinding protein activity in vascular smooth muscle. J Biol Chem. 2013;288(47):33519–29.
383. Ma H, Groth RD, Cohen SM, Emery JF, Li B, Hoedt E, et al. γcaMKII shuttles Ca2+/CaM to the nucleus to trigger CREB phosphorylation and gene expression. Cell. 2014;159(2):281–94.
384. Cai H, Davis ME, Drummond GR, Harrison DG. Induction of endothelial NO synthase by hydrogen peroxide via a Ca(2+)/calmodulin-dependent protein kinase II/janus kinase 2-dependent pathway. Arterioscler Thromb Vasc Biol. 2001 Oct;21(10):1571–6.
385. Li H, Burkhardt C, Heinrich U-R, Brausch I, Xia N, Förstermann U. Histamine upregulates gene expression of endothelial nitric oxide synthase in human vascular endothelial cells. Circulation. 2003 May;107(18):2348–54.
386. Gray CBB, Suetomi T, Xiang S, Blackwood EA, Glembotski CC, Miyamoto S, et al. CaMKIIδ subtypes differentially regulate infarct formation following ex vivo myocardial ischemia/reperfusion through NF-κB and TNF-α. J Mol Cell Cardiol. 2017;103:48–55.
387. Zhuang X, Zhang H, Li X, Li X, Cong M, Peng F, et al. Differential effects on lung and bone metastasis of breast cancer by Wnt signalling inhibitor DKK1. Nat Cell Biol. 2017 Oct;19(10):1274–85.

388. Ikeda S, Matsushima S, Okabe K, Ikeda M, Ishikita A, Tadokoro T, et al. Blockade of L-type Ca(2+) channel attenuates doxorubicin-induced cardiomyopathy via suppression of CaMKII-NF-κB pathway. Sci Rep. 2019 Jul;9(1):9850.
389. Yan X, Liu J, Ye Z, Huang J, He F, Xiao W, et al. CaMKII-Mediated CREB phosphorylation is involved in Ca2+-Induced BDNF mRNA transcription and neurite outgrowth promoted by electrical stimulation. PLoS One. 2016;11(9):1–22.
390. Cai H, Liu D, Garcia JGN. CaM Kinase II-dependent pathophysiological signalling in endothelial cells. Cardiovasc Res. 2008;77(1):30–4.
391. Wang Z, Ginnan R, Abdullaev IF, Trebak M, Vincent PA, Singer HA. Calcium/calmodulin-dependent protein kinase II delta 6 (CaMKIIδ 6) and RhoA involvement in thrombin-induced endothelial barrier dysfunction. J Biol Chem. 2010;285(28):21303–12.
392. Li W, Li H, Sanders PN, Mohler PJ, Backs J, Olson EN, et al. The multifunctional Ca2+/Calmodulin-dependent Kinase II δ (CaMKIIδ) controls neointima formation after carotid ligation and vascular smooth muscle cell proliferation through cell cycle regulation by p21. J Biol Chem. 2011;286(10):7990–9.
393. Gao J, Wang X, Sun H, Cao Y, Liang S, Wang H, et al. Neuroprotective effects of docosahexaenoic acid on hippocampal cell death and learning and memory impairments in a valproic acid-induced rat autism model. Int J Dev Neurosci. 2016;49:67–78.
394. Bie N, Feng X, Li C, Meng M, Wang C. The Protective Effect of Docosahexaenoic Acid on PC12 Cells in Oxidative Stress Induced by H2O2through the TrkB-Erk1/2-CREB Pathway. ACS Chem Neurosci. 2021;12(18):3433–44.
395. House SJ, Ginnan RG, Armstrong SE, Singer HA. Calcium/calmodulin-dependent protein kinase II-δ isoform regulation of vascular smooth muscle cell proliferation. Am J Physiol Physiol. 2007 Jun 1;292(6):C2276–87.
396. House SJ, Singer HA. CaMKII-delta isoform regulation of neointima formation after vascular injury. Arterioscler Thromb Vasc Biol. 2008 Mar;28(3):441–7.
397. House SJ, Potier M, Bisaillon J, Singer HA, Trebak M. The non-excitable smooth muscle: calcium signaling and phenotypic switching during vascular disease. Pflugers Arch. 2008 Aug;456(5):769–85.
398. Bowman L, Mafham M, Wallendszus K, Stevens W, Buck G, Barton J, et al. Effects of n-3 Fatty Acid Supplements in Diabetes Mellitus. N Engl J Med. 2018 Oct;379(16):1540–50.

399. Manson JE, Cook NR, Lee I-M, Christen W, Bassuk SS, Mora S, et al. Marine n-3 Fatty Acids and Prevention of Cardiovascular Disease and Cancer. N Engl J Med. 2019 Jan;380(1):23–32.
400. Innes JK, Calder PC. Marine omega-3 (N-3) fatty acids for cardiovascular health: An update for 2020. Int J Mol Sci. 2020;21(4):1–21.
401. Giltay EJ, Gooren LJG, Toorians AWFT, Katan MB, Zock PL. Docosahexaenoic acid concentrations are higher in women than in men because of estrogenic effects. Am J Clin Nutr. 2004 Nov 1;80(5):1167–74.
402. Childs CE, Kew S, Finnegan YE, Minihane AM, Leigh-Firbank EC, Williams CM, et al. Increased dietary α-linolenic acid has sex-specific effects upon eicosapentaenoic acid status in humans: re-examination of data from a randomised, placebo-controlled, parallel study. Nutr J. 2014;13(1):113.
403. Plourde M, Chouinard-Watkins R, Vandal M, Zhang Y, Lawrence P, Brenna JT, et al. Plasma incorporation, apparent retroconversion and β-oxidation of 13C-docosahexaenoic acid in the elderly. Nutr Metab. 2011;8:1–9.
404. Schuchardt JP, Ostermann AI, Stork L, Fritzsch S, Kohrs H, Greupner T, et al. Effect of DHA supplementation on oxylipin levels in plasma and immune cell stimulated blood. Prostaglandins Leukot Essent Fat Acids. 2017;121(May):76–87.
405. Meuronen T, Lankinen MA, Fauland A, Shimizu B ichi, de Mello VD, Laaksonen DE, et al. Intake of Camelina Sativa Oil and Fatty Fish Alter the Plasma Lipid Mediator Profile in Subjects with Impaired Glucose Metabolism – A Randomized Controlled Trial. Prostaglandins Leukot Essent Fat Acids. 2020;159(January):102143.
406. Calder PC. Eicosapentaenoic and docosahexaenoic acid derived specialised pro-resolving mediators: Concentrations in humans and the effects of age, sex, disease and increased omega-3 fatty acid intake. Biochimie. 2020;178:105–23.
407. Du Y, Taylor CG, Aukema HM, Zahradka P. Role of oxylipins generated from dietary PUFAs in the modulation of endothelial cell function. Prostaglandins Leukot Essent Fat Acids. 2020;160(May):102160.
408. Chattopadhyay R, Mani AM, Singh NK, Rao GN. Resolvin D1 blocks H(2)O(2)-mediated inhibitory crosstalk between SHP2 and PP2A and suppresses endothelial-monocyte interactions. Free Radic Biol Med. 2018 Mar;117:119–31.
409. Yeganeh A, Taylor CG, Tworek L, Poole J, Zahradka P. Trans-10,cis-12 conjugated linoleic acid (CLA) interferes with lipid droplet accumulation during 3T3-L1 preadipocyte differentiation. Int J Biochem Cell Biol. 2016;76:39–50.

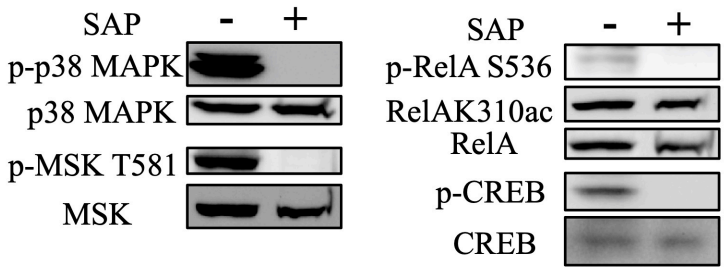

Figure 26. Validation of primary antibodies for some phospho-proteins and RelAK310ac.

EA.hy926 cells were treated with 125 μM DHA for 8 h at which time cell lysates were prepared and subjected to alkaline phosphatase treatment as previously described [409]. Briefly, after DHA treatment, hypotonic lysis buffer (HLB) (100 mM Tris pH 7.4, 2 mM EDTA, and 1× Protease Inhibitor cocktail set III (Millipore, #539134)) was used to lyse cells. Then, 1× phosphatase inhibitor cocktail was immediately added to 40 μL of the cell lysate, while another 40 μL of the lysate was incubated with 2 μL rCutSmart™ buffer and 1 μL Shrimp Alkaline Phosphatase (SAP, NEB, #M0371S) at 37 ºC for 30 min followed by 65 ºC for 5 min. Both phosphatase-treated (SAP+) and non-treated (SAP-) samples were then sonicated and analyzed by Western blotting. The absence of bands in the SAP+ sample lysates together with the visible bands for SAP- sample lysates indicate that the tested phospho-antibodies were specific for the phosphoproteins under investigation. In addition, the similar band intensities in RelAK310ac between the SAP- and SAP+ sample lysates imply that this RelA acetylation was not affected by phosphorylation.

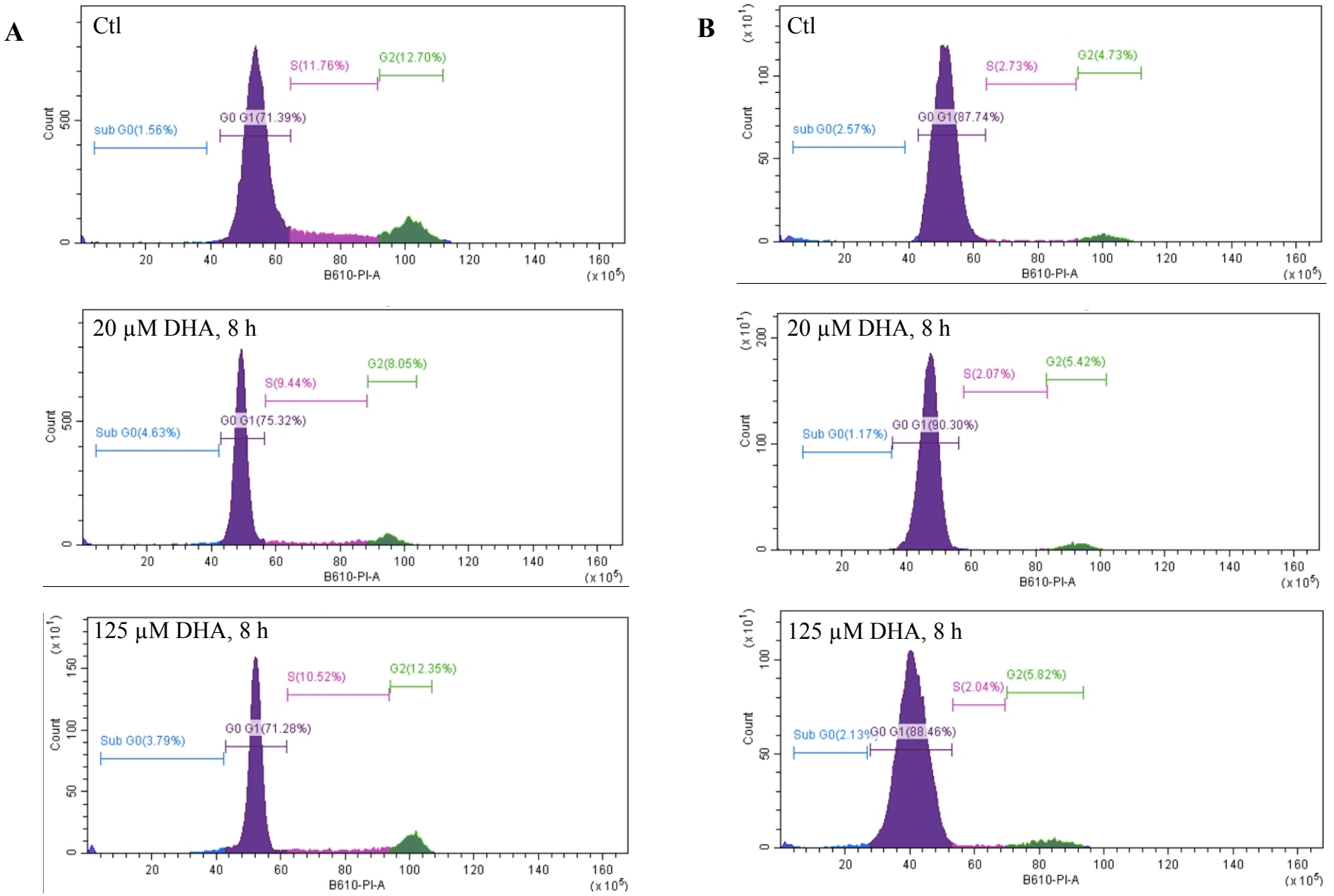
A
Ctl
S(11.76%)
G2(12.70%)
sub G0(1.56%)
G0 G1(71.39%)
20 µM DHA, 8 h
G2(8.05%)
S(9.44%)
G0 G1(75.32%)
Sub G0(4.63%)
125 µM DHA, 8 h
S(10.52%)
G2(12.35%)
Sub G0(3.79%)
G0 G1(71.28%)
B
Ctl
S(2.73%)
G2(4.73%)
sub G0(2.57%)
G0 G1(87.74%)
20 µM DHA, 8 h
S(2.07%)
G2(5.42%)
Sub G0(1.17%)
G0 G1(90.30%)
125 µM DHA, 8 h
S(2.04%)
G2(5.82%)
Sub G0(2.13%)
G0 G1(88.46%)
Count
B610-PI-A
(x10^5)
(x10^1)

Figure 27. Representative histograms for flow cytometry of PI-stained EA.hy926 cells.

EA.hy926 cells were treated with various concentrations of DHA for 2 or 8 h. Then the cells were subjected to PI staining and flow cytometry analysis with an established protocol from Dr. Peter Pelka's lab (University of Manitoba). Representative histograms for growing cells (panel A on the left) and quiescent cells (panel B on the right) are displayed. Ctl: control with 0 μM DHA treatment.